Report No. BMI-1298
UC-25 Metallurgy and Ceramics
(TID-4500, 14th Ed.)

Contract No. W-7405-eng-92

CONSTITUTION, METALLURGY, AND OXIDATION RESISTANCE OF IRON-CHROMIUM-ALUMINUM ALLOYS

by

Walston Chubb
Sam Alfant
Arthur A. Bauer
Edward J. Jablonowski
Fred R. Shober
Ronald F. Dickerson

October 16, 1958

BATTELLE MEMORIAL INSTITUTE
505 King Avenue
Columbus 1, Ohio

DISCLAIMER

TABLE OF CONTENTS

CONSTITUTION, METALLURGY, AND OXIDATION RESISTANCE OF IRON-CHROMIUM-ALUMINUM ALLOYS

Walston Chubb, Sam Alfant, Arthur A. Bauer, Edward J. Jablonowski, Fred R. Shober, and Ronald F. Dickerson

The constitution of iron-chromium-aluminum alloys has been investigated employing high-purity materials. Ternary sections illustrating the results are presented. The limits of the alpha-plus-sigma region are found to extend from 33 to 63 w/o chromium at 600 C. At 750 C these limits decrease to 38 and 57 w/o chromium. Sigma is found in alloys containing a maximum of about 9 w/o aluminum at 600 C and 4 w/o aluminum at 750 C. The limits of the alpha solid-solution region were investigated between 500 and 900 C. No observable change in limits occurred between 500 and 750 C. However, between 750 and 900 C the $AlCr_2$ phase decomposes resulting in a slightly expanded alpha region in the high-chromium alloys. Sigma is found to be unstable below 600 C in alloys of sigma-phase composition. Sigma formation and decomposition occur reversibly above and below this temperature. The nature of the products of the reaction below 600 C has not been determined.

A detailed investigation of the physical metallurgy of iron alloys containing 25 to 35 w/o chromium and 3 to 8 w/o aluminum has been made in an attempt to define the limits of usefulness of these materials as structural materials. It is possible to melt and fabricate all alloys within this composition range, but extraordinary care must be used to avoid embrittlement from undesirable impurities such as carbon, from oxide drosses, from unfavorable grain size and structure, and from internal cracking caused by rapid cooling. Suitable methods for casting and fabricating these alloys are described. The deformation processes of iron-chromium-aluminum alloys are reported and a ductility transition which varies with alloy content is attributed to the interaction of a twinning mode of plastic deformation and a cleavage mode of fracture.

The oxidation resistances of iron-23.7 w/o chromium-6.0 w/o aluminum alloy and of nickel-20.0 w/o chromium-1.1 w/o niobium alloy have been compared at 1900 and 2100 F (1040 and 1150 C) in air atmospheres containing additions of (1) water vapor, (2) carbon dioxide, and (3) combinations of water vapor and carbon dioxide. The iron-chromium-aluminum alloy was more oxidation resistant than the nickel-chromium-niobium alloy in all atmospheres at 2100 F (1150 C). Minimum oxidation of both alloys occurred in an atmosphere of air plus 2.5 volume per cent water vapor.

INTRODUCTION

Iron-chromium-aluminum alloys have been used commercially for many years as electrical-resistance heating elements. In this application, they have distinguished themselves for superior oxidation resistance at very high temperatures (up to 1300 C). This oxidation resistance has been attributed to the formation of a dense protective film of nearly pure alumina on the surface of the alloys.[1-3] As electrical heating ele-

(1) References at end of report.

ments, iron-chromium-aluminum alloys have also developed a reputation for sagging and becoming brittle in use. Low creep strength and rapid grain growth are reported to be the causes of this behavior[1]. The sagging tendency can be corrected by proper design and support of the heating elements; the grain growth is reported to be retarded by the addition of certain inhibitors, such as titanium or zirconium[1].

With structural applications in mind, the engineering properties of iron-chromium-aluminum alloys have been investigated.[2-6] As expected, the high-temperature strength of the alloys was found to be low, but not prohibitively low for such an application. More serious, however, was the discovery that the alloys did not show reproducible cold-rolling ductility at the iron-25 w/o chromium-5 w/o aluminum level and that the iron-35 w/o chromium-7.5 w/o aluminum alloy could not be cold rolled at all, and often showed poor hot-fabrication characteristics.[6] The work reported herein represents a continuation of these studies. The metallurgy of iron-chromium-aluminum alloys has been further detailed, and an attempt has been made to clarify the lack of reproducible fabrication characteristics of the materials.

Because of this lack of reproducibility of the fabrication behavior of iron-chromium-aluminum alloys, the character of secondary phases normally, or even rarely, present has received special scrutiny. The iron-chromium sigma phase with its occasional habit of appearing in steels of compositions far removed from the stoichiometric, FeCr, composition has been the subject of an investigation intended to show whether sigma or any aluminum-rich compound could be a contributing factor to the brittle behavior of some alloys. An investigation of the physical metallurgy of iron-chromium-aluminum alloys was undertaken on the supposition that the irreproducibility might be caused by some minor impurity or by some chance variation in melting, casting, or fabrication techniques. Studies of the oxidation behavior of iron-chromium-aluminum alloys at very high temperatures represent extensions of previous studies[2,3,6] which were also intended to define the utility and limitations of this remarkable group of ferritic alloys. Additional work of this type will undoubtedly be required as the techniques for preparing these materials become more thoroughly understood and as materials of more uniform behavior become available and as engineers become acquainted with their unusual properties and ranges of application. Recent studies of the casting, fabrication, mechanical properties, and oxidation resistance of alloys containing up to 25 w/o chromium and 11 w/o aluminum[7] suggest that these materials may find use as boiler tubes.

CONSTITUTION OF IRON-CHROMIUM-ALUMINUM ALLOYS

Background

As early as 1927, Chevenard[8] suggested that a compound existed at approximately 50 a/o chromium in the binary iron-chromium system. In 1927, Bain and Griffiths[9] confirmed the existence of an intermetallic compound in iron-chromium alloys, and called it the sigma phase. Cook and Jones[10], in 1943, investigated the iron-chromium system and showed that at 600 C, sigma extended from 42 to 48 w/o chromium. They also showed that sigma existed in alloys containing as little as 24 w/o

chromium. However, it was later shown by Anderson and Jette[11] that the limits of existence of the sigma phase were altered by the presence of silicon and manganese. According to Vollers[12], silicon greatly promoted the formation of the sigma constituent. High-purity alloys that contained less than 25 w/o chromium after extended heat treatments showed no sigma phase, and iron-chromium alloys containing between 8 and 10 w/o silicon and only 11 w/o chromium showed definite evidences of sigma phase. Nicholson, Samans, and Shortsleeve[13] reported that an increase in carbon content accelerated the formation of the sigma phase. The effect of carbon was determined by comparing the threshold time of two alloys which contained the same amount of chromium in solid solution, but which contained different amounts of carbon. (They defined "threshold time" as the minimum time required to develop enough sigma to produce detectable X-ray diffraction lines.) The threshold time for both of these alloys was determined for a series of temperatures between 595 and 745 C. In every case the threshold time for the higher carbon alloy was less than the threshold time for the lower carbon alloy.

In previous work it was found that the precipitation of cubic chromium carbide was complete before sigma began to form. It appears that the primary influence of carbon was to combine with chromium and iron, and, thereby, to reduce the "effective" amount of chromium, that is, the chromium in solid solution. According to Tofaute, Küttner, and Büttenghaus[14], the cubic carbide for these alloys should contain 68 w/o chromium, 26.5 w/o iron, and 5.5 w/o carbon.

With regard to the ternary iron-chromium-aluminum system, the only reported original work was completed in 1940 by I. I. Kornilov[15]. This study was subsequently discussed by Case and Van Horn[1]. Kornilov reported an incomplete phase diagram at room temperature, as shown in Figure 1, and a similar section for the same alloys after quenching from 1150 C, shown in Figure 2. In regard to the nomenclature used by Kornilov, α_3 designated an iron-chromium-aluminum solid solution; ϵ_3 was a product of a peritectic reaction, liquid plus $\alpha_3 \rightarrow \epsilon_3$; and sigma, σ, designated the compound FeCr. He also reported that alloys quenched from 1150 C and containing approximately 30 to 40 w/o aluminum produced two phases, α_3 and ϵ_3, and, as the concentration of aluminum was increased, the quantity of ϵ_3 was increased, with the disappearance of α_3 in alloys above 40 w/o aluminum.

The problem of the hardening and embrittlement of ferritic chromium stainless steels at temperatures below 600 C has not been clearly resolved in spite of extensive investigations. Fisher, Dulis, and Carrol[16] discovered a chromium-rich body-centered-cubic precipitate in alloys annealed below 600 C. Williams and Paxton[17,18] reported that a miscibility gap existed below 600 C and was joined by one or two eutectoid reactions to the sigma-forming regions, and that this gap resulted in the precipitation of a chromium-rich phase which was always coherent with the matrix. Tisinai and Samans[19] studied the hardening effects of several 24 to 30 w/o chromium steels at 475 C, and found that hardening at that temperature was the result of coherent precipitation of a chromium-rich phase, the nature of which was not entirely clear. They showed that in alloys containing normal amounts of carbon, the temperature and time of prior heat treatments affected the hardening, apparently because of destruction of potential hardening nuclei by carbide nucleation. And in corroboration of these observations, Wright[20] and Lorrel[21] showed that 475 C hardening occurred in relatively pure iron-chromium alloys, but that the rate of hardening in high-purity alloys seemed to be appreciably lower, due probably to the absence of hardening and straining effects from precipitated carbides.

α_3 - Designates the Iron - Chromium - Aluminum solid solution

ϵ_3 - Designates a product of a preitectic reaction, liquid + $\alpha_3 \rightarrow \epsilon_3$

The broken line outlines the limits of magnetic transformation

β - A chromium - aluminum compound

γ_2 - A chromium - aluminum compound

δ - Sigma phase, Fe Cr

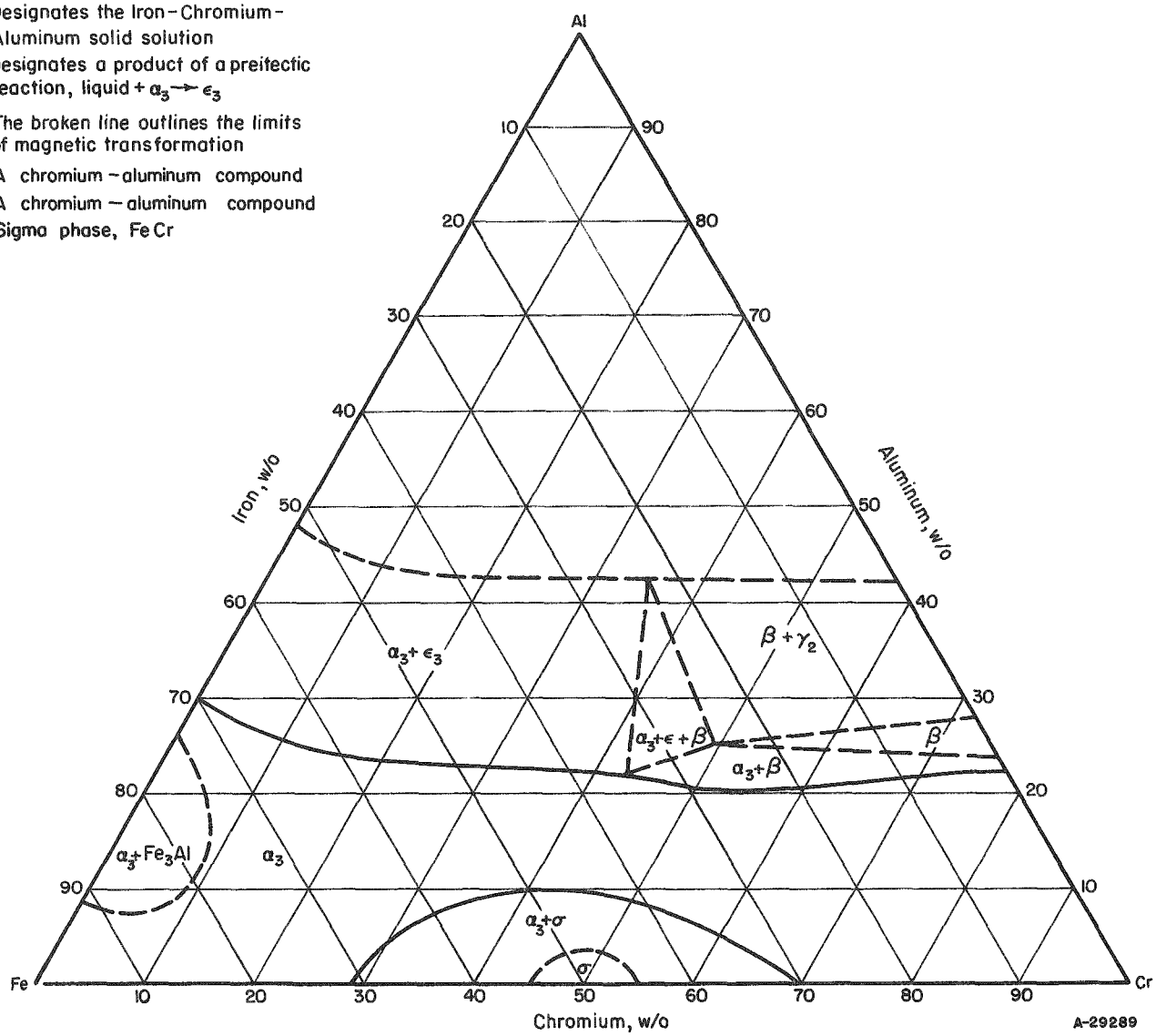

FIGURE 1. ROOM-TEMPERATURE PHASE DIAGRAM FOR IRON-CHROMIUM-ALUMINUM SYSTEM

After Kornilov[15].

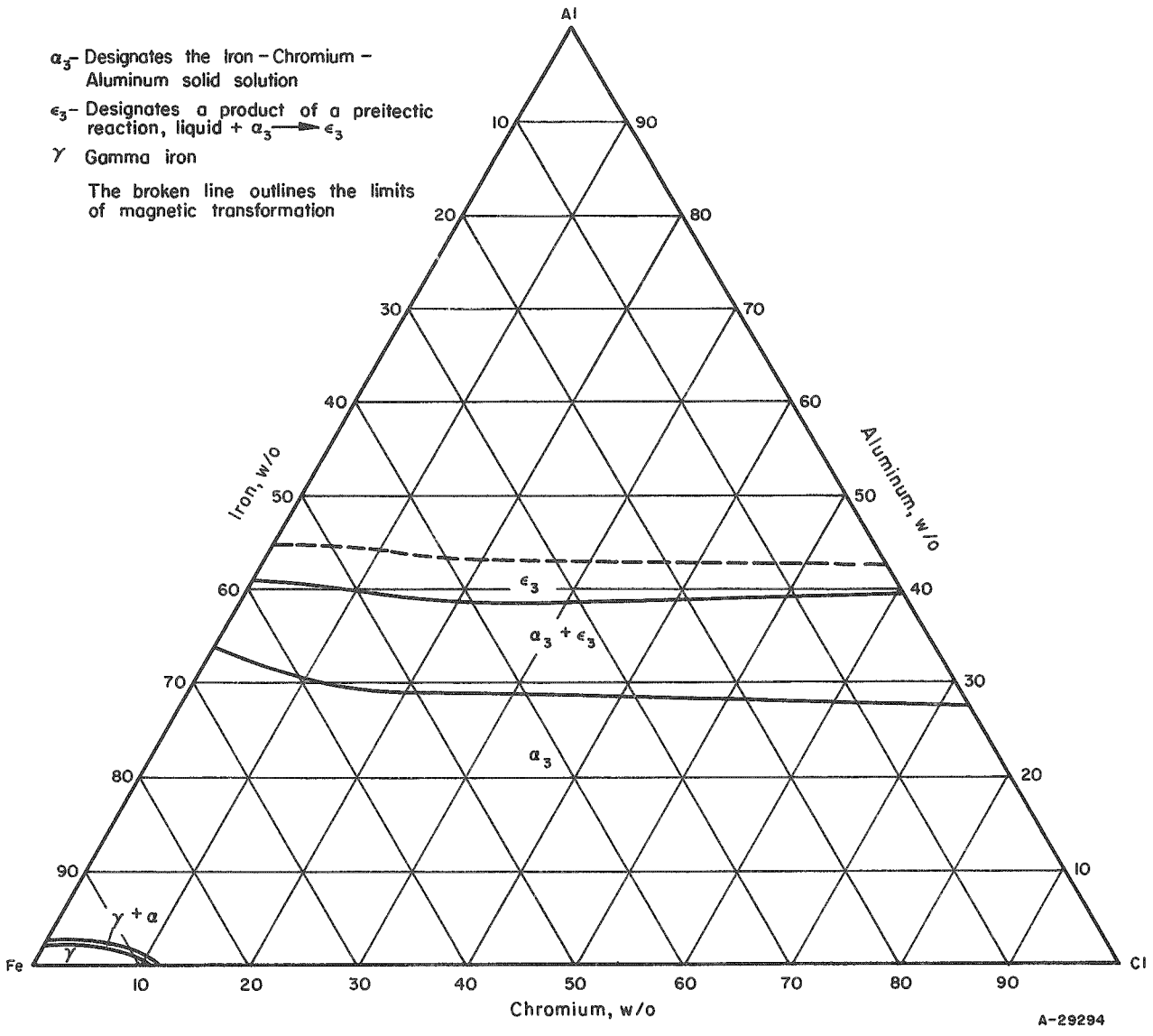

FIGURE 2. PHASE DIAGRAM OF THE IRON-CHROMIUM-ALUMINUM SYSTEM AT 1150 C

After Kornilov[15].

The presently reported investigation was prompted by a desire to provide a more detailed knowledge of the constitution of iron-chromium-aluminum alloys than was reported by Kornilov[15]. Materials of the highest purity available were employed. Principal emphasis was placed on determining the limits of the sigma phase and related phase regions in the system since the formation of appreciable amounts of the brittle sigma phase in an alloy precludes its application as a structural material. In addition, a survey of the alpha-phase region was conducted to provide an indication of its composition range as a prelude to possible future alloy development.

Experimental Procedures

Initially, the limits of the sigma- and alpha-plus-sigma-phase regions in the iron-chromium-aluminum system were investigated employing iron-rich alloys only. While these studies were only partially complete, the investigation was extended to include a study of these same regions in chromium-rich alloys and to include a study of the composition limits of the alpha-phase region. As a result, while the techniques of specimen preparation and examination were similar in all phases of the program, times of heat treatment were not necessarily the same throughout. Since heat treatments were designed to insure the development of equilibrium structures for each specific composition, the later data obtained are valid, and perhaps more reliable because of the use of more effective heat-treatment procedures.

Alloys were cast and then hot and cold rolled, if possible, or, when fabrication was not possible, given a homogenization anneal. Specimens were heat treated for various times at temperatures from 480 to 900 C and then examined metallographically. X-ray diffraction examinations were also conducted to aid in interpreting metallographic data. Attempts to perform thermal analysis on high-aluminum alloys were unsuccesful since such alloys are not amenable to the machining or spot-welding operation which is required for the preparation of thermal-analysis specimens.

Alloy Preparation

High-purity aluminum, iodide chromium, and electrolytic iron were employed for this study. Carbon, hydrogen, nitrogen, and oxygen analyses on these materials are given below.

	Analysis, ppm by weight			
	Carbon	Hydrogen	Nitrogen	Oxygen
Aluminum	40	0.9	10	12
Chromium	20	3	10	83
Iron	60	<0.7	10	47

Charges of 40-g size were prepared using an analytical balance and were melted in an inert-electrode arc furnace. Charges were melted seven times to insure homogeneity. Chemical analyses of the ingots indicated insignificant departures from the intended compositions. Consequently, all compositions are reported in terms of nominal composition.

The arc-melted buttons were hot rolled at 1095 C to 3/16-in. flat plate, where possible, and were then cold reduced 98 per cent by cold rolling. The purpose of cold reduction was to accelerate the formation of sigma. Those alloys which could not be either hot or cold rolled were given a homogenization anneal of 100 hr at 1000 C and furnace cooled prior to subsequent heat treatment.

The compositions of all alloys prepared for this study are shown in Figure 3. The compositional ranges of hot and cold fabricability are also shown on this diagram. It should be noted that these fabrication data apply to 40-g ingots and that fabricability is used here only in the sense that some reduction occurred and sufficient material was recovered for further tests.

Heat Treatment

Specimens were heat treated in argon-flushed and -filled Vycor tubes which were quenched and broken in water after the heat treatments were completed. All specimens were heat treated for a minimum of two periods of time and examined metallographically. The absence of change in structure, and consequent specification of phase-boundary limits, between these two periods served to establish the equilibrium-phase boundaries.

The alloys prepared for the initial study of the sigma-phase region were all high in iron (50 w/o or more) and could all be hot worked and cold reduced. Total times and temperatures of heat treatment used in arriving at a determination of phase-boundary limits in the high-iron regions are given below:

	Time at Temperature, hr	
Temperature, C	First Period	First Period Plus Second Period
480	1200	2200
500	1000	2000
500	360	720
650	360	720
700	480	1000
750	360	720

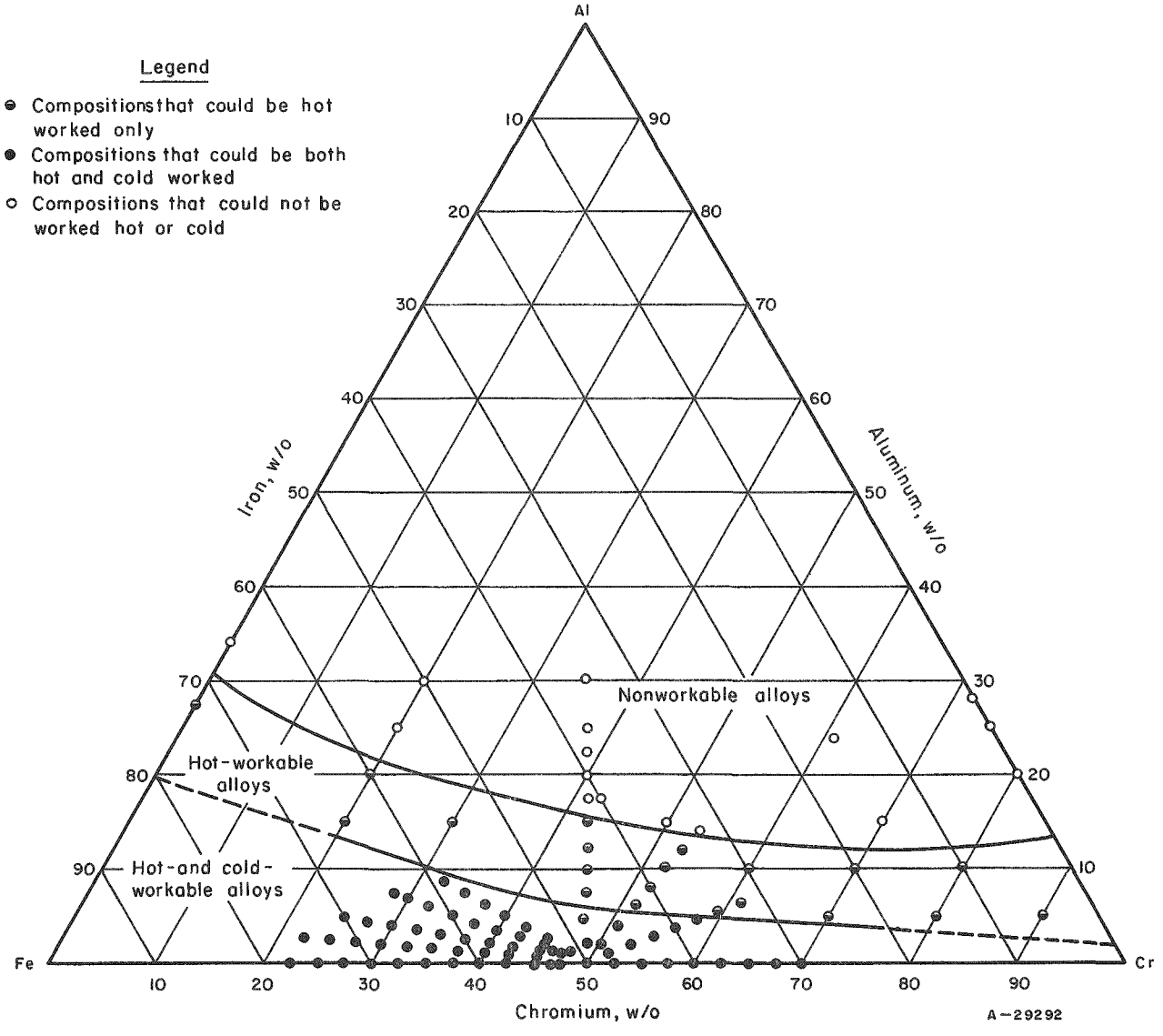

FIGURE 3. ALLOY COMPOSITIONS AND FABRICABILITY LIMITS

40-g ingots.

A study of the effect of cold work on the rate of sigma formation in these iron-rich alloys was also conducted. For this purpose, specimens in the as-hot-rolled condition and as-cold-reduced 90 per cent and 98 per cent conditions were heat treated for 240, 480, and 2400 hr at 700 C. In addition, alloy specimens of approximately single-phase sigma composition were heat treated at 700 C for periods of time up to 5000 hr to determine if overaging and softening of the sigma phase occurs.

Only a portion of the alloys prepared for a study of the sigma-phase region in chromium-rich alloys could be cold worked. In order to compensate for the lack of cold work introduced into many of these alloys, the times of heat treatment were increased. Temperatures and total times of heat treatment for the cold-worked alloys and those not cold worked in the high-chromium and high-aluminum regions are given below:

	Time at Temperature, hr			
	Cold-Worked Alloys		Alloys Not Cold Worked	
Temperature, C	First Period	First Period Plus Second Period[a]	First Period	First Period Plus Second Period[a]
480	1400	2400	1800	2300
500	1200	2200	1600	2000
600	1000	1300	1400	1800
650	850	1200	1200	1600
700	700	1000	1000	1400
750	600	900	900	1300

(a) Total of first period and second period.

Those alloys prepared specifically for a study of the high-aluminum alpha-phase boundary and generally containing 10 w/o or more aluminum were heat treated as tabulated below. Since the sluggish sigma-phase transformation was not involved, only a single period of heat treatment at each temperature was employed.

Temperature, C	Time, hr
500	1200
600	250
650	250
700	500
750	200
900	100

Metallography and Hardness

Specimens were mounted either in Bakelite or Kold-Weld* and were wet ground through 600-grit paper. The specimens were then given an intermediate polish on felt cloth with diamond abrasive using kerosene as the lubricant. Final polishing was performed on Buehler Microcloth with Linde B abrasive in water suspension.

In order to differentiate alpha from sigma in alpha-plus-sigma alloys, an electrolytic etchant was employed consisting of 10 g of oxalic acid in 100 cm^3 of water. This etch attacked the alpha phase, leaving the sigma phase in relief. This etchant was also employed for etching high-aluminum alloys.

Specimens containing large amounts of sigma were etched to outline the sigma-phase grain boundaries by employing an etchant consisting of 40 cm^3 of glycerine, 15 cm^3 of nitric acid, and 30 cm^3 of hydrochloric acid. The etchant was applied by swabbing for 30 sec to 2 min.

Hardness measurements were made on all specimens using a Tukon hardness tester with a Knoop diamond indenter and a 300-g load.

X-Ray Diffraction Examination

X-ray diffraction examinations were generally made by taking a sliver sample of conical shape from each specimen. In cases where the material was too brittle to be ground to the desired shape, samples were obtained by shattering the specimen in a diamond mortar, and selecting a piece with the required thickness. Specimens from which satisfactory slivers could not be obtained were crushed to powder.

The samples were then generally etched in 10 volume per cent oxalic acid for 5 min to etch either the sigma phase or other compounds, in relief, so as to enhance their respective pattern intensities. However, some samples were electropolished in phosphoric-sulfuric acid solution to obtain diffraction photograms representative of the total sample.

The X-ray photograms were taken in a 57.3-mm Debye camera, using 8-hr exposures to unfiltered chromium radiation.

Experimental Results

The results of this investigation are summarized in Figures 4, 5, 6, 7, and 8. The limits of the sigma, alpha-plus-sigma, and alpha regions are shown. Tentative phase relationships for high-aluminum alloys are shown. These diagrams are based primarily upon metallographic determinations supplemented by X-ray diffraction and hardness data. The X-ray diffraction data are presented in Table 1.

*Product of Precision Dental Mfg. Co., Chicago, Illinois.

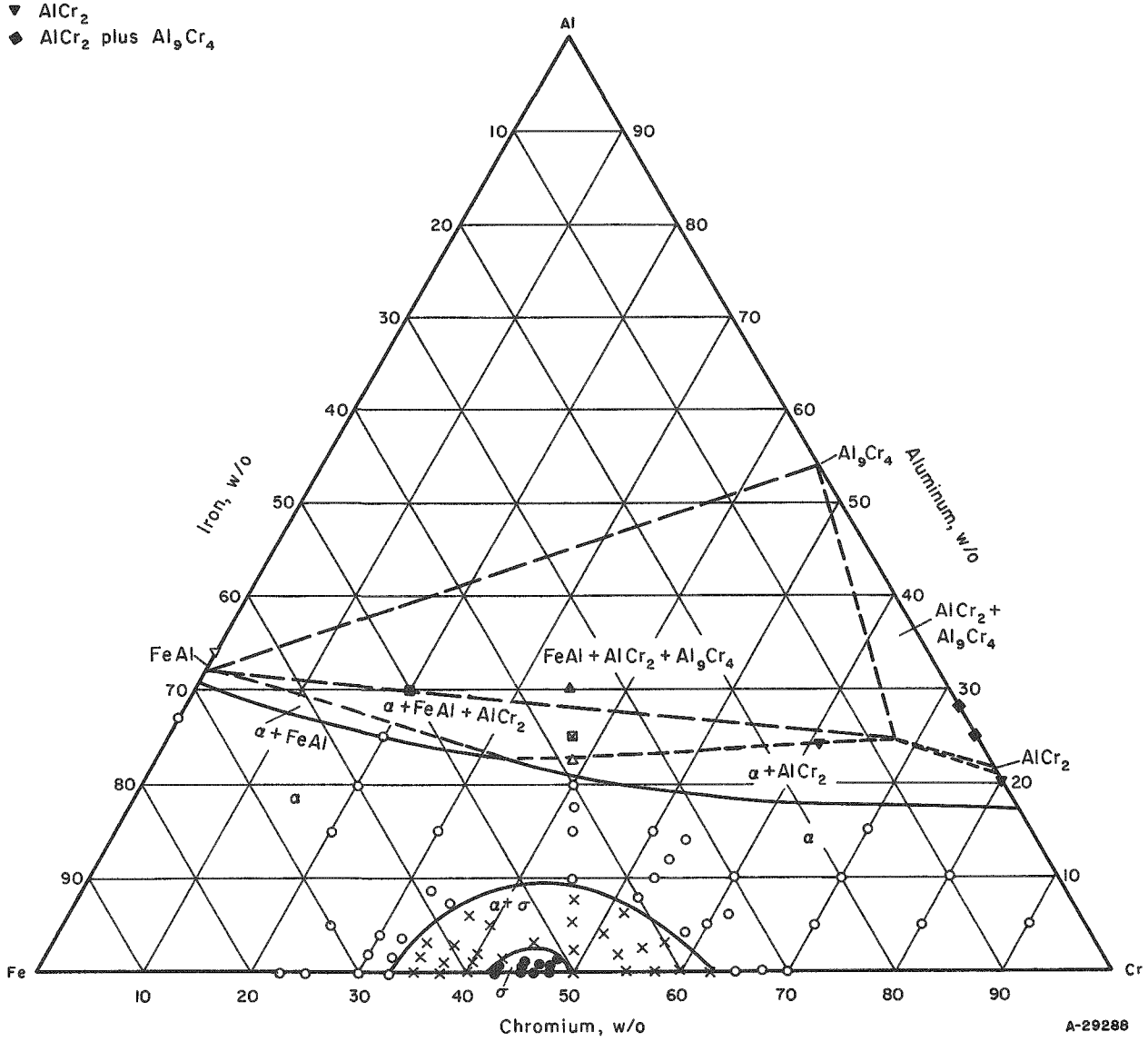

FIGURE 4. IRON-CHROMIUM-ALUMINUM TERNARY SECTION AT 600 C

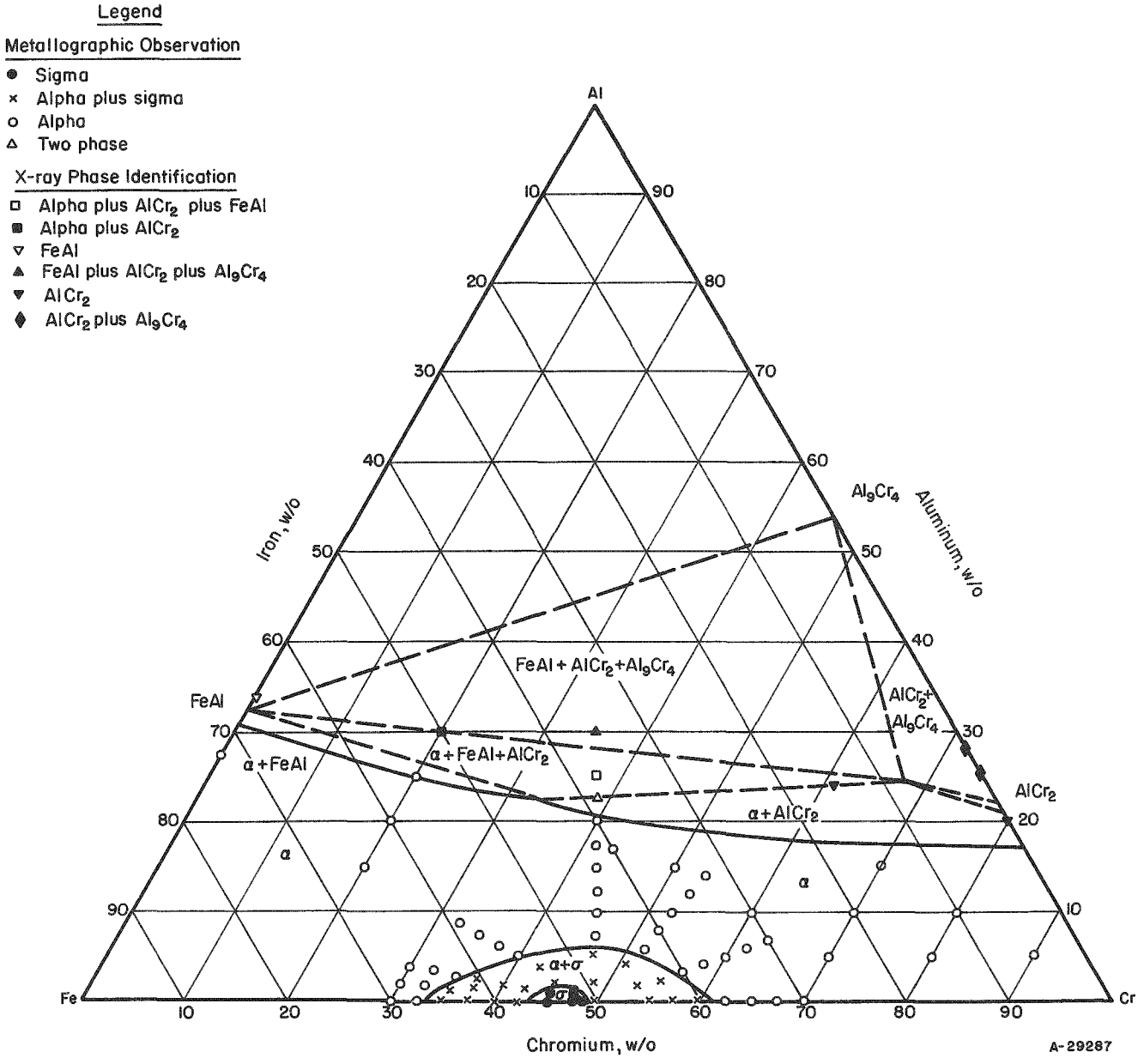

FIGURE 5. IRON-CHROMIUM-ALUMINUM TERNARY SECTION AT 650 C

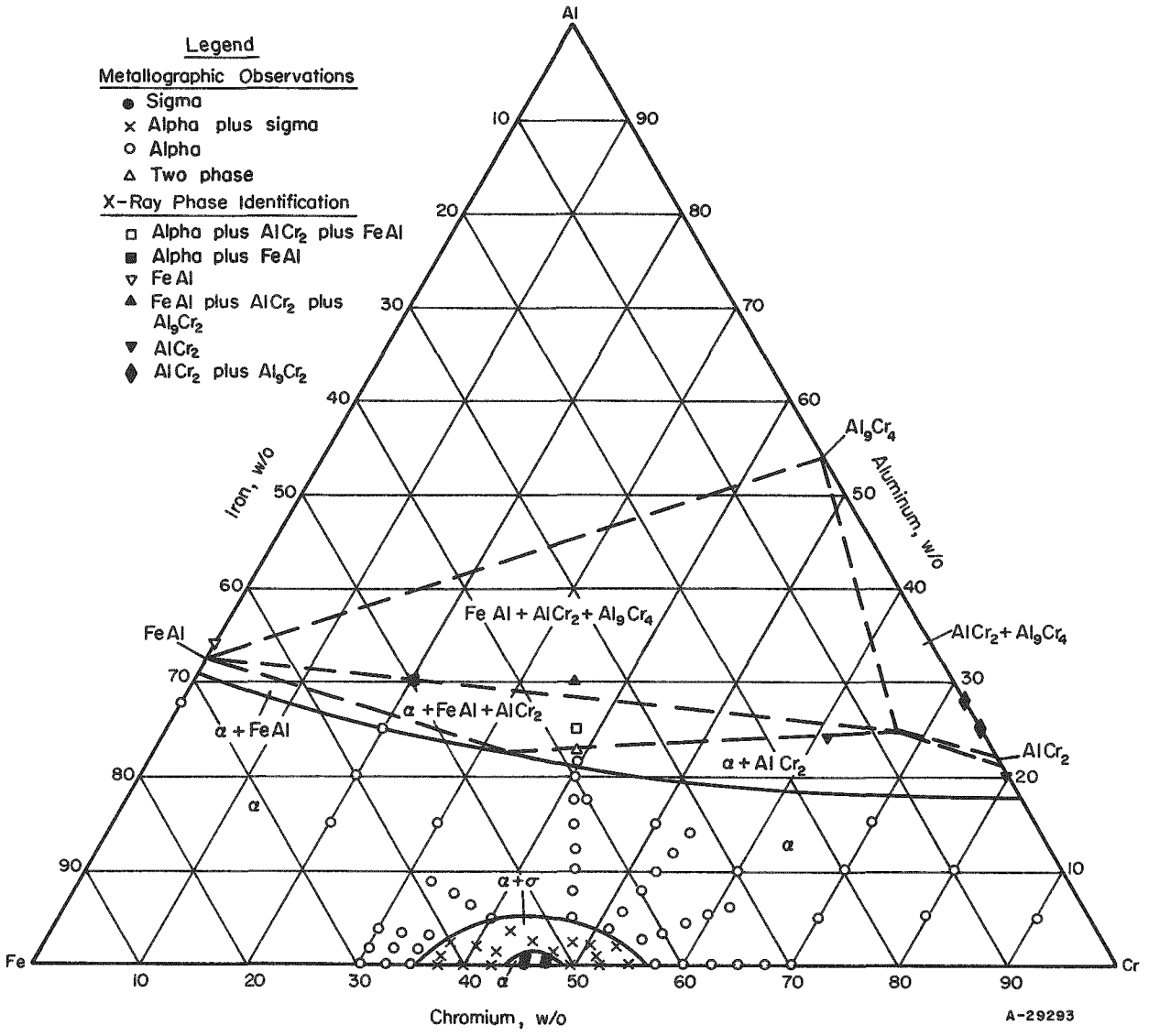

FIGURE 6. IRON-CHROMIUM-ALUMINUM TERNARY SECTION AT 700 C

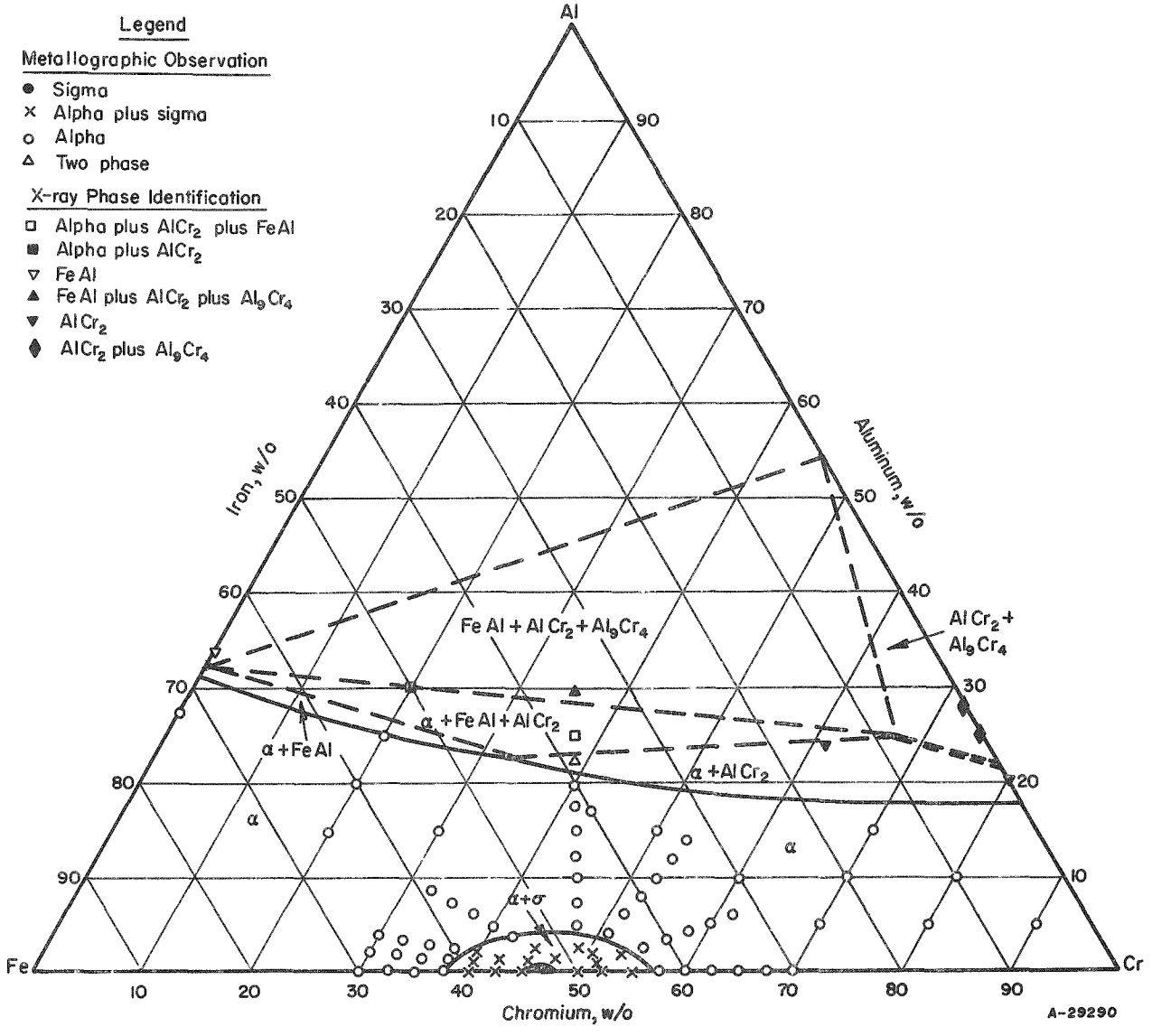

FIGURE 7. IRON-CHROMIUM-ALUMINUM TERNARY SECTION AT 750 C

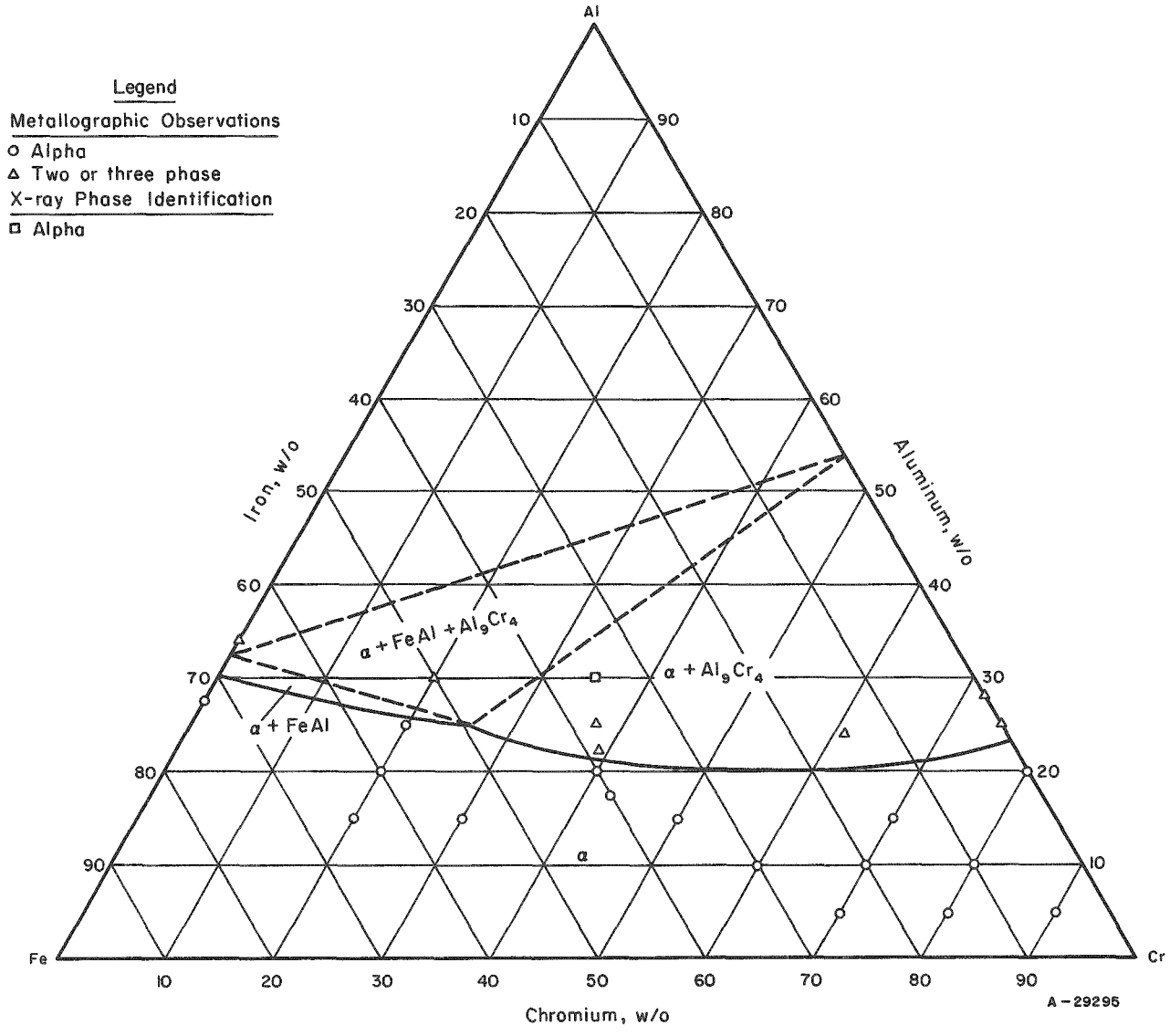

FIGURE 8. IRON-CHROMIUM-ALUMINUM TERNARY SECTION AT 900 C

TABLE 1. RESULTS OF X-RAY DIFFRACTION EXAMINATIONS OF IRON-CHROMIUM-ALUMINUM ALLOYS

Composition, w/o			Heat Treatment		Intensities of Phase Patterns Observed(a)				
			Time,	Temperature,					
Fe	Cr	Al	hr	C	Alpha	$AlCr_2$	FeAl	Al_9Cr_4	Sigma
45	51	4	850	650	VS	0	0	0	0
40	60	--	850	650	S	0	0	0	MF
42.5	57.5	--	850	650	VS	0	0	0	M
47.5	51.75	0.75	850	650	VS	0	0	0	F
45	55	--	850	650	VS	0	0	0	VF
45	53.25	1.75	850	650	VS	0	0	0	0
48.75	48.75	2.5	1000	700	VS	0	0	0	MS
47.5	50.5	2	850	650	VS	0	0	0	0
42.5	51.5	6	1400	600	VS	0	0	0	0
37.5	52.5	10	1400	600	VS	0	0	0	0
15	61	24	250	600	0	S	0	0	0
41.25	41.25	17.5	1000	700	VS	0	0	0	0
--	80	20	250	650	0	VS	0	0	0
--	72	28	250	650	0	S	0	MF	0
--	75	25	250	650	0	VS	0	MF	0
66	--	34	250	650	0	0	VS	0	0
37.5	37.5	25	1000	700	VVF	S	S	0	0
35	35	30	250	700	0	S	S	MF	0
35	35	30	100	900	MS	0	0	0	0
50	20	30	200	700	MF	0	S	0	0

(a) V = very.
S = strong.
M = medium.
F = faint.
0 = not detected.

The results are presented in three parts: those applicable to the sigma-phase regions, those applicable to the alpha-phase region and its limits, and the results on alloys of sigma-phase composition annealed at temperatures below 600 C, at which temperature the sigma phase is unstable.

Sigma-Phase Regions

The single-phase sigma and alpha-plus-sigma regions were found to expand with decreasing temperature, as shown in Figures 4 through 7. In binary alloys the iron-rich boundary for the alpha-plus-sigma region occurs at about 38 w/o chromium at 750 C and 33 w/o chromium at 600 C; corresponding values for the chromium-rich boundary are 57 w/o and 63 w/o chromium, respectively. Sigma is found in alloys containing a maximum of about 4 w/o aluminum at 750 C and 9 w/o aluminum at 600 C.

Sigma-phase structures are shown in Figures 9a and 9b. The etchant, consisting of glycerine and nitric and hydrochloric acids, has developed the microstructure of the sigma phase of the specimen shown in Figure 9a. By comparison, the oxalic acid etch which was employed for developing alpha-plus-sigma structures, only succeeds in pitting the sigma phase.

A general characteristic of sigma-phase formation at 700 and 750 C is illustrated in Figure 9a, namely the tendency for sigma to form massively at the center of cold-worked specimens. Thus, in this specimen, transformation to sigma is complete at the center of the specimen, while alpha remains at the surface. Figure 9c also illustrates this tendency of sigma-phase formation at these temperatures. At lower temperatures, 600 or 650 C, sigma formation is much more likely to be initiated at the specimen surface.

The hardness impressions appearing in Figure 9a also serve to illustrate the remarkable difference in hardness between the alpha and sigma phases. For this reason hardness measurements serve as a useful tool in the identification of sigma. In Figure 9d a typical alpha-plus-sigma structure is shown. While only slight differences in color or shading exist between the alpha and sigma phases, hardness impressions clearly differentiate between the two phases. It will be noted that the hardness impressions show a considerable range in size, depending upon the relative amounts of sigma and alpha covered by an impression. Consequently an average hardness value for a specimen such as this must be based on a considerable number of hardness impressions.

Cracks in the brittle sigma phase are also evident in Figures 9a, 9b, and 9c. Such cracking was usually observed whenever sigma was the predominant phase.

Typical alpha-plus-sigma structures are shown in Figures 10 and 11.

The microstructures appearing in Figure 10 are of binary alloys. In Figure 10a, sigma is the predominant phase, with small islands of alpha present in the sigma matrix. In the specimen shown in Figure 10b, sigma has precipitated at and surrounds the alpha grains. In both Figures 10c and 10d, sigma is present primarily near the specimen surface, the amount present decreasing with increasing chromium content. An

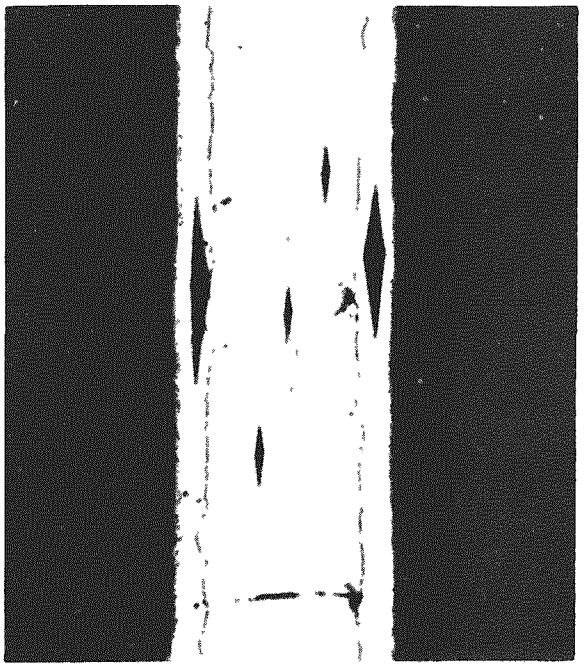

250X Glycerine, HNO_3, HCl Etch N48719

a. Iron-46.25 w/o Chromium Heated 2400 Hr at 700 C and Water Quenched

Knoop Hardness: Sigma 1092
Alpha 206

250X Oxalic Acid Etch N48725

b. Iron-45 w/o Chromium-0.5 w/o Aluminum Heated 720 Hr at 650 C and Water Quenched

Knoop Hardness: 1275

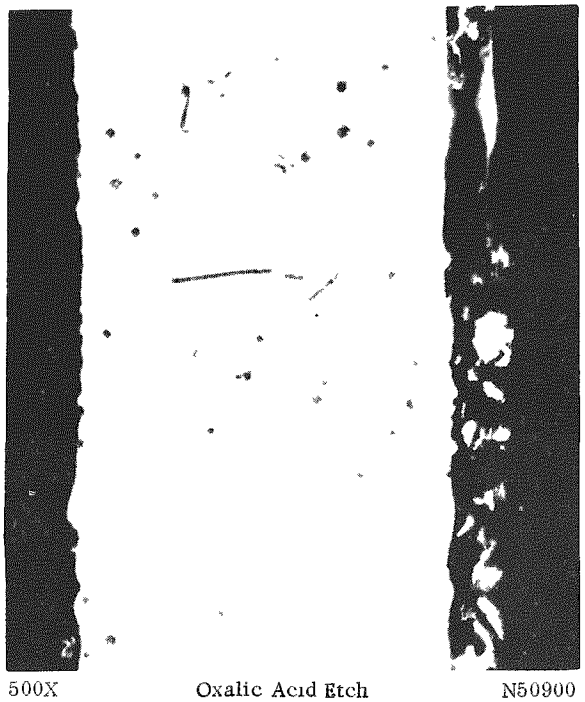

500X Oxalic Acid Etch N50900

c. Iron-40 w/o Chromium Heated 720 Hr at 750 C and Water Quenched

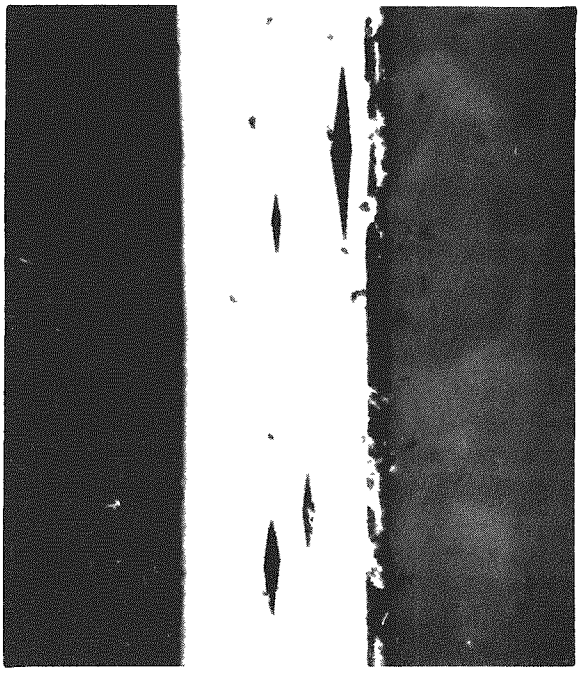

250X Oxalic Acid Etch N48723

d. Iron-47.5 w/o Chromium-1 w/o Aluminum Heated 2400 Hr at 700 C and Water Quenched

Knoop Hardness: Sigma 1182
Alpha 259

FIGURE 9. SIGMA- AND ALPHA-PLUS-SIGMA-PHASE STRUCTURES

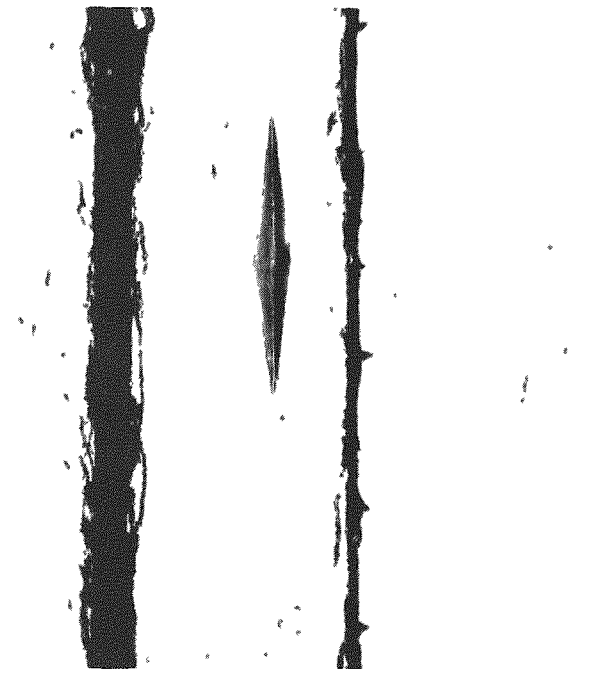

500X N49094

a. Iron-50 w/o Chromium

Knoop Hardness: 740

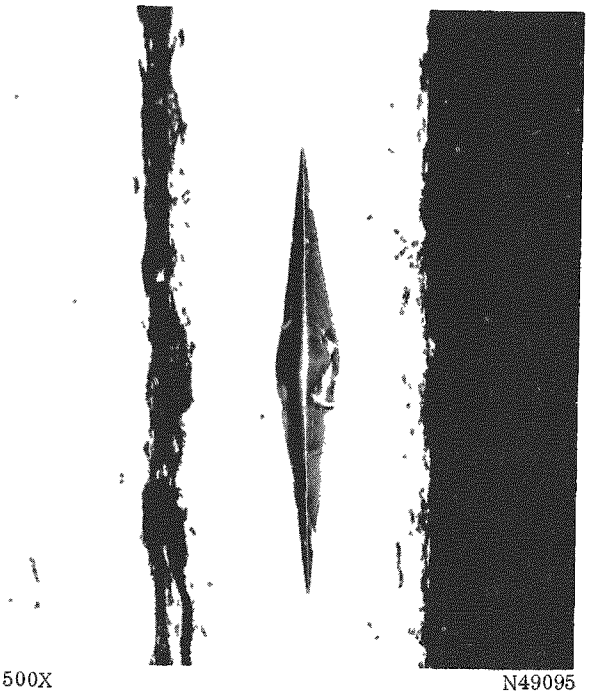

500X N49095

b. Iron-52.5 w/o Chromium

Knoop Hardness: 412

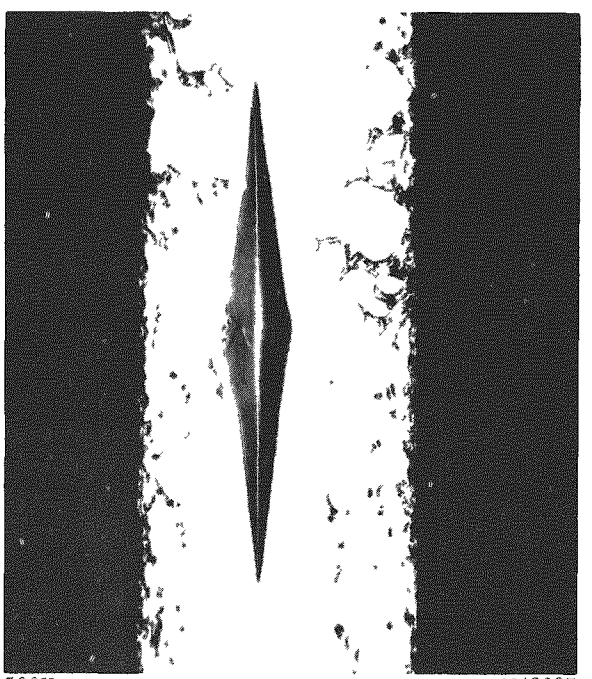

500X N49097

c. Iron-55 w/o Chromium

Knoop Hardness: 363

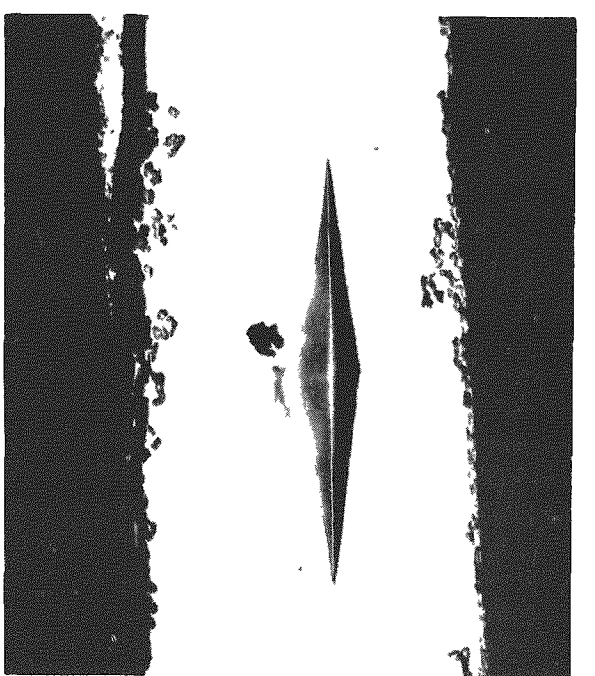

500X N49096

d. Iron-57.5 w/o Chromium

Knoop Hardness: 301

FIGURE 10. ALPHA-PLUS-SIGMA-PHASE STRUCTURES IN BINARY ALLOYS HEATED 1200 HR AT 650 C AND WATER QUENCHED

Oxalic Acid Etch.

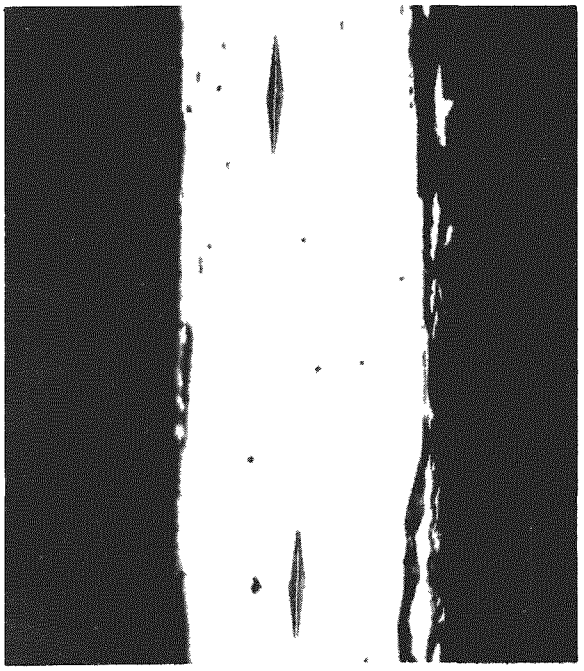

465X N48733

a. Iron-47.5 w/o Chromium-0.25 w/o Aluminum

Knoop Hardness 1282

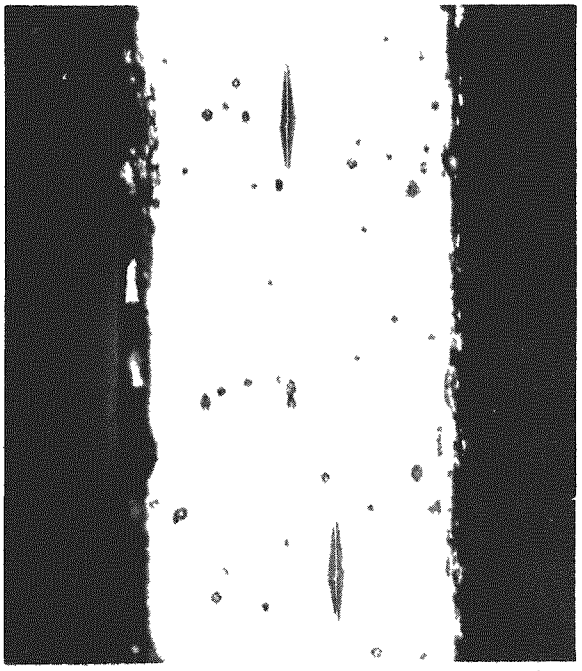

465X N48734

b. Iron-45 w/o Chromium-0.5 w/o Aluminum

Knoop Hardness 1275

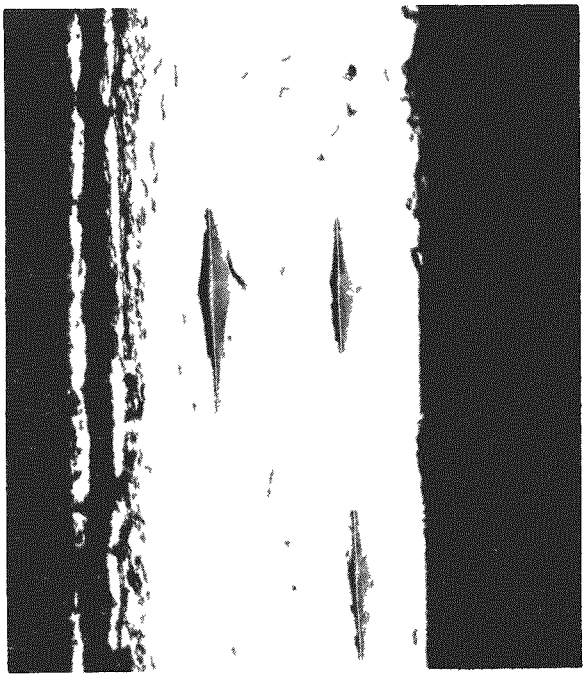

465X N48728

c. Iron-42.5 w/o Chromium-0.75 w/o Aluminum

Knoop Hardness 558

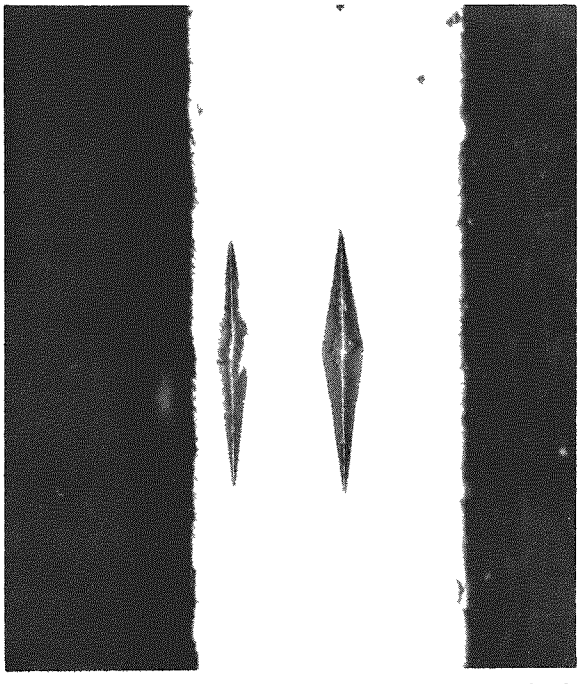

465X N48732

d. Iron-40 w/o Chromium-1 w/o Aluminum

Knoop Hardness 360

FIGURE 11. SIGMA- AND ALPHA-PLUS-SIGMA-PHASE STRUCTURES IN TERNARY ALLOYS HEATED 720 HR AT 650 C AND WATER QUENCHED

Oxalic Acid Etch.

iron-60 w/o chromium alloy contains only alpha. A small particle of sigma near the center of the specimen shown in Figure 10d is responsible for the distorted hardness impression.

The microstructures appearing in Figure 11 are a series of alloys which lie on a line radiating out from the iron-50 w/o chromium composition. Both of the specimens shown in Figures 11a and 11b contain sigma. Pitting of the sigma phase by the oxalic acid etchant employed is evident. In Figure 11c, sigma is the matrix phase with the alpha remaining enveloped in sigma. In Figure 11d, sigma appears primarily near the specimen surface, the structure consisting principally of alpha.

The X-ray identification of sigma is reported in Table 1. It will be noted that in some cases where sigma was observed metallographically the amount present was insufficient for detection by X-ray analysis.

The aging characteristics of predominantly sigma-phase alloys were studied. Specimens were aged at 700 C for times up to 5000 hr. The results are summarized in Figure 12.

The hardness curves are seen to fall into two groups. In the one group hardness increases rapidly and reaches a maximum within approximately 100 hr, showing little change thereafter, except for fluctuations assignable to experimental technique. These are the binary iron-46.25 w/o and -47.5 w/o chromium alloys. In the second group, little change in hardness is noted until after 100 hr, at which point hardness begins to increase gradually and continues to increase up to 5000 hr.

Microstructures taken showing the gradual transformation of the iron-47.5 w/o chromium-1 w/o aluminum alloy are shown in Figure 13. After 10 and 100 hr, only the alpha phase is present. However, after 1000 hr the structure consists of a sigma matrix and alpha islands. The amount of alpha present shows a further decrease after 2000 hr. Cracks through the sigma phase are seen to stop at the alpha grain boundaries.

On the basis of these results it may be concluded that the rate of transformation of alpha to sigma is decreased considerably by additions of aluminum.

The effect of cold work on sigma formation was also investigated. Hardness data illustrating the effect of cold reduction and time on hardness, indicative of sigma formation, are given in Table 2. There is a marked difference in behavior between material which is hot rolled and then annealed at 700 C and material which is cold reduced either 90 or 98 per cent prior to annealing at 700 C. The difference between material receiving either 90 or 98 per cent cold work is not as great, although the effect of the greater reduction can be noted in some cases. Thus the iron-50 w/o chromium and iron-46.25 w/o chromium-1.25 w/o aluminum specimens which had been cold reduced 98 per cent and annealed for 480 hr at 700 C show substantially higher hardnesses than do their companion specimens which were cold reduced 90 per cent.

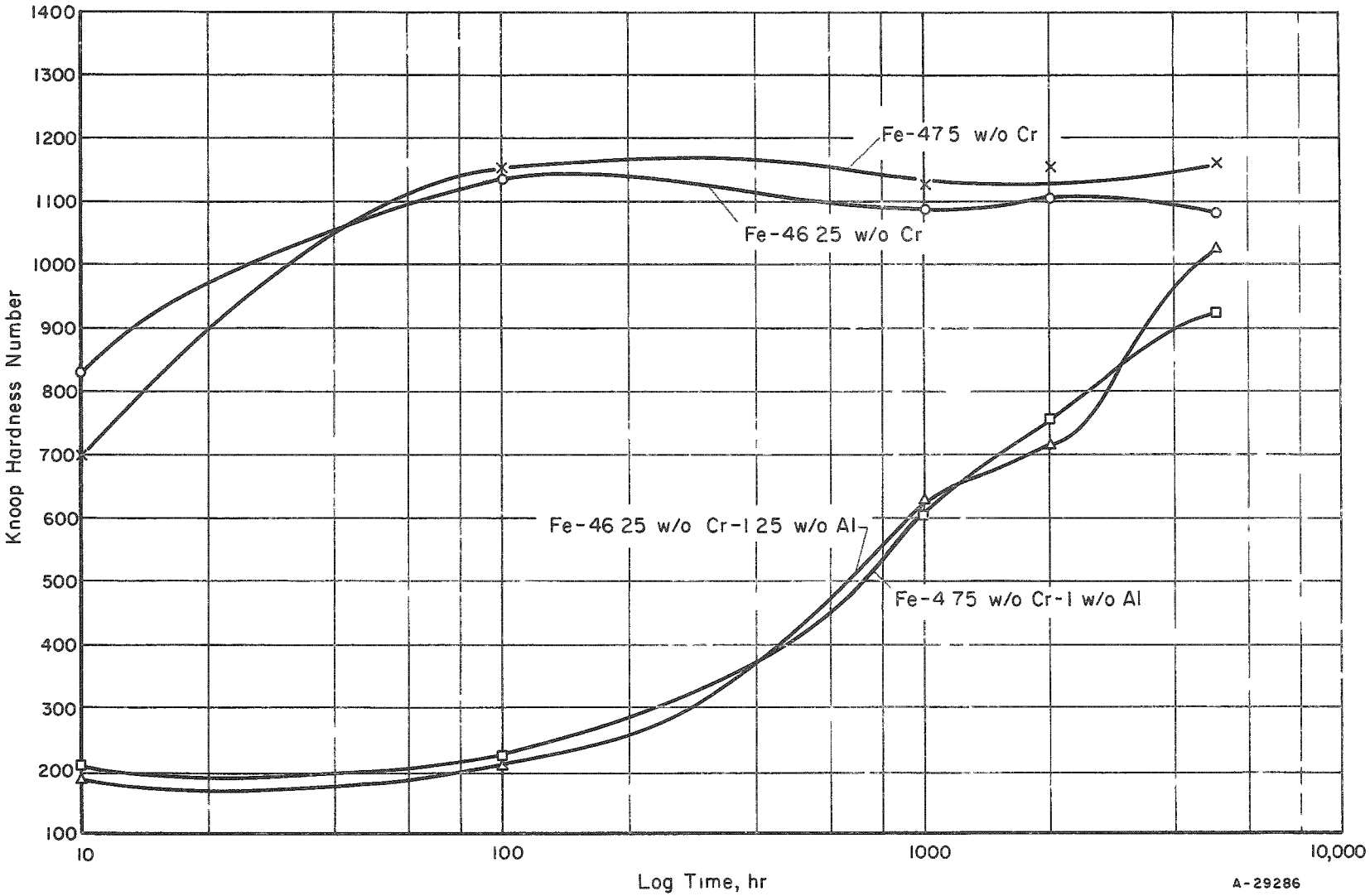

FIGURE 12. HARDENING CHARACTERISTICS OF IRON-CHROMIUM AND IRON-CHROMIUM-ALUMINUM SIGMA-PHASE ALLOYS AT 700 C

1000X N43167

a. 10 Hr at 700 C

Knoop Hardness, 210
Alpha Structure

1000X N43172

b. 100 Hr at 700 C

Knoop Hardness 228
Alpha Structure

1000X N43177

c. 1000 Hr at 700 C

Knoop Hardness 606
Alpha-plus-Sigma Structure

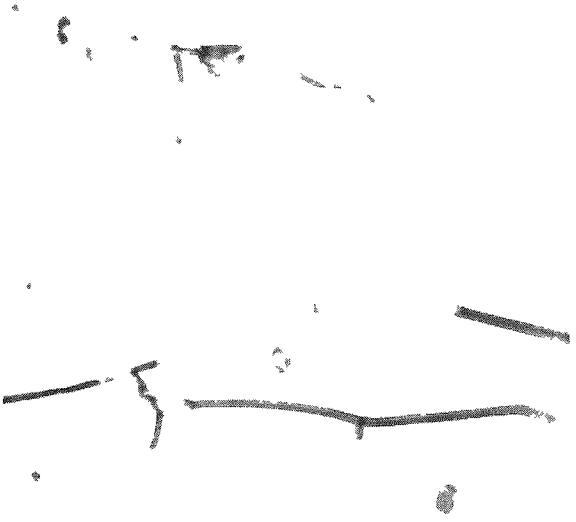

1000X N43182

d. 2000 Hr at 700 C

Knoop Hardness 757
Alpha-plus-Sigma Structure

FIGURE 13. CHANGES IN STRUCTURE AND HARDNESS OF IRON-47.5 w/o CHROMIUM-1 w/o ALUMINUM ALLOY WITH TIME AT 700 C

Oxalic Acid Etch.

TABLE 2. EFFECT OF COLD WORK ON RATE OF TRANSFORMATION TO SIGMA

Composition, w/o			Knoop Hardness After Annealing at 700 C for Time Indicated								
			240 Hr			480 Hr			2400 Hr		
				90	98		90	98		90	98
Fe	Cr	Al	Hot Rolled	Per Cent Reduction	Per Cent Reduction	Hot Rolled	Per Cent Reduction	Per Cent Reduction	Hot Rolled	Per Cent Reduction	Per Cent Reduction
60	40	--	373	1098	978	613	1148	1105	953	1167	1008
62.5	37.5	--	203	189	210	212	182	203	306	647	633
65.0	35.0	--	197	179	176	170	198	178	181	205	244
50	50	--	181	379	475	296	558	944	367	813	839
52.5	47.5	--	812	1251	1225	1106	1312	1193	1256	1166	1186
53.75	46.25	--	394	693	1169	1282	1252	1206	1219	1287	1230
51.5	47.5	1.0	264	248	240	273	295	--	263	793	799
57.5	46.25	1.25	249	242	255	255	236	543	477	905	877

Alpha-Phase Alloys

The aluminum-rich limits of the single-phase alpha region are shown in Figures 4 through 8. No variation in the limits was detected between 500 and 750 C; at 900 C the alpha region expanded slightly in chromium-rich alloys as $AlCr_2$ decomposed between 750 and 900 C.

Tentative phase regions have been sketched on the diagrams. While the alpha-phase limits are based primarily upon metallographic examination, the phase regions shown are based upon X-ray diffraction identification as reported in Table 1 and shown in Figures 4 through 8. The "Al_9Cr_4" phase is of doubtful identity, insufficient information being available to specify its stoichiometry. The $AlCr_2$-phase identification is based upon comparison with available standards and its similarity to the U_2Mo phase, which has a tetragonal (AlB_2 type) structure. FeAl is identified as a body-centered-cubic phase of the CsCl (B-2) type. No higher iron compounds were identified. The indicated solubility range for $AlCr_2$ is based upon observed variations in lattice parameter for this phase with variations in composition.

Insufficient data are available to completely specify the ternary-phase relationships in the high-aluminum alloys. For this reason, while the relationships shown are regarded as probable, the phase boundaries can not be located exactly.

While X-ray data were obtained only at 650 or 750 C, the lack of pronounced microstructural change between 500 and 750 C indicates little change in phases present over the latter temperature range. Consequently, phase-identification data are shown in Figures 4 through 7 independently of temperature. At 900 C, only a single specimen was examined by X-ray diffraction techniques, an iron-35 w/o chromium-30 w/o aluminum alloy which was found to consist primarily of alpha, although metallographically the structure contained three phases. At 700 C this same alloy contained alpha, $AlCr_2$, and FeAl. Since $AlCr_2$ was found to decompose between 750 C and 900 C and no evidence for the decomposition of either FeAl or Al_9Cr_4 was obtained, the phase relationships shown are inferred as being the most probable.

In considering the X-ray data it should be realized that X-ray detection of small amounts of a second or third phase is not always obtained. Consequently, while in some cases only a single phase is reported by X-ray, two or three phases may actually be present. In such cases, metallographic examination is necessary and provides the additional information required in specifying the phase region involved.

Metallographic structures of high-aluminum alloys are shown in Figures 14 and 15. Figures 14a through 14e show binary alloy structures. The iron-28 w/o aluminum alloy, Figure 14a, consists of single-phase alpha, while the matrix of the iron-34 w/o aluminum alloy, Figure 14b, consists of FeAl. The second phase was not identified, but its appearance suggests a compound, possibly $FeAl_2$. The structure of the latter alloy showed little change between 600 and 900 C aside from a slight coarsening of the second-phase particles at higher temperatures. The coarse particles appearing in the structure shown were produced during the homogenization anneal at 900 C prior to heat treatment at 700 C. In Figure 14c is shown the microstructure of the chromium-20 w/o aluminum alloy after annealing at 600 C. Between 600 and 750 C the only change

500X N49077

a. Iron-28 w/o Aluminum Heated 250 Hr at 650 C and Water Quenched

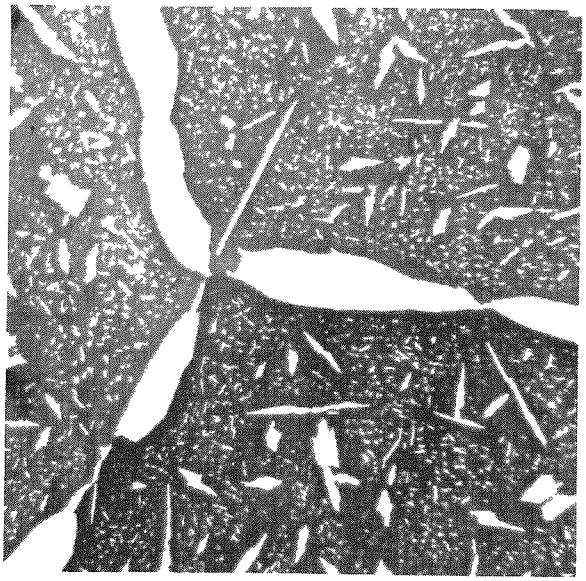

500X N50640

b. Iron-34 w/o Aluminum Heated 250 Hr at 650 C and Water Quenched

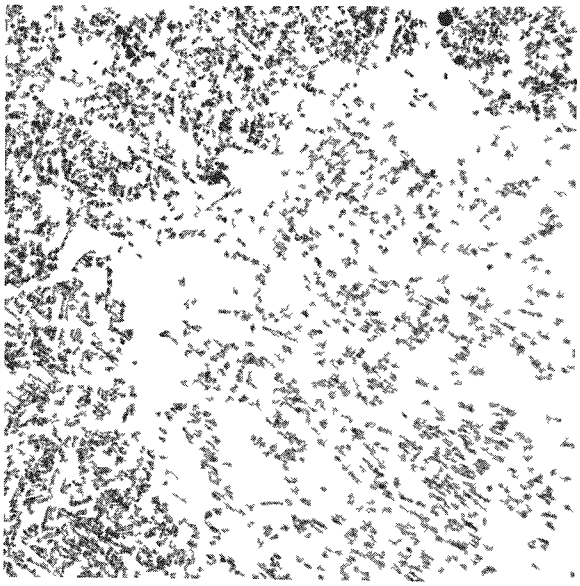

500X N50643

c. Chromium-20 w/o Aluminum Heated 250 Hr at 600 C and Water Quenched

FIGURE 14. BINARY IRON-ALUMINUM AND CHROMIUM-ALUMINUM ALLOYS

Oxalic Acid Etch.

250X RM10060

d. Chromium-20 w/o Aluminum Heated 100 Hr at 900 C and Water Quenched

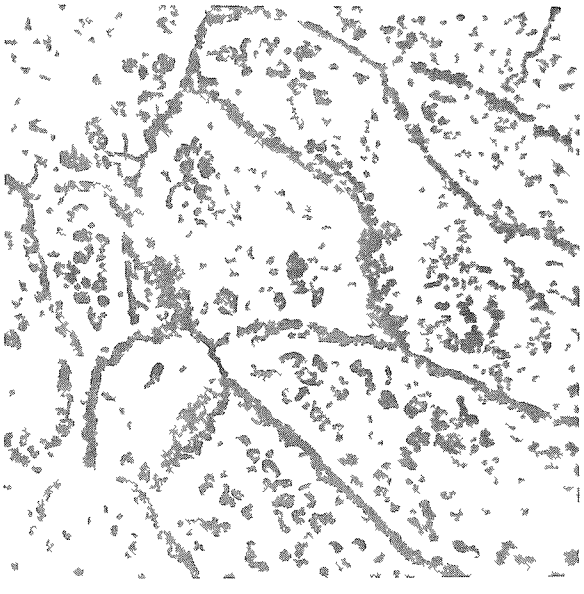

250X RM10062

e. Chromium-28 w/o Aluminum Heated 100 Hr at 900 C and Water Quenched

FIGURE 14 (CONTINUED)

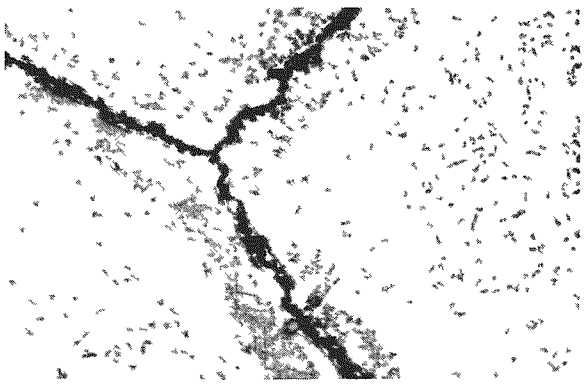

250X N50646

a. Iron-37.5 w/o Chromium-25 w/o Aluminum Heated 1000 Hr at 700 C and Water Quenched

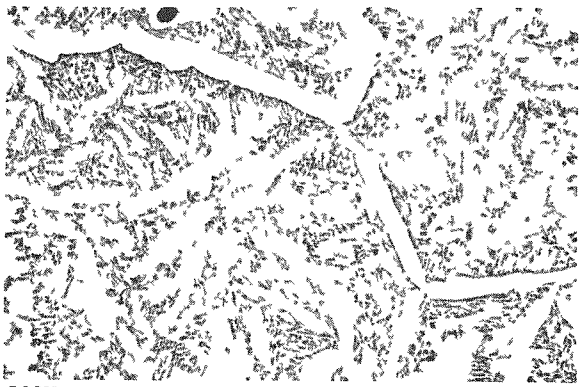

500X N50650

b. Iron-35 w/o Chromium-30 w/o Aluminum Heated 250 Hr at 700 C and Water Quenched

500X N49080

c. Iron-70 w/o Chromium-15 w/o Aluminum Heated 200 Hr at 750 C and Water Quenched

500X N50641

d. Iron-61 w/o Chromium-24 w/o Aluminum Heated 200 Hr at 750 C and Water Quenched

500X N49078

e. Iron-20 w/o Chromium-25 w/o Aluminum Heated 500 Hr at 700 C and Water Quenched

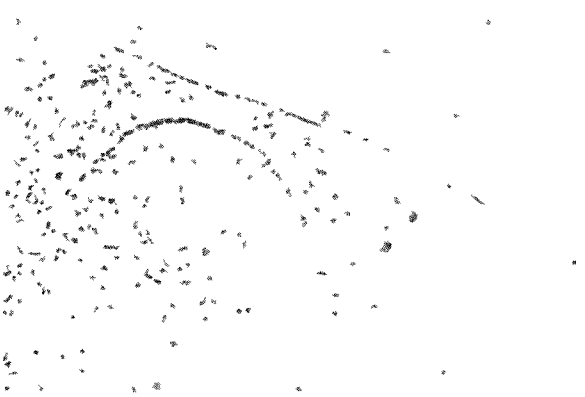

500X N50649

f. Iron-20 w/o Chromium-30 w/o Aluminum Heated 200 Hr at 700 C and Water Quenched

FIGURE 15. STRUCTURES OF TERNARY IRON-CHROMIUM-ALUMINUM ALLOYS

Oxalic Acid Etch.

produced was a coarsening of the phase particles. However, at 900 C this alloy is single-phase alpha (See Figure 14d), a result of $AlCr_2$ decomposition between 750 and 900 C. A chromium-28 w/o aluminum alloy (Figure 14e) contains two phases at 900 C.

Ternary alloy structures appear in Figure 15.

In Figures 15a and 15b the structures of the iron-37.5 chromium-25 w/o aluminum and iron-35 w/o chromium-30 w/o aluminum alloys consist, respectively, of alpha, FeAl, and $AlCr_2$ and of FeAl, $AlCr_2$, and Al_9Cr_4. Figures 15c and 15d illustrate the alpha-phase boundary between an iron-70 w/o chromium-15 w/o aluminum alloy, which is single-phase alpha, and an iron-61 w/o chromium-24 w/o aluminum alloy which contains alpha and $AlCr_2$. Similarly, an iron-20 w/o chromium-25 w/o aluminum alloy is single-phase alpha (Figure 15e), while an iron-20 w/o chromium-30 w/o aluminum alloy contains alpha and FeAl (Figure 15f).

Sigma-Phase Instability Below 600 C

Alloys in the sigma-phase composition range were annealed at temperatures of 480, 500, and 550 C to study the aging characteristics of these alloys at temperatures below 600 C. All evidence indicates that sigma is unstable at these temperatures. Hardness increases accompanying the low-temperature anneals were noted, but these increases were not within the range which accompanies the formation of sigma. Furthermore, specimens annealed for 1000 or 2200 hr at 500 C showed essentially the same hardnesses, indicating that a hardness plateau had been reached. X-ray examination of specimens annealed for up to 2200 hr at 500 C revealed only a strong alpha pattern and metallographically only alpha was observed.

Typical hardness data for alloys annealed at 480 and 500 C are given in Table 3. Little difference in hardness can be noted for alloys annealed either for 1000 or 2200 hr at 500 C. In order to determine if cold-worked specimens responded differently from annealed specimens, one set of specimens was annealed at 800 C to recrystallize the initially cold-worked alpha phase prior to annealing at 500 C. As shown in Table 3, very little difference can be noted, indicating substantially the same behavior for either type of material. In examining the hardness data it should be realized that the hardness of untreated alpha-phase material of the compositions listed is on the order of 200 KHN. Thus, substantial increases in hardness have resulted from the low-temperature heat treatments.

A further indication of the instability of sigma at low temperatures was obtained from a group of alloys initially annealed at 700 C to produce the sigma phase and subsequently reannealed at temperatures of 480 to 550 C. Hardness data are given in Table 4. Typical sigma hardness values were obtained after the 700 C heat treatment while heat treatment at the lower temperatures resulted in decreased hardnesses indicative of sigma-phase decomposition.

Metallographic changes accompanying this type of treatment are shown in Figures 16a and 16b. The sigma phase developed after a heat treatment of 720 hr at 650 C is shown in Figure 16a and has an average hardness of 1280 KHN. A specimen heat treated at 650 C for 1000 hr had an average hardness of 1200 KHN. After an additional treat-

TABLE 3. HARDNESS OF IRON-CHROMIUM-ALUMINUM ALLOYS AFTER HEAT TREATMENT AT 480 AND 500 C

Composition, w/o			Knoop Hardness After Heat Treatment Indicated			
			Annealed at 500 C			Annealed at 480 C
Fe	Cr	Al	1000 Hr[a]	2200 Hr[a]	1000 Hr[b]	for 2200 Hr[a]
50.0	50.0	--	541	502	513	541
52.5	47.5	--	590	515	543	402
53.75	46.25	--	531	504	490	511
51.5	47.5	1.0	556	432	493	473
52.5	46.25	1.25	526	466	488	472
60.0	40.0	--	433	410	466	460
62.5	37.5	--	494	388	431	356
65.0	35.0	--	360	382	415	356
51.0	48.0	1.0	568	521	471	485
47.5	52.5	--	--	449	--	522
45.0	55.0	--	--	527	--	520
47.5	51.75	0.75	--	563	--	574
45.0	53.25	1.75	--	580	--	619

(a) Specimens annealed at 480 or 500 C in the cold-worked condition.
(b) Specimens annealed at 800 C for 1 hr before annealing at 500 C.

TABLE 4. EFFECT OF LOW-TEMPERATURE HEAT TREATMENT ON HARDNESS OF SIGMA-PHASE ALLOYS

Composition, w/o			Knoop Hardness After	Additional Heat Treatment		Final Knoop
Fe	Cr	Al	700 C Treatment	Time, hr	Temperature, C	Hardness
50.	50.	--	941	1000	550	755
47.5	52.5	--	1256	1500	480	917
46.25	53.75	--	1219	1200	500	838
40.	60.	--	824	1200	500	806
47.5	52.25	0.75	1178	1000	550	711

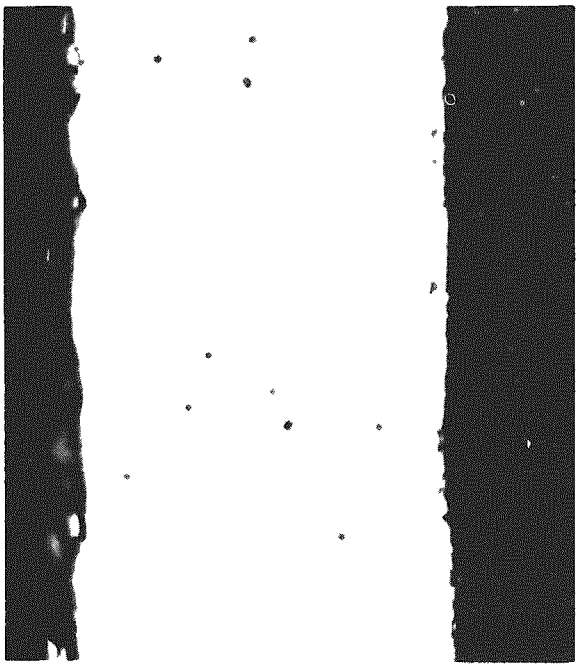

500X N51356

a. Iron-46.25 w/o Chromium Heated 720 Hr at 650 C and Water Quenched

Knoop Hardness: 1280

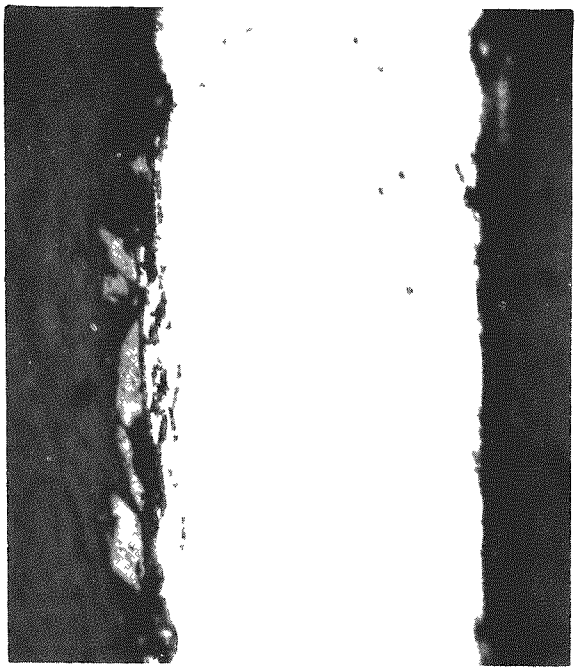

500X N51091

b. Iron-46.25 w/o Chromium Heated 1000 Hr at 650 C and Water Quenched, 1200 Hr at 500 C and Water Quenched

Knoop Hardness: 610

500X N50957

c. Iron-50 w/o Chromium Heated 1600 Hr at 500 C and Water Quenched

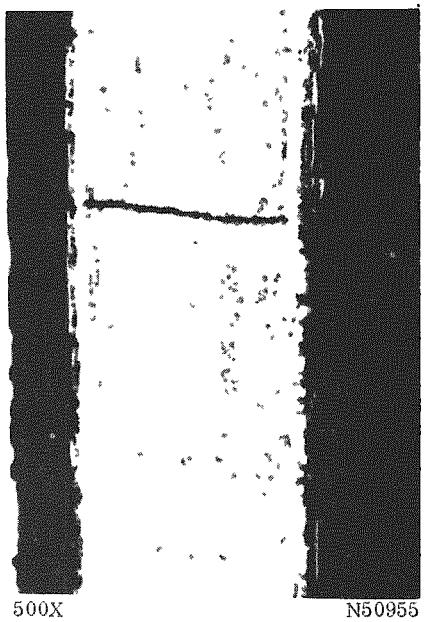

500X N50955

d. Iron-50 w/o Chromium Heated 1600 Hr at 500 C and Water Quenched, 400 Hr at 700 C and Water Quenched

FIGURE 16. STRUCTURES OF SIGMA-PHASE ALLOYS ACCOMPANYING HEAT TREATMENTS AT 500 AND 700 C Oxalic Acid Etch.

ment of 1200 hr at 500 C the hardness decreased to 610 KHN and had the structure shown in Figure 16b. The matrix phase is sigma and the second-phase particles are alpha or modified alpha as identified by relative hardnesses of the two phases. These photomicrographs and hardness data constitute substantial evidence suggestive of sigma-phase decomposition.

In order to determine if the transformation was reversible, a second specimen was annealed first at 500 C for 1600 hr and then heated to 700 C for 400 hr. Resultant microstructures appear in Figures 16c and 16d, respectively. After treatment at 500 C, only a cold-worked alpha structure is apparent. However, on annealing at 700 C sigma forms in the alpha matrix. These results indicate the reversible formation and decomposition of sigma above and below 600 C, respectively.

Summary and Discussion

The limits of the sigma-, alpha-plus-sigma-, and alpha-phase regions have been determined for the iron-chromium-aluminum system. While direct comparison with the results of Kornilov[15] is not possible since his data are incompletely available, fairly general agreement with the form and phase limits shown in his room-temperature ternary section was obtained. The ternary-phase relationships in high-aluminum alloys have been tentatively outlined as a result of this program in a more complete fashion than by Kornilov. One area of agreement in these regions is the apparent extensive solubility of iron in the Cr_2Al phase, although the exact extent cannot be specified at this time.

The limits of the alpha-plus-sigma region in binary alloys were found to be considerably more restricted than those reported by Cook and Jones[10], who reported values of 24 w/o chromium, and between 60 and 67 w/o chromium at 600 C for the iron- and chromium-rich boundaries, respectively. In this investigation, using high-purity materials, values of about 33 and 63 w/o chromium, respectively, were obtained at 600 C. As noted by other investigators[11,12], common impurities found in iron, such as silicon and manganese, can cause extension of this phase region.

Evidence has been obtained that sigma is unstable below 600 C. No evidence for the formation of sigma at temperatures of 480 to 550 C was obtained. Further, sigma formed at higher temperatures was found to decompose at these lower temperatures. The formation and decomposition of sigma above and below 600 C was found to be reversible. These results are in agreement with those of Williams and Paxton[17,18], who have reported that sigma is unstable at low temperatures. However, the nature of the reaction below 600 C was not determined in the present study, although a hardness increase was found to accompany low-temperature annealing treatments. No evidence of a phase change was detected either metallographically or by X-ray diffraction analysis to account for the hardness increase. Williams and Paxton suggest a process involving the formation of two coherent alpha phases, one chromium-rich the other iron-rich, at low temperatures. This process may account for both the hardness increases observed and the inability to detect any observable phase changes.

PHYSICAL METALLURGICAL STUDIES OF IRON-CHROMIUM-ALUMINUM ALLOYS

Background

Although there are a number of commercial iron-chromium-aluminum alloys, virtually all previous work on the metallurgical and mechanical properties of these alloys was done by I. I. Kornilov[1,15]. A study involving about six alloys of different compositions was reported recently by J. E. Srawley[7]. The commercial alloys, Kanthal (iron-25 w/o chromium-5 w/o aluminum-3 w/o cobalt) and Smith No. 10 (iron-37.5 w/o chromium-7.5 w/o aluminum), are used extensively in this country for electrical-heating elements. These alloys have high electrical resistivities and are oxidation resistant to higher temperatures than nickel-chromium-iron alloys. Unfortunately, the iron-chromium-aluminum alloys are based on body-centered-cubic iron (ferrite) and as a result they are extremely weak at elevated temperatures, and if unsupported tend to sag under their own weight. This weakness causes designers to request alloys of higher and higher alloy contents and this results in alloys of lower fabricability and lower room-temperature ductility.

Published information on the fabrication and mechanical properties of iron-chromium-aluminum alloys is summarized in Figures 17 through 21. Kornilov's data are shown in Figures 17, 18, 20, and 21. Srawley's recent data[7] are shown in Figure 19. In general, Kornilov's alloys were based on low-carbon steel and typically contained 0.02 to 0.10 w/o carbon, 0.3 to 1.0 w/o silicon, plus manganese, sulfur, phosphorus, and unknown amounts of nitrogen. For alloys of this purity, he found that the impact transition temperature was raised above room temperature by binary additions to iron of about 20 w/o chromium or about 5 w/o aluminum. By comparison of Figure 20 with Figure 17, it is apparent that the impact transition temperature can be raised considerably above room temperature by addition of aluminum and chromium before cold fabricability is completely lost.

Figures 18 and 19 demonstrate the effect of temperature upon the strength and ductility of iron-chromium-aluminum alloys prepared by Kornilov and Srawley. Above about 500 C, these alloys lose strength rapidly and their strength is more properly defined for engineering purposes by stress-rupture or creep data. The elongation data in Figures 18 and 19 and the impact data of Figure 20 show that these alloys of commercial purity were subject to the "blue-brittleness" phenomenon in the temperature interval from 300 to 600 C. Blue brittleness has been attributed to precipitation effects caused by the presence of very small amounts of carbon, nitrogen, or oxygen in ferrite.[22] These impurities have also been related to a variety of other deformation phenomena in ferrite such as "quench aging", "strain aging", and upper and lower yield phenomena. Figure 20 suggests that blue brittleness in Kornilov's alloys may have been caused by carbon since the blue brittleness disappears at a lower temperature in the lower carbon alloy. Srawley's alloys were purer than Kornilov's, containing on the order of 0.01 w/o carbon and 0.1 w/o manganese. The lower strength and higher ductility of Srawley's alloy described in Figure 19 reflects this higher purity. The higher ductility of Srawley's alloy in the temperature interval from 300 to 600 C tends to support the contention that carbon is responsible for the blue brittleness of these alloys.

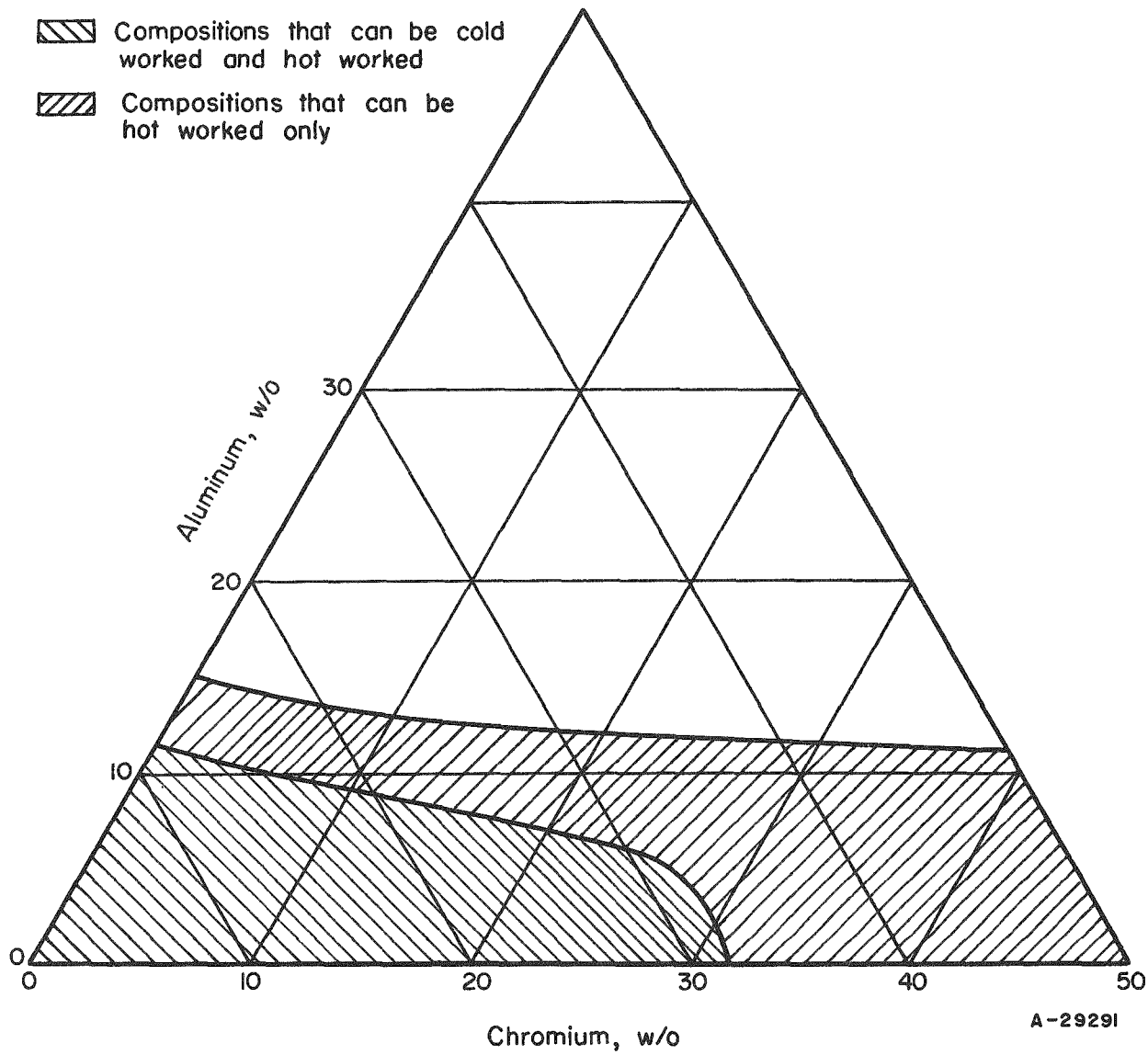

FIGURE 17. FABRICABILITY LIMITS OF IRON-CHROMIUM-ALUMINUM ALLOYS ACCORDING TO KORNILOV[1, 15]

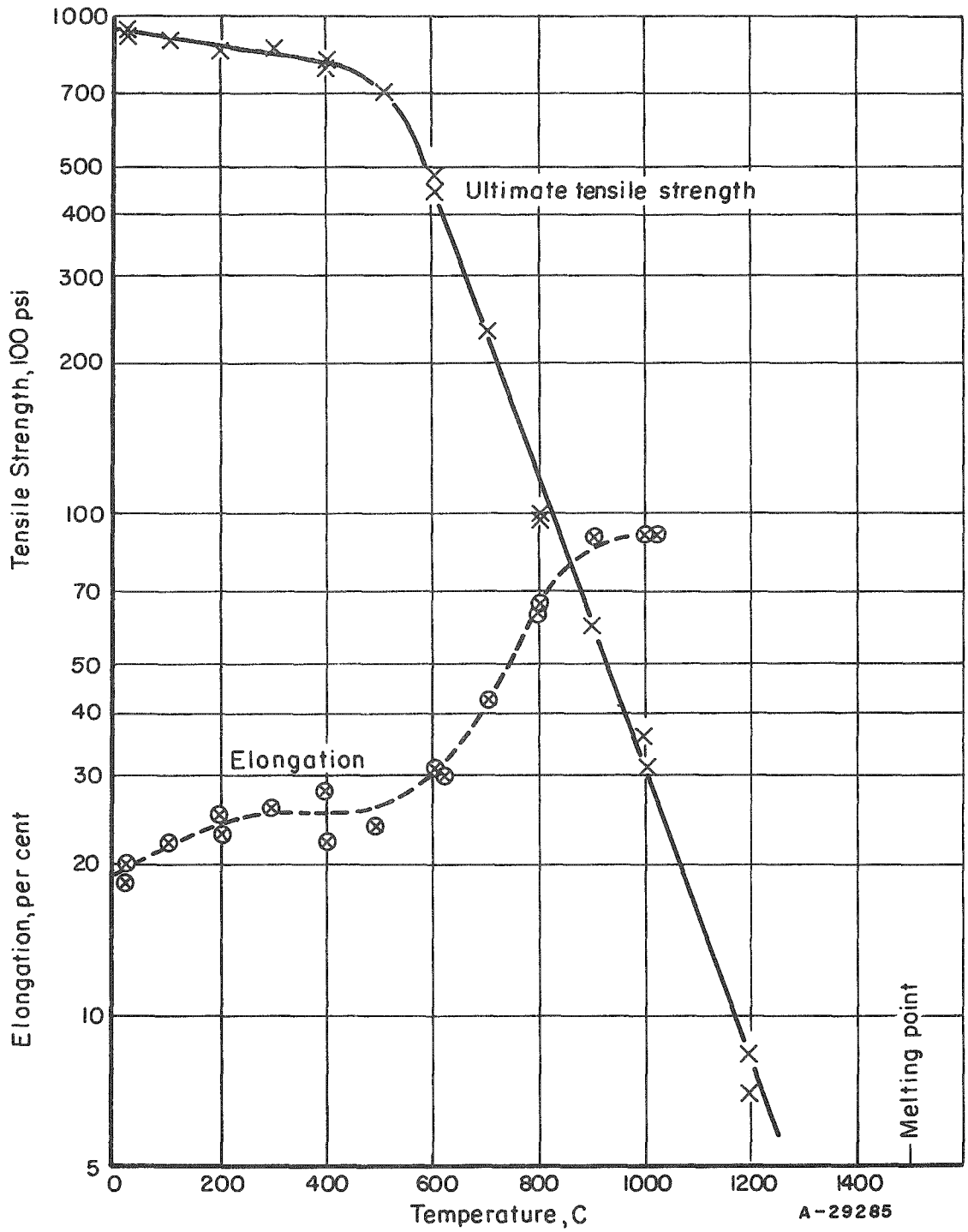

FIGURE 18. TENSILE PROPERTIES OF IRON-17 TO 25 w/o CHROMIUM-5 w/o ALUMINUM ALLOYS ACCORDING TO KORNILOV[1, 15]

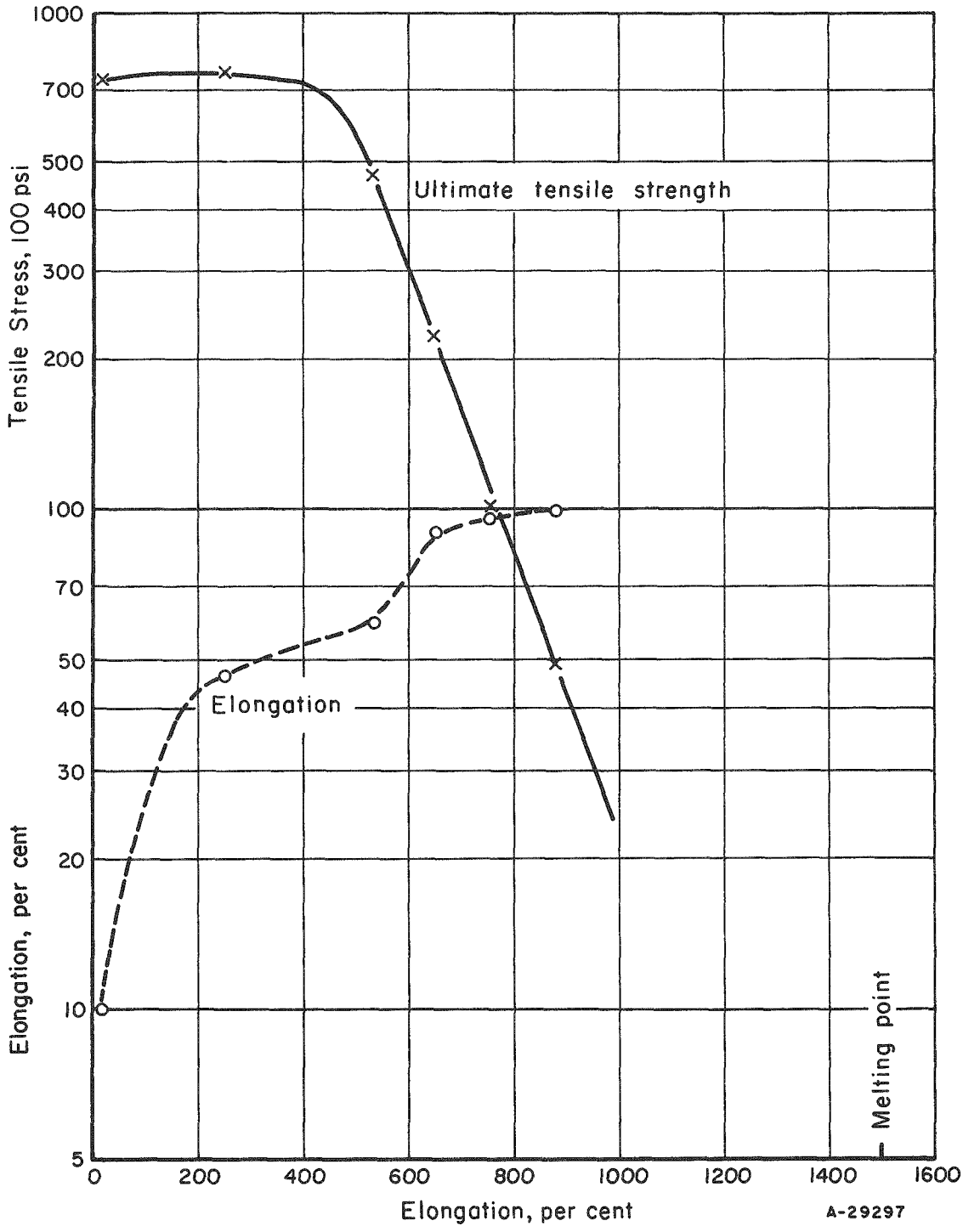

FIGURE 19. TENSILE PROPERTIES OF VACUUM-MELTED IRON-26 w/o CHROMIUM-6 w/o ALUMINUM ALLOY ACCORDING TO SRAWLEY[7]

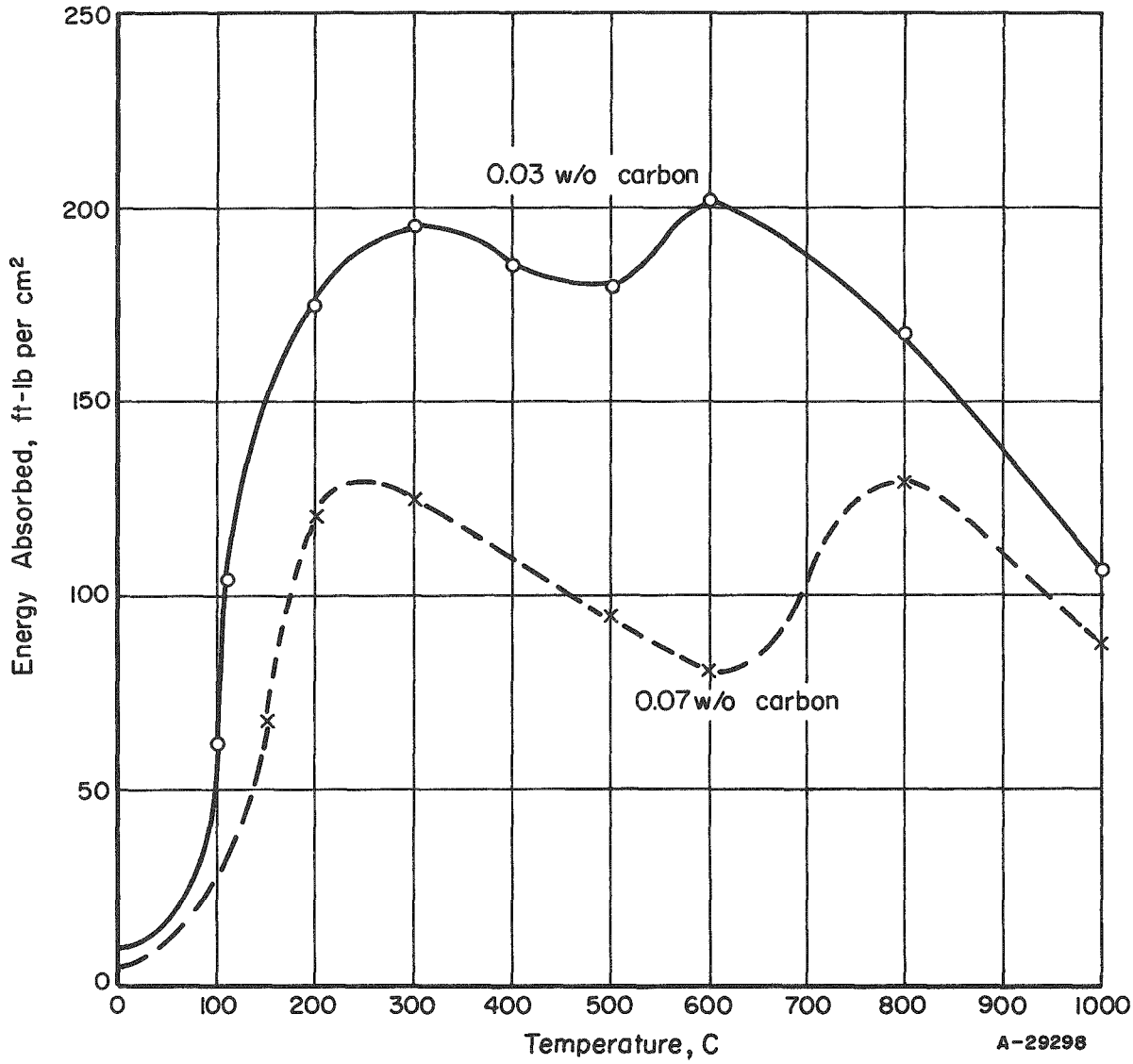

FIGURE 20. EFFECT OF CARBON ON THE IMPACT STRENGTH OF IRON-25 w/o CHROMIUM-5 w/o ALUMINUM ALLOY ACCORDING TO KORNILOV[1, 15]

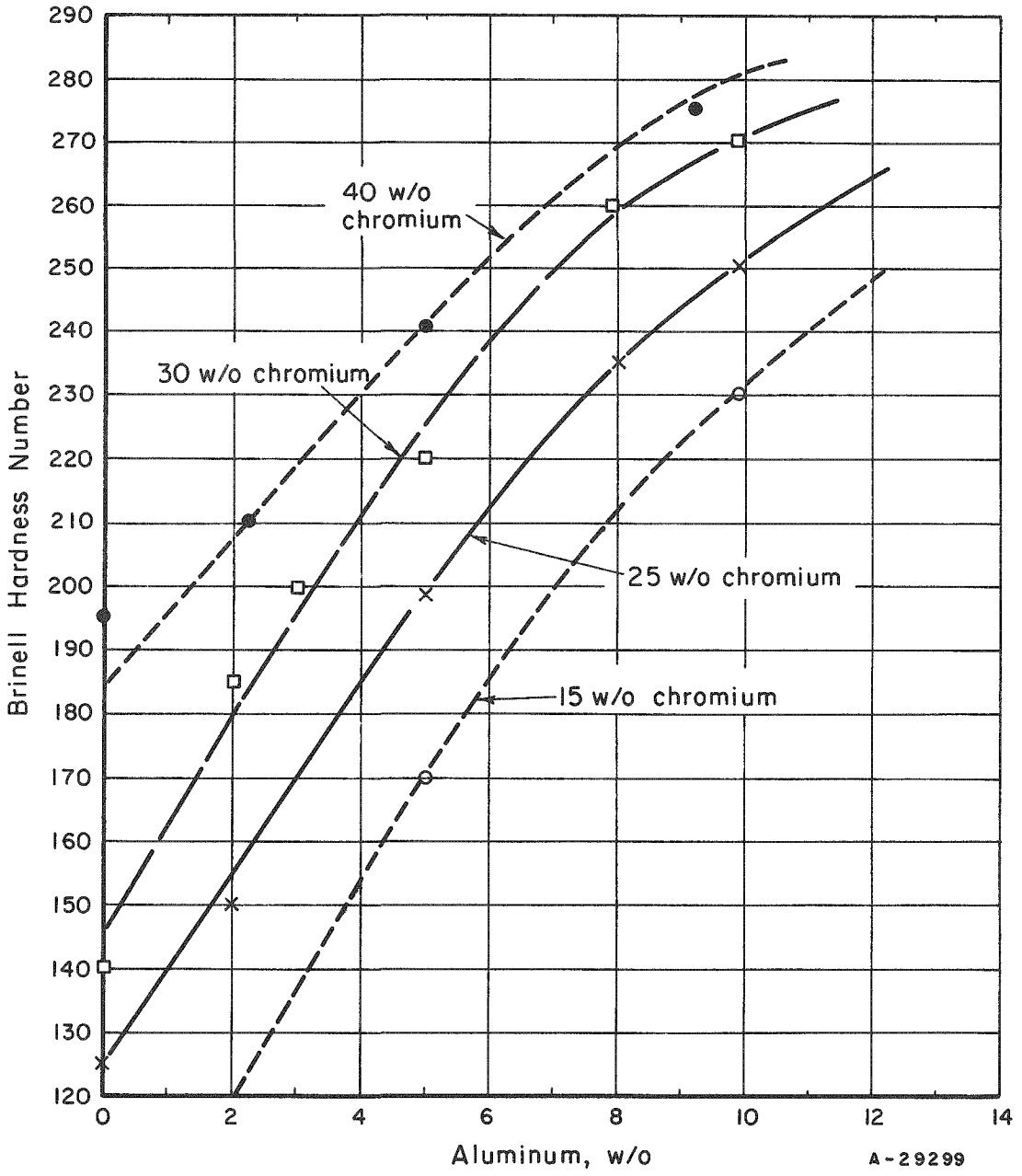

FIGURE 21. HARDNESS OF IRON-CHROMIUM-ALUMINUM ALLOYS AS A FUNCTION OF COMPOSITION ACCORDING TO KORNILOV[1, 15]

Figure 21 shows Kornilov's data for the effect of chromium and aluminum upon the hardness of ferrite.[15] On the basis of these data, it is not too surprising to find that aluminum increases the strength and decreases the ductility of ferrite with increasing composition at a rather rapid rate. Changes in chromium content affect the properties of ferrite somewhat more slowly.

Much has been written and said about brittleness in the body-centered-cubic metals: iron, chromium, molybdenum, niobium, and vanadium. Oxygen is reported to by the major source of embrittlement of molybdenum[23]. Wain, Henderson, and Johnstone[24] and Abrahamson and Grant[25] report that nitrogen embrittles chromium. The brittle behavior of iron has been attributed to carbon, hydrogen, nitrogen, and oxygen, grain size, stress raisers, and impurities in and out of solution separately and in combination.[26,27] For vacuum-melted iron-chromium alloys, Ham and Carr found that the impact "transition temperature of quenched alloys in the 35 to 50 per cent chromium range depends on the composition of the solid solution rather than on the amount of oxide or the grain size. In the range from 35 to 50 per cent chromium, the ductile-to-brittle transition temperature can be predicted from the chromium, carbon, and nitrogen concentrations, and is independent of oxygen content up to at least 0.1 per cent."[28]

The iron-aluminum alloys have been studied in considerable detail.[29-34] It appears that by paying exceptional attention to metal cleanliness, ingot-cooling and -heating rates, and ingot breakdown, ductile iron-aluminum alloys containing 12 to 14 w/o aluminum may be obtained. In agreement with Kornilov's results for iron-chromium-aluminum alloys (Figure 20), Justusson, Zackay, and Morgan[34] found that carbon was very detrimental to the impact resistance of iron-14 w/o aluminum alloys, and that cast grain size could be greatly reduced by keeping the pouring temperature down to 1600 C, just a few degrees above the solidus. Zackay and Goering[33], on the other hand, emphasize the importance of removal of aluminum oxide dross from the melt, and of careful handling of the ingots to prevent internal cracking prior to rolling.

In addition to the above data, there have been a few more basic studies of the behavior of alloying elements in iron which have a bearing on the brittleness of iron-chromium-aluminum alloys. Rees reports that pure iron has an impact transition temperature of -10 C.[35] This is raised to 20 C by 37 ppm oxygen and to 90 C by 160 ppm oxygen, and at 2700 ppm oxygen the first visible iron oxide appears as distinct spheroidal particles. The transition temperature of iron containing 100 ppm carbon is -5 C; 300 ppm carbon raises the transition to 90 C, while 500 ppm carbon raises it only to 70 C. The addition of 2 w/o manganese to iron containing 300 ppm or 500 ppm carbon lowers the transition to -60 or -65 C. Gokcen and Chipman[36] investigated the aluminum-oxygen equilibria in iron and found that the activity of oxygen in iron is strongly reduced by the presence of aluminum. For example, in the presence of aluminum and essentially independent of the aluminum concentration, the solubility of oxygen in iron at 1600 C in the liquid state is about 7 ppm, and the indicated solubility of oxygen in solid iron containing only 100 ppm aluminum at 1260 C is about 0.02 ppm. It should be clear that if the aluminum oxide dross formed on and in iron-aluminum alloys can be removed to a satisfactorily low level to achieve metal cleanliness in the liquid state, then oxygen can be disregarded as a possible source of brittleness in these alloys.

Green and Brick[37] studied the flow and fracture stresses of ferrites containing up to 2.4 w/o aluminum and concluded that as much as 0.2 w/o silicon in aluminum ferrites acts only as another solute element and does not specifically embrittle iron under conditions of uniaxial static tensile deformation. They noted that in these alloys a change in mode of deformation occurred below about -100 C in static tension tests. This change in mode of deformation was associated with decreased ductility, the appearance of mechanical twinning, and lowering of the fracture stress. In all alloys the fracture stress decreased with decreasing temperature until fracture occurred at the 0.2 per cent offset yield stress at about -185 C. It can be assumed that the impact transition temperature for these alloys occurs at some temperature well above -185 C, and that this transition also is associated with the same change in deformation behavior; i.e., the appearance of mechanical twinning and a lowering of the fracture stress.

Wessel[38] has prepared an extremely interesting mechanical model for the occurrence of preyield plastic deformation, abrupt yielding, and brittle fracture in mild steel, molybdenum, niobium, and tantalum. Unfortunately, this model is applicable only to those metals and alloys whose initial or limiting mode of deformation is by slip; i.e., those metals whose critical stress for deformation by slip is lower than their critical stress for deformation by twinning. Green and Brick[37] showed that at low temperatures, just above the brittle-ductile transition temperature, the major mode of plastic deformation was by twinning in iron-aluminum alloys. The present investigation indicates similar behavior for iron-chromium-aluminum alloys. Wessel's mechanism for the formation of cracks indicates that high local stresses are necessary to initiate cracking. This implies that the critical stress for cleavage and fracture is higher than the critical stress for plastic flow; this need not be the case. It is interesting to note that certain minerals, such as calcite, exhibit cleavage along certain very distinct crystallographic planes and that under certain conditions twinning can occur on these same crystallographic planes (the $0\bar{1}11$ plane in the case of calcite). If this is true of iron-aluminum ferrites, then the transition from twinning to cleavage can be regarded as a gradual and continuous lowering of the critical stress for cleavage toward the critical stress for twinning. This would account for the extremely strong dependence of ductility in these alloys upon grain size, strain rate, temperature, stress raisers, and stress conditions. Twinning is a rather massive and abrupt mode of deformation, and, as Chalmers[39] has observed in tetragonal tin, the propagation of strain across grain boundaries by twinning often is imperfect so that some separation of crystals usually occurs.* Either sufficiently large separation or the occurrence of such an event in the area of a brittle intergranular particle could lead to propagation of a macrocrack.. Large separation is most likely to occur in coarse-grained metal where orientations may be unfavorable for propagation of strain from one grain to the next.

Figure 22 is a simplified version of the iron-25 w/o chromium-5 w/o aluminum-carbon phase diagram.[15,40] In this diagram the horizontal lines represent three phase regions and have a slight upward or downward curvature toward the right. Figure 23 shows the solubility of hydrogen in iron at 1 atm of pressure.[41] The dashed line represents the hypothetical solubility for ferrite in the temperature range from 910 to 1400 C. This diagram makes it possible to predict that vacuum-melted iron and iron alloys will contain virtually no hydrogen. Figure 24 is a similar diagram describing the behavior of nitrogen in iron. This figure suggests that vacuum treatment of molten iron will reduce the nitrogen content to a low level; but it is not clear that vacuum treatment

*Chalmers did not associate or attribute the observed grain separation to twinning. However, it is well known that tin deforms by twinning at room temperature, producing the so-called tin "cry".

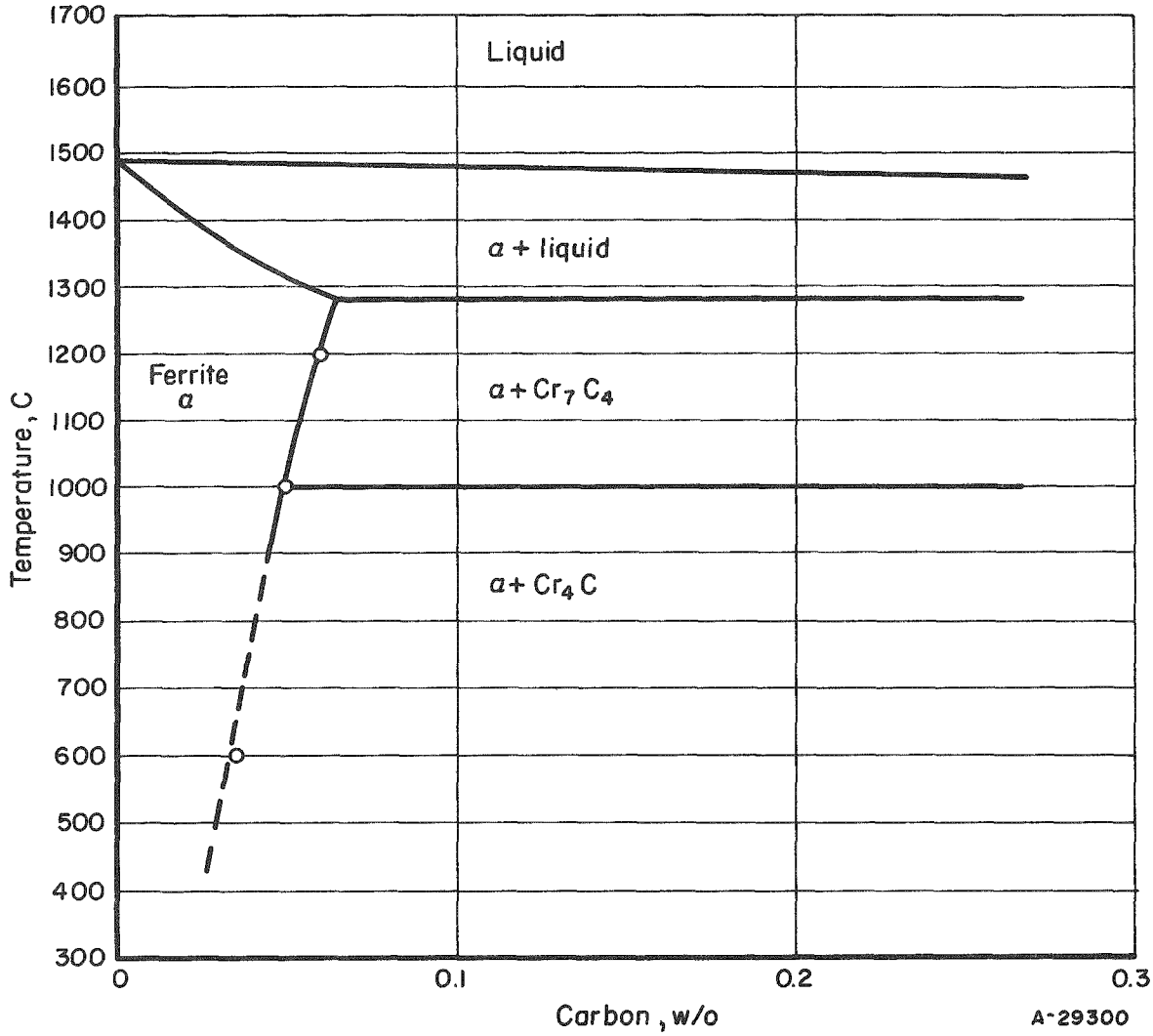

FIGURE 22. CONSTITUTION OF IRON-25 w/o CHROMIUM-5 w/o ALUMINUM-CARBON ALLOYS

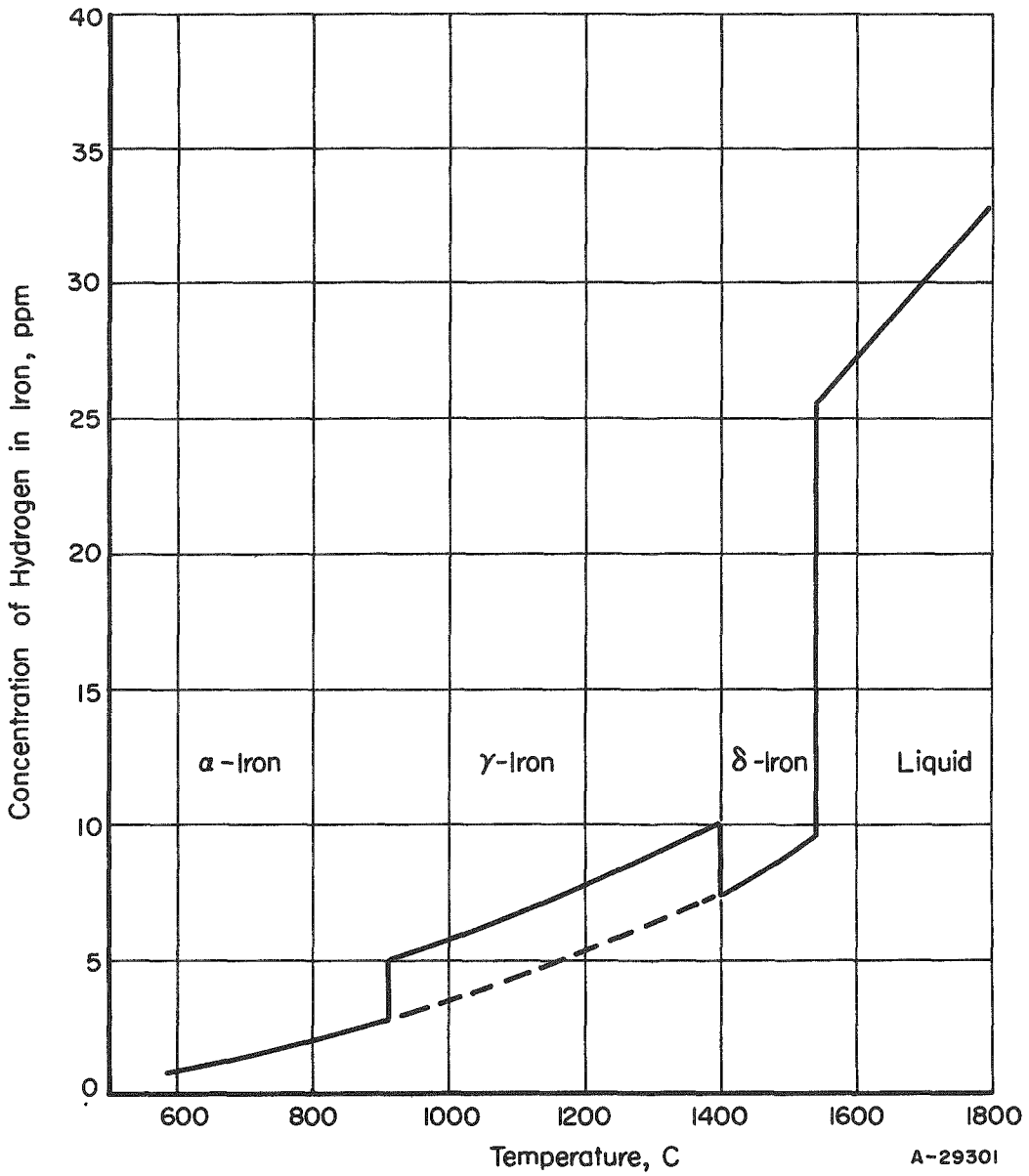

FIGURE 23. CONCENTRATION OF HYDROGEN IN IRON UNDER A 1-ATM PRESSURE OF HYDROGEN GAS

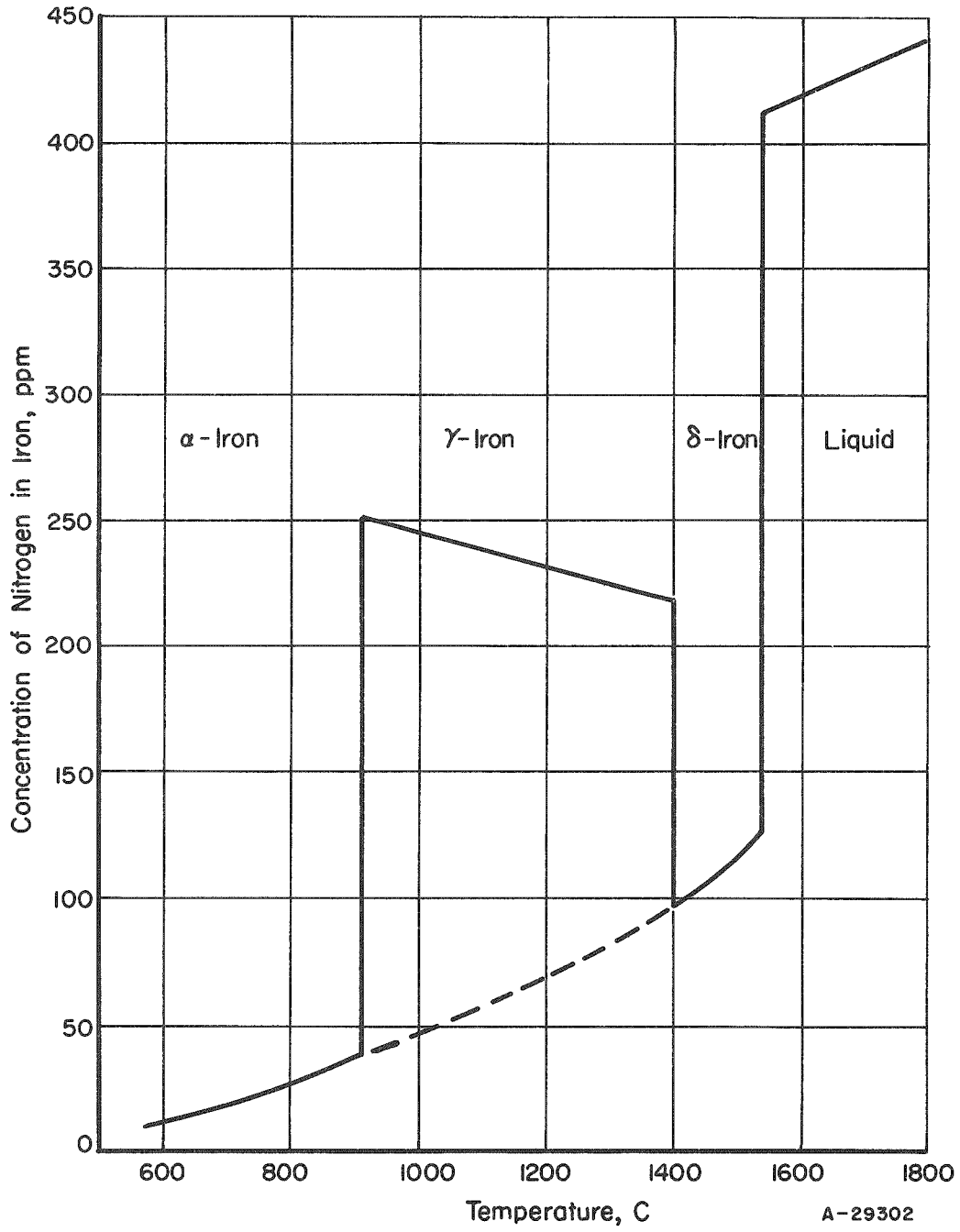

FIGURE 24. CONCENTRATION OF NITROGEN IN IRON UNDER A 1-ATM PRESSURE OF NITROGEN GAS

will reduce nitrogen to the level of insignificance, particularly in the presence of appreciable quantities of chromium and aluminum. It appears that carbon and nitrogen are the most likely contenders for the dubious honor of causing the blue-brittleness phenomenon and other low-temperature-ductility problems in iron-chromium-aluminum alloys.

Physical Metallurgical Studies

Iron-25 w/o Chromium-5 w/o Aluminum Alloy

From prior physical metallurgical studies on iron-25 w/o chromium-5 w/o aluminum alloys it was reported that "in some instances, quenching in water from 1300 to 1400 F (700 to 760 C) improves both hot and cold working characteristics".[4] This rather improbable statement suggests that the increase in ductility attributed to quenching was not reproducible and was, therefore, possibly a function of random, uncontrolled impurities or possibly a function of quenching rate. How water quenching from 700 C could affect subsequent hot-working characteristics at 900 C is inexplicable; perhaps the writers had reference to warm-working characteristics at temperatures below 700 C.

Initial physical metallurgical studies were performed on an iron-25 w/o chromium-5 w/o aluminum alloy melted in a vacuum in a magnesia crucible and cast as two 150-lb ingots. These were hot rolled to 1/8 in. at 1180 C and warm rolled to 1/16 in. at 260 C. The analyses obtained on this material are shown in Table 5. It is noteworthy that these analyses show that this alloy contains less residual impurities than usually specified for austenitic or ferritic high-chromium stainless steels. The manganese and silicon contents are somewhat higher than usually found in ingot iron, but the presence of these elements should be beneficial. Figure 25 shows microstructures of this material in the as-received warm-worked condition and as annealed at 1260 C. These photomicrographs show that recrystallization causes the rejection of some impurities to the grain boundaries while others, noticeably the large round globs and the stringers, remain unaffected. It is presumed that at least two different impurities are associated with the phases appearing in Figure 25.

Because "excessive grain growth" has been given as the nominal cause of brittleness of iron-chromium-aluminum alloys for many years[1], a study of the annealing and grain-growth behavior of the above-mentioned material was undertaken. Table 6 lists the results of these studies. These data show that a blue-brittleness range probably exists in this alloy near 400 C; they show also that brittleness is not associated with a critical temperature or recrystallization in this particular material below 800 C, that brittleness is associated with grain growth and redistribution of impurities above 800 C, and that probably some of these impurities are dissolved at 1200 C and are retained in solution by rapid quenching from 1200 C. The data also show that elimination of internal gases and external oxides by vacuum annealing does not reduce brittleness in this alloy. Likewise, altering the surface of the metal by a skin-pass (10 per cent) cold reduction did not improve the ductility, but electropolishing the material by removal of about 0.010 in. from each side may have produced an effect. Electropolishing apparently did not increase brittleness by loading the alloy with hydrogen, but unfortunately the results are not clear since the increased ductility may be attributed to a decrease in thickness as well as to surface effects.

TABLE 5. ANALYSIS OF THE IRON-25 w/o CHROMIUM-5 w/o ALUMINUM ALLOY

Element	Analysis (Balance Nominally Iron), w/o
Chromium	24.2-24.5
Aluminum	5.3-5.5
Manganese	0.04-0.20
Silicon	0.06
Copper	0.04
Nitrogen	0.02-0.06
Carbon	0.014-0.015
Phosphorus	0.014
Sulfur	0.010-0.014
Oxygen	0.0073
Hydrogen	0.0006

100X RM4208

a. As warm rolled at 260 C from 0.125 to 0.062 in.

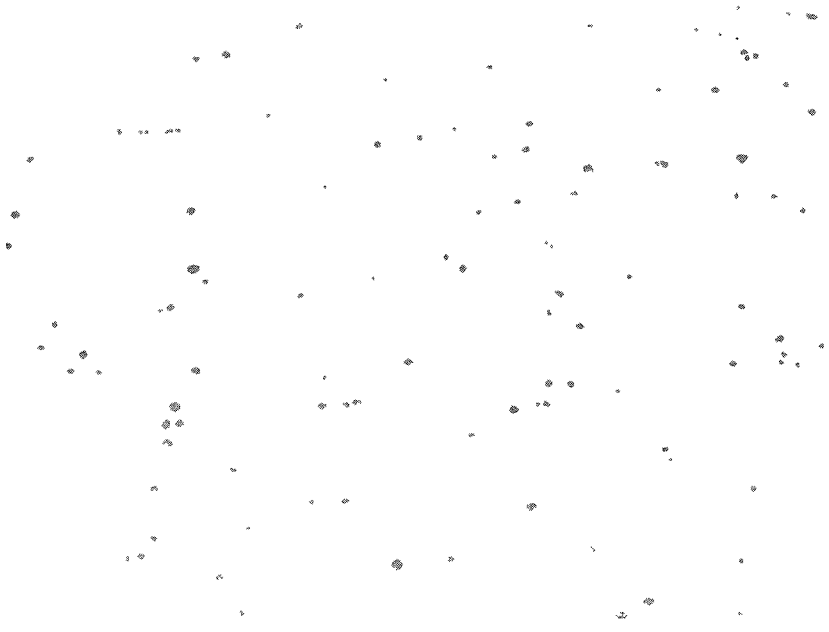

100X RM4209

b. As annealed at 1260 C

FIGURE 25. IRON-25 w/o CHROMIUM-5 w/o ALUMINUM ALLOY

See analysis in Table 5.

TABLE 6. GRAIN GROWTH, HARDNESS, AND DUCTILITY OF IRON-25 w/o CHROMIUM-5 w/o ALUMINUM AS A FUNCTION OF HEAT TREATMENT

Heat Treatment	Hardness, DPH	ASTM Grain Size	Results of Bend Test (Simple 90-Deg Bend in Vise)
As warm rolled 50 per cent at 260 C	336	(a)	Full bend without cracking
Annealed 1 hr at 400 C	350	(a)	Full bend without cracking
Annealed 1 hr at 600 C	312	(a)	Full bend without cracking
Annealed 1 hr at 800 C	221	7	Full bend without cracking
Annealed 1 hr at 1000 C	210	2	Cracked at less than 30 deg
1 hr at 1000 C, water quenched	207	--	Cracked at less than 30 deg
Annealed 1 hr at 1100 C in vacuum	212	--	Cracked at less than 30 deg
Annealed 1 hr at 1200 C	210	--	Cracked at less than 30 deg
1 hr at 1200 C, water quenched	210	--	Cracked at about 80 deg
Annealed 1 hr at 1260 C	203	--	Cracked at less than 30 deg
1 hr at 1000 C, rolled 10 per cent at 300 C	312	--	Cracked at less than 30 deg
Annealed 1 hr at 1000 C; electropolished	210	--	Cracked at about 45 deg

(a) Cold-worked grains. See Figure 25.

The fact that a highly fibered and fine-grained structure in this alloy is ductile, and that quenching from 1200 C tends to improve the ductility of a coarse-grained structure, is indicative of some sort of grain-boundary precipitate which is present in very limited amounts and is partially soluble at high temperatures and which may form an almost invisible grain-boundary film. The sensitivity of the alloy to the presence of this precipitate, and the alloy's response to electropolishing, suggested that it was extremely notch sensitive. Proof of the notch sensitivity of the material was obtained in the following manner: A sample of the as-received warm-rolled sheet was lightly notched on one surface with a sharp chisel. When subjected to the bend test with the notch in tension, this sample cracked at the notch before it had bent 30 deg. An identical sample was electropolished and notched and tested. This sample also cracked in a brittle fashion at the notch before it had bent 30 deg. Adjacent unnotched material was bent 90 deg without difficulty.

Because there exists a rather elaborate and authoritative theoretical basis for the plastic deformation and brittle fracture of body-centered-cubic iron by the Cottrell dislocation-locking mechanism[42], it was considered very important to achieve an understanding of the deformation modes of the alloy, and of the effect of cold work upon the ductility of the metal. To this end, the data shown in Table 7 were obtained. The data do not support a Cottrell dislocation-locking mechanism as being responsible for the brittleness of this alloy. According to the theory a small amount of cold work should free dislocations from their locking atmospheres and should increase ductility to some slight extent. Aging or annealing should allow the locking atmospheres to rejoin the wandering dislocations and should reduce ductility. Small reductions by cold or warm rolling did not improve ductility, while annealing after these same small reductions did in some cases improve ductility.

The increase in ductility at about 30 per cent reduction is in itself inexplicable; however, an examination of the microstructures shown in Figures 26 through 29 indicates quite graphically that twinning is the dominant mode of deformation in this alloy at 25 C. These photomicrographs clearly show the grain surface markings and grain-boundary offsetting characteristic of deformation by twinning. Figure 28 is particularly interesting because it shows that when twinning strains do not terminate within a grain they must propagate into the next grain with only a minor change in direction. Figure 29 suggests that the number of possible twinning planes in a single grain is quite small, but that it is not necessary for twinning to occur precisely on a single plane. Deformation by utilization of several adjacent atomic planes in succession must account for the convergence of twin markings in Figure 29. This possibility allows for some adjustment of the direction of strain and permits limited plasticity.

Since a twin boundary represents a change in lattice orientation, twinning can be regarded to some extent as similar to the formation of small grains from large ones with the reservation that the twinning process also produces strain hardening. Thus, a metal which deforms by twinning can become harder and more brittle in the direction of the stress producing the twinning while at the same time it acts in a more ductile fashion to a stress producing deformation in another direction. In addition, twins produced by cold deformation can contain no brittle layer at the twin boundary, so that nucleation of brittle fracture at such layers is less likely to occur during the transmission of a strain across such a boundary. This may explain why the hardness of iron-25 w/o chromium-5 w/o aluminum increases steadily during cold rolling while the bend ductility of this cold-rolled material shows a marked increase at about 30 per cent reduction.

TABLE 7. EFFECT OF COLD WORK UPON THE HARDNESS AND DUCTILITY OF IRON-25 w/o CHROMIUM-5 w/o ALUMINUM

Heat Treatment	Hardness, DPH	Results of Bend Test (Simple 90-Deg Bend in Vise)
As warm rolled 50 per cent at 260 C	336	Full bend without cracking
Annealed 1 hr at 1100 C	212	Cracked at less than 30 deg
1 hr at 1100 C, rolled 15 per cent at 600 C	265	Cracked at less than 30 deg
Above plus 1 hr at 750 C	220	Cracked at about 60 deg
Above plus 7 per cent reduction at 25 C	258	Cracked at less than 30 deg
Above plus 1 hr at 750 C	216	Cracked at about 45 deg
1 hr at 1000 C, water quenched	207	Cracked at less than 30 deg
Above plus 10 per cent reduction at 25 C	251	Not tested
Above plus 1 hr at 750 C	220	Cracked at less than 30 deg
Above plus 7 per cent reduction at 25 C	258	Cracked at less than 30 deg
Above plus 1 hr at 750 C	218	Cracked at less than 30 deg
Annealed 1 hr at 1000 C	212	Cracked at less than 30 deg
1 hr at 1000 C, rolled 10 per cent at 25 C	270	Cracked at less than 30 deg
1 hr at 1000 C, rolled 20 per cent at 25 C	283	Cracked at less than 30 deg
1 hr at 1000 C, rolled 30 per cent at 25 C	309	Full bend without cracking
1 hr at 1000 C, rolled 50 per cent at 25 C	327	Full bend without cracking
1 hr at 1000 C, rolled 20 per cent, 1 hr at 750 C	209	Full bend without cracking

250X RM5578

FIGURE 26 IRON-25 w/o CHROMIUM-5 w/o ALUMINUM ALLOY ANNEALED 1 HR AT 1000 C AND ROLLED 10 PER CENT AT 25 C

250X RM5579

FIGURE 27 IRON-25 w/o CHROMIUM-5 w/o ALUMINUM ALLOY ANNEALED 1 HR AT 1000 C AND ROLLED 20 PER CENT AT 25 C

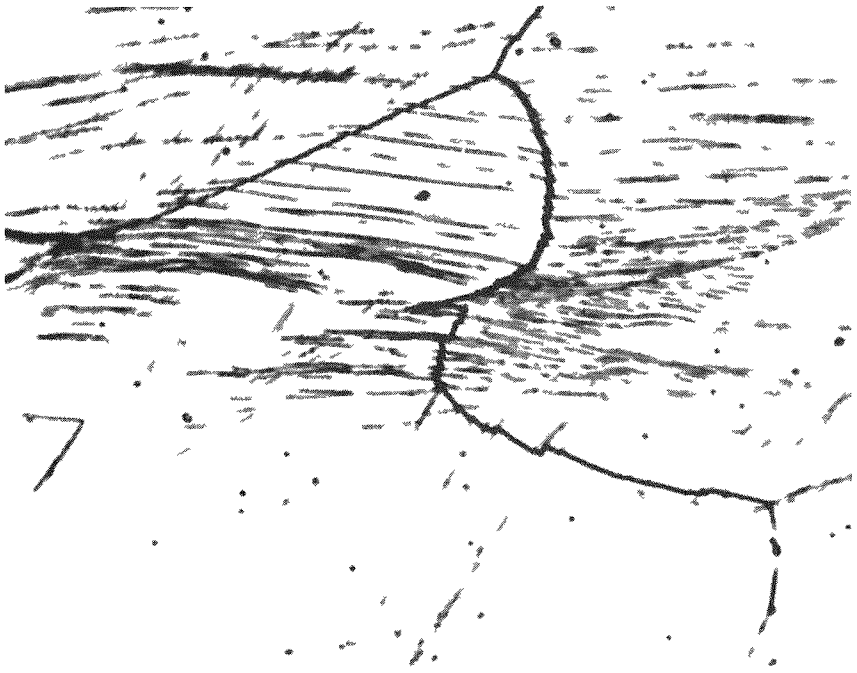

1000X Nitric Acid Methanol Electrolytic Etch RM5590

FIGURE 28 IRON 25 w/o CHROMIUM-5 w/o ALUMINUM ALLOY ANNEALED 1 HR AT 1000 C AND ROLLED 30 PER CENT AT 25 C

250X RM5581

FIGURE 29 IRON-25 w/o CHROMIUM-5 w/o ALUMINUM ALLOY ANNEALED 1 HR AT 1000 C AND ROLLED 50 PER CENT AT 25 C

The increases in ductility with annealing at 750 C are readily explicable in terms of elimination of strain hardening and grain refinement. "Grain refinement" is used in a dual sense here; recrystallization does occur in this alloy at 750 C; but any stress-relieved portion of a twin is also equivalent to a new grain.

Examination of the fractures produced in the course of the bend tests reported in Tables 6 and 7 showed that fracture in the iron-25 w/o chromium-5 w/o aluminum alloy is mainly transgranular. The transgranular cracks appear to follow crystallographic directions as indicated by Figure 30, and the broken surfaces show facets typical of cleavage along crystallographic planes. Figure 30 shows some auxiliary cracks through a group of three large grains. The main fracture cut across the center grain at the top edge of this photomicrograph. In the light of Chalmers' observation of crystal separations probably caused by twinning[39], it is readily understandable why cracks can originate in cleavage planes or grain boundaries and grow in a coarse-grained alloy where few changes in crystallographic direction at grain boundaries are necessary; and why, conversely, crack growth is more difficult in a fine-grained or heavily twinned metal where the crack (or crystal separation) encounters frequent changes in the direction of cleavage planes and opportunities for plastic deformation before its length becomes very great.

This information, plus the knowledge that certain impurities tend to segregate to grain boundaries (Figure 25), and that the material is extremely notch sensitive, suggested that the ductility of the material might be improved by identifying and eliminating those impurities which tend to segregate to the grain boundaries as weak and brittle layers. The behavior of oxygen in iron-chromium-aluminum alloys has been suggested by Gokcen and Chipman[36](see the Background to this section), and the identification of aluminum oxide in these alloys is unusually definitive. Figure 31 is a photograph of an iron-35 w/o chromium-7 w/o aluminum alloy ingot prepared by consumable-electrode arc melting. The dark areas in this ingot are slag inclusions (no slag was added). Some of this material was chipped out, cleaned with a magnet, and analyzed for iron and aluminum. The iron content was 0.85 w/o and the aluminum content was 51.3 w/o. Since aluminum oxide contains only 53 w/o aluminum, this slag is nearly pure alumina. Two other ingots of iron-25 w/o chromium-5 w/o aluminum alloy prepared by induction melting were analyzed first for oxygen content by vacuum-fusion analysis. Then a rather large portion of the ingot was chipped and dissolved in hydrochloric acid; the residue of this operation was collected, weighed, and analyzed for aluminum, and the oxygen associated with this amount of aluminum was calculated. The results shown in the following tabulation suggest that the oxygen in iron-chromium-aluminum alloys is all combined with aluminum as aluminum oxide. The higher oxygen content indicated by the insoluble technique probably derives from the oxidation of some aluminum during the involved procedure.

Ingot	Vacuum-Fusion Oxygen Analysis, ppm	Total Insoluble, w/o	Alumina in Insoluble, w/o	Oxygen Analysis by Insoluble Method, ppm
B	12	0.06	14.2	40
3	220	0.08	77.5	290

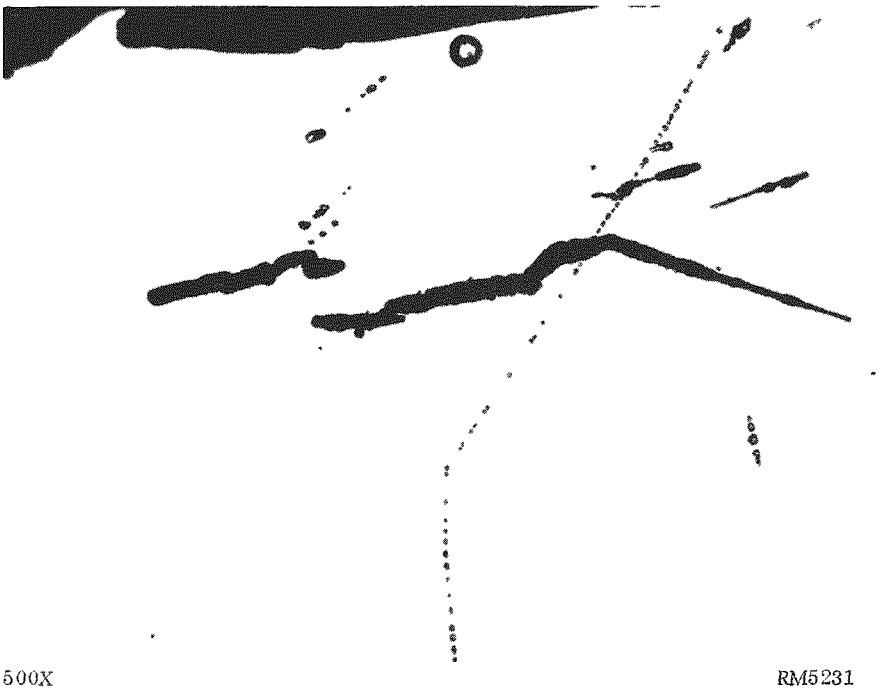

500X RM5231

FIGURE 30. AUXILIARY CRACKS IN AN IRON-25 w/o CHROMIUM-5 w/o ALUMINUM ALLOY

Note change in direction of crack at grain boundary. Sample annealed 1 hr at 1200 C, water quenched, and bent to fracture. Fracture surface shown at top of photomicrograph.

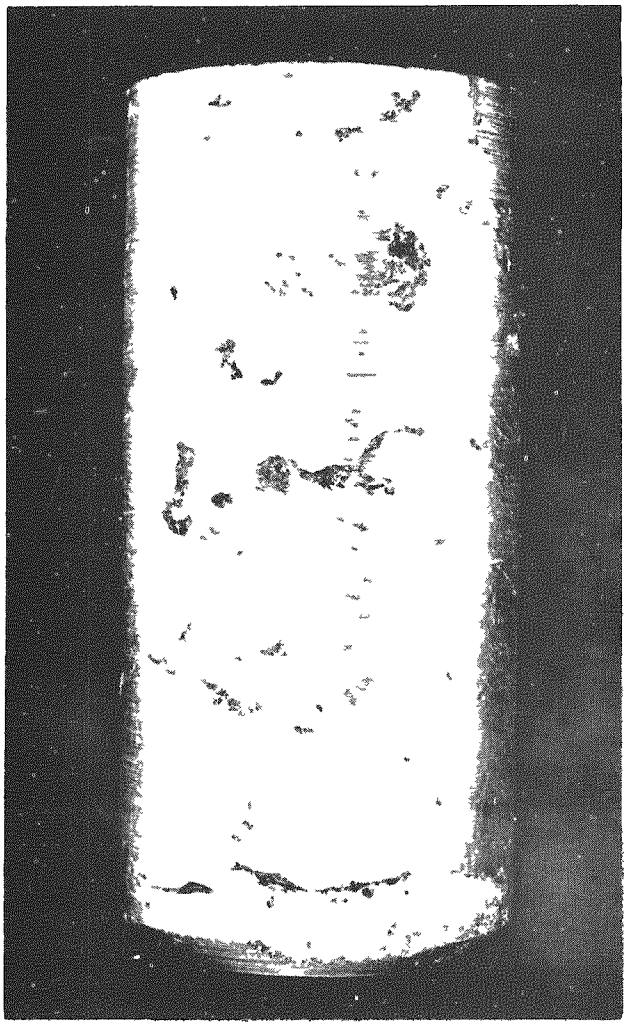

1X RM8344

FIGURE 31 INGOT OF IRON-35 w/o CHROMIUM-7 w/o ALUMINUM ALLOY PREPARED BY CONSUMABLE-ELECTRODE ARC MELTING

Figures 32 through 35 show the appearance of alumina in cast and wrought samples of iron-chromium-aluminum alloys. The drosslike character of alumina in these alloys suggests that oxygen is virtually insoluble in the molten metal. It is also noticeable that the presence of this dross in the alloys restricts grain growth in the areas where it is present; grain-boundary movement tends to stop when a dross particle is encountered. The dross appears at grain boundaries because of this tendency, not because the alumina tends to migrate to the boundaries. The fact that these alloys were readily cold reduced with up to 510 ppm oxygen suggests that oxygen is not an undesirable impurity in these alloys. It is believed, however, that quantities of oxygen in excess of about 500 ppm will result in so much dross and dirt that ingot fabricability may be impaired. The ingot shown in Figure 31 could not be fabricated at 1230 C possibly because of the form of the oxides present.

According to Kornilov[15] (see Figure 22), about 350 ppm carbon is soluble in the iron-25 w/o chromium-5 w/o aluminum alloy at 600 C. Figures 35 and 36 are believed to show the appearance of carbide in iron-chromium-aluminum alloys. If this grain-boundary constituent has been correctly identified, then its solubility in these alloys is less than 50 ppm at about 600 C. Metallographic observation of this constituent indicated that it was opaque and had the metallic luster characteristic of carbides. X-ray diffraction methods indicated the presence of the compound $(Fe,Cr)_{23}C_6$ in a sample showing this opaque grain-boundary constituent; this compound is often referred to as Cr_4C for purposes of simplification. In view of the fact that the solubility of carbon in chromium is given as about 60 ppm at 900 C[43], while the solubility of carbon in pure ferritic iron at 723 C is about 250 ppm, it seems probable that the solubility of carbon in iron-25 w/o chromium-5 w/o aluminum alloy is considerably less than 250 ppm at 723 C. It appears that Figure 22 is grossly in error, at least for temperatures below 1000 C, and that perhaps as little as 50 ppm carbon is soluble in this alloy at about 600 C. The high mobility and ready appearance of this carbide phase at grain boundaries suggest that, in agreement with Figure 22, the solubility of carbon in these alloys increases with increasing temperatures. A solubility on the order of 100 ppm carbon at 1260 C is suggested by the quenching studies reported in Tables 5 and 6.

In the course of these studies it was suggested that the increase in ductility associated with quenching from very high temperatures might be associated with some basic heat-treatment effect such as is commonly found in iron alloys which undergo the austenite-ferrite transformation. Local concentrations of carbon or nitrogen around carbides or nitrides might easily result in some austenite formation at temperatures above 725 C. To check on this possibility, a sample of iron-20 w/o chromium-5 w/o aluminum alloy containing 170 ppm carbon and 25 ppm oxygen was heated to 1000 C for 1 hr and end quenched. Examination of this bar showed that it had uniform grain size, uniform structure, and, within experimental error, uniform hardness from one end to the other. The mean hardness was 207 DPH which is not unusual for an alloy of this composition and treatment; and no trend in the hardness variations was observed. This result caused the abandonment of this trend of thought, and focused attention on the behavior of trace impurities.

Iron-35 w/o Chromium-7 w/o Aluminum Alloy

The iron-chromium-aluminum phase diagram suggests that any differences between the iron-25 w/o chromium-5 w/o aluminum alloy and the iron-35 w/o chromium-

100X Etch: 10 Parts Nitric Acid, 10 Parts Hydrochloric Acid, 30 Parts Lactic Acid N38271

FIGURE 32 DROSS-TYPE CLUSTERS OF ALUMINA IN AN AS-CAST SAMPLE OF IRON-24 w/o CHROMIUM-3.3 w/o ALUMINUM ALLOY CONTAINING 250 PPM OXYGEN AND 20 PPM CARBON

250X Nitric Acid, Methanol, Electrolytic Etch RM6784

FIGURE 33 PARTIALLY ELONGATED DROSS-TYPE CLUSTERS OF ALUMINA IN WROUGHT AND ANNEALED SAMPLE OF IRON-26 w/o CHROMIUM-3 w/o ALUMINUM ALLOY CONTAINING 197 PPM OXYGEN AND 20 PPM CARBON

Sample reduced 80 per cent at 25 C and annealed 1 hr at 1000 C Hardness: 258 DPH.

500X 10 Volume Per Cent Oxalic Acid, Electrolytic Etch RM6328

FIGURE 34. PARTICLES OF ALUMINA IN WROUGHT AND ANNEALED SAMPLE OF IRON-24 w/o CHROMIUM-4.3 w/o ALUMINUM ALLOY CONTAINING 220 PPM OXYGEN AND 20 PPM CARBON

Sample reduced 80 per cent at 25 C and annealed 1 hr at 1000 C. Hardness: 202 DPH.

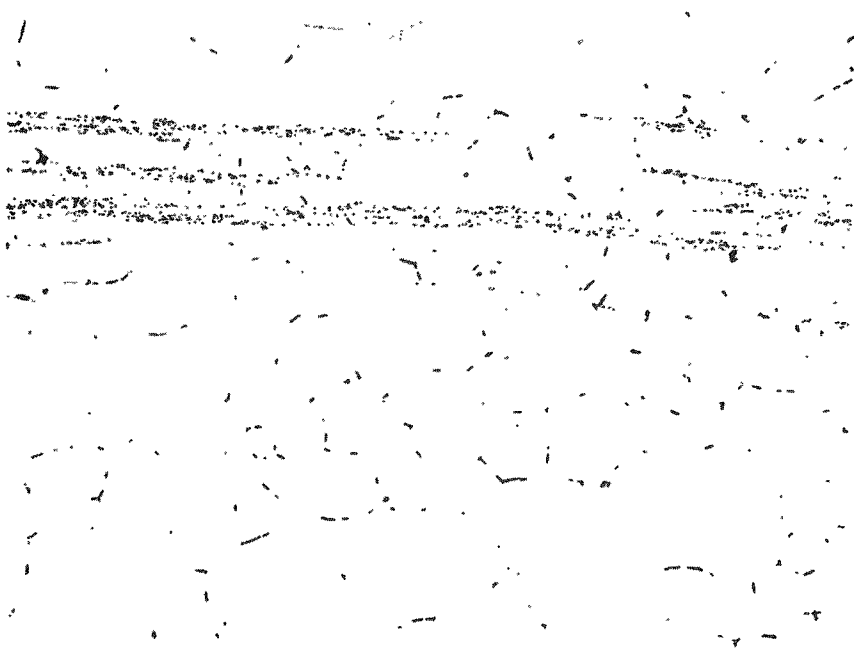

FIGURE 35. STRINGERS OF ALUMINA IN WROUGHT AND ANNEALED SAMPLE OF IRON-23 w/o CHROMIUM-5.6 w/o ALUMINUM ALLOY CONTAINING 510 PPM OXYGEN AND 50 PPM CARBON

Sample reduced 80 per cent at 25 C and annealed 1 hr at 1000 C. Hardness: 230 DPH. Grain-boundary constituent is probably carbide.

500X 10 Per Cent Oxalic Acid, Electrolytic Etch RM5373

a. The light-gray globular particles are believed to be oxides.

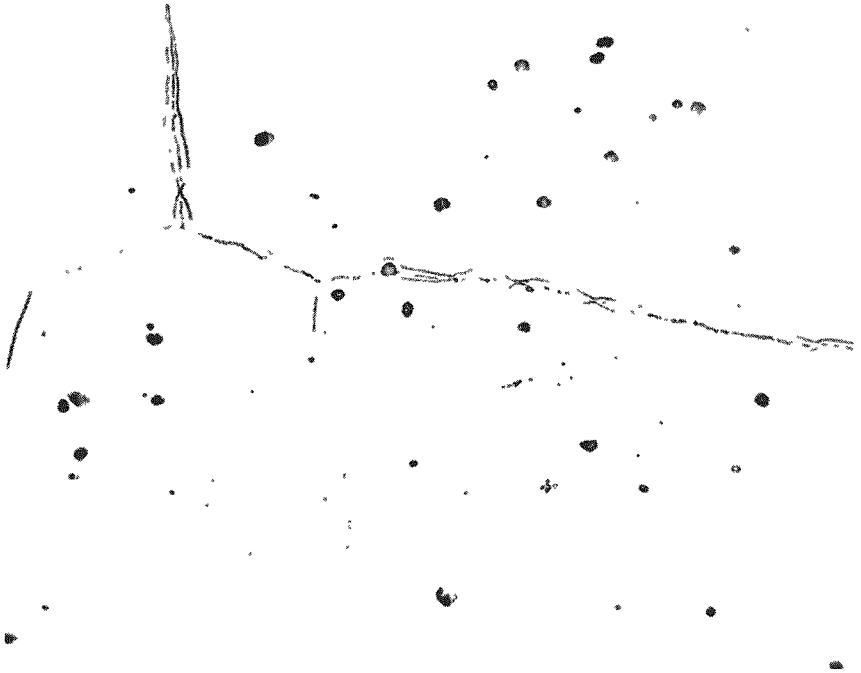

250X 1 Part Nitric Acid, 2 Parts Methanol, Electrolytic Etch RM5374

b. The carbide is outlined in this photomicrograph by a stain produced by the etchant. Only the carbide is outlined.

FIGURE 36. GRAIN-BOUNDARY PHASE, IDENTIFIED AS Cr_4C, IN AN IRON-25 w/o CHROMIUM-5 w/o ALUMINUM ALLOY CONTAINING 55 PPM CARBON AND 73 PPM OXYGEN

Sample annealed 1 hr at 1100 C.

7 w/o aluminum alloy are purely matters of degree. However, Kornilov[1,15] has indicated that both these alloys are hot fabricable, but that only the former is cold fabricable. This suggested that there might be a fundamental difference between the alloys, and led to a physical metallurgical search for such a difference.

Tests were made on samples of an iron-35 w/o chromium-7 w/o aluminum alloy melted in a vacuum in an alumina crucible and cast as a single 15-lb ingot. The ingot was forged at 1260 C and hot rolled to 0.060-in. sheet of high quality at 1000 C. On analysis, this material contained 34.8 w/o chromium, 6.9 w/o aluminum, 70 ppm carbon, and 96 ppm oxygen. Warm rolling of the 0.060-in. sheet was attempted at 590 C and at 350 C, and in both cases no cracking of the slightest degree was observed in reductions as high as 33 per cent. However, it was found that when the warm-rolled sheet was annealed for 1 hr at 1100 C and cold rolled at 25 C, cracking began at reductions of about 5 per cent. This suggests that the iron-35 w/o chromium-7 w/o aluminum alloy differs from the iron-25 w/o chromium-5 w/o aluminum alloy by having a cold-deformation brittle-ductile transition temperature above room temperature, while that of the iron-25 w/o chromium-5 w/o aluminum alloy is below room temperature. This change in transition temperature is a gradual change as a function of composition, as is shown later for the impact transition temperature. Bend-ductility tests performed on this alloy are shown in Table 8. These data show that the recrystallization temperature of the iron-35 w/o chromium-7 w/o aluminum alloy is about the same as that of the iron-25 w/o chromium-5 w/o aluminum alloy. The grain-growth rate of the iron-35 w/o chromium-7 w/o aluminum alloy is noticeably slower than that of the iron-25 w/o chromium-5 w/o aluminum alloy reported in Table 6, so that the ductility of the former shows a tendency to improve as hardness decreases with increasing annealing temperature while the rapid grain growth of the iron-25 w/o chromium-5 w/o aluminum alloy causes it to become brittle when annealed for 1 hr at 1000 C. Figure 37 shows some of the test specimens mentioned in Table 8. These photomicrographs are comparable with those in Figures 25 and 26, and show that the iron-25 w/o chromium-5 w/o aluminum and iron-35 w/o chromium-7 w/o aluminum alloys are metallurgically similar.

Figure 38 shows hot-hardness data for representative iron-chromium-aluminum alloys. The data show that increasing alloy content increases high-temperature hardness, and that forging and rolling temperatures for the higher alloy will be approximately 100 C above the respective forging and rolling temperatures of the leaner alloy. The similarity of the low-temperature hardnesses of these alloys is believed to be a function of the relatively higher impurity content of the iron-25 w/o chromium-5 w/o aluminum alloy (compare Figures 25 and 37a).

Figure 39 is comparable to Figure 30 and shows subsidiary or auxiliary cracking in an iron-35 w/o chromium-8 w/o aluminum alloy. This specimen is part of an impact bar broken at 275 C with an absorption of 14 ft-lb of energy. The fracture was entirely brittle by visual examination, but the auxiliary cracks in Figure 39 show evidence of very slight ductility. As in Figure 30, the cracking is almost entirely transgranular and seems to follow straight lines through grains with only minor changes in direction at grain boundaries.

Figure 40 shows the appearance of the constituent believed to be Cr_4C in an iron-30 w/o chromium-7 w/o aluminum alloy containing 80 ppm carbon and 30 ppm oxygen. This photomicrograph is comparable with those in Figures 35 and 36, and suggests that the solubility of carbon in this alloy is much less than 80 ppm.

TABLE 8. EFFECT OF VARIOUS TREATMENTS UPON THE HARDNESS, GRAIN SIZE, AND DUCTILITY OF THE IRON-35 w/o CHROMIUM-7 w/o ALUMINUM ALLOY

Heat Treatment	Rockwell A Hardness	Grain Size	Results of Bend Test (Simple 90-Deg Bend in Vise)
As hot rolled at 1000 C	57	--	--
Warm rolled 33 per cent at 590 C	69	(a)	--
Warm rolled 33 per cent at 350 C	70	(a)	Cracked at less than 10 deg
Warm rolled 33 per cent, annealed 2 hr at 600 C	67	(a)	Cracked at less than 10 deg
Warm rolled 33 per cent, annealed 1 hr at 700 C	62	(b)	Cracked at about 30 deg
Warm rolled 33 per cent, annealed 1 hr at 800 C	59	6	Cracked at about 20 deg
Warm rolled 33 per cent, annealed 1 hr at 900 C	58	5	Cracked at about 30 deg
Warm rolled 33 per cent, annealed 1 hr at 1000 C	57	4	Cracked at about 60 deg
Warm rolled 33 per cent, annealed 1 hr at 1100 C	56	--	--

(a) Cold-worked grains, about ASTM Grain Size 4. See Figure 37.
(b) See Figure 37. ASTM Grain Size 4 and 9, mixed.

100X RM9422

a. Annealed 2 hr at 600 C. Note cold worked grains and twin markings as in Figure 28.

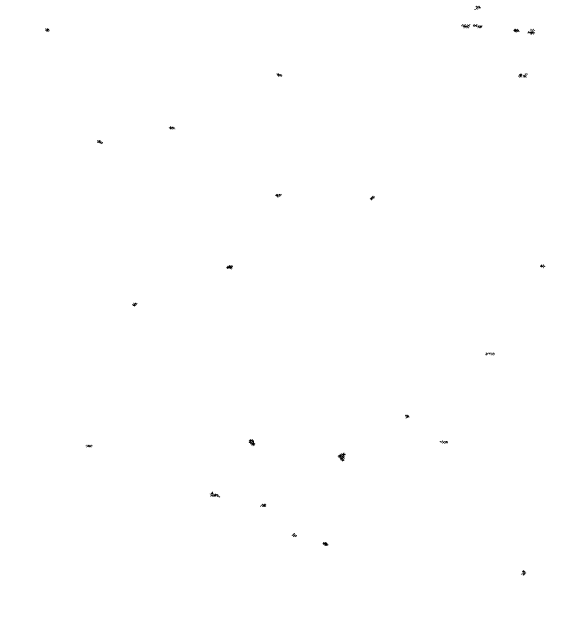

100X RM9423

b Annealed 1 hr at 700 C Partial recrystallization.

100X RM9424

c Annealed 1 hr at 800 C. ASTM Grain Size 6.

FIGURE 37. EFFECT OF INCREASED ANNEALING TEMPERATURES ON THE MICROSTRUCTURE OF IRON-35 w/o CHROMIUM-7 w/o ALUMINUM WARM ROLLED 33 PER CENT AT 350 C

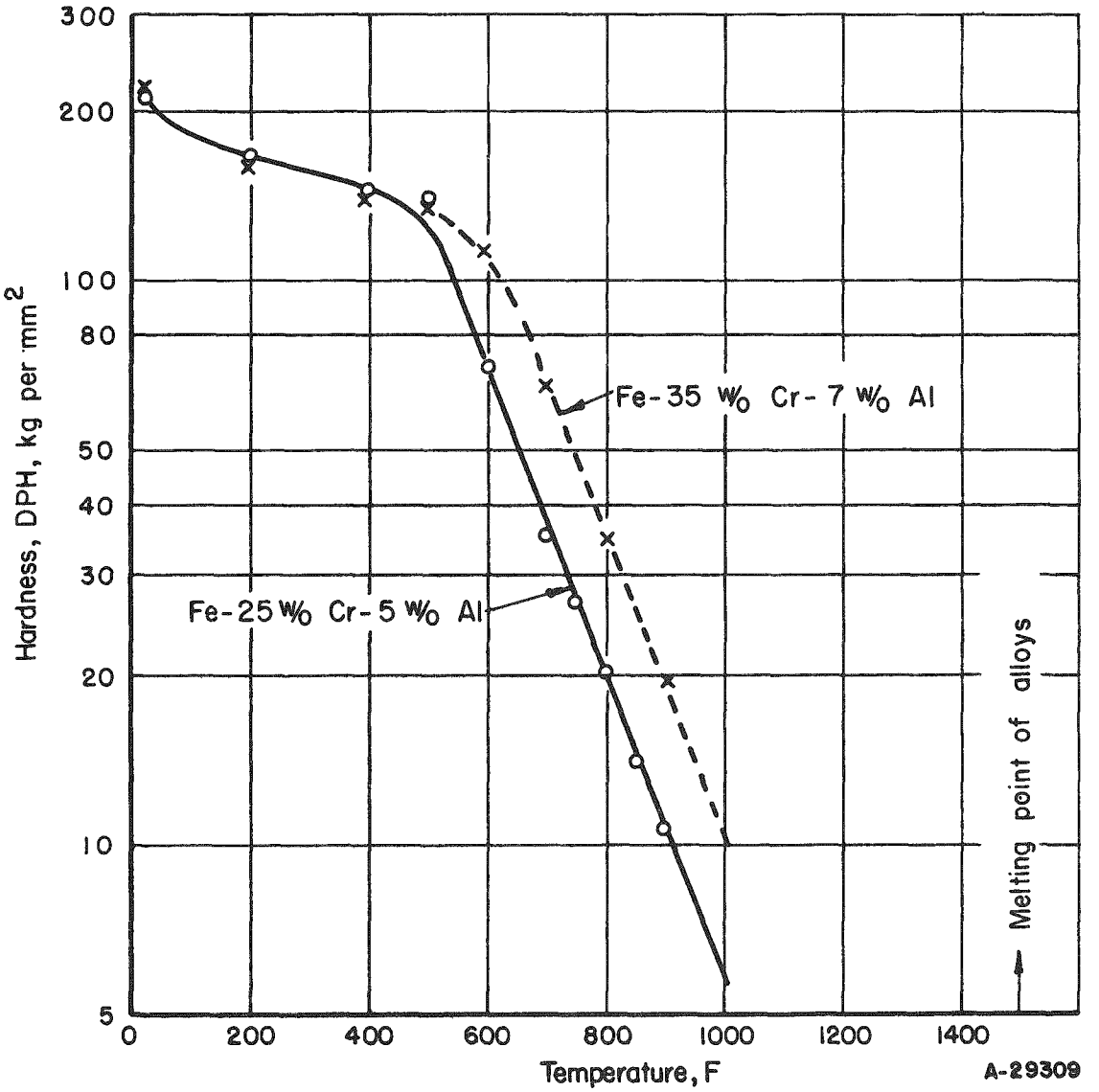

FIGURE 38. HARDNESS OF IRON-CHROMIUM-ALUMINUM ALLOYS AS A FUNCTION OF TEMPERATURE

100X RM8787

FIGURE 39. AUXILIARY CRACKS IN AN IRON-35 w/o CHROMIUM-6 w/o ALUMINUM ALLOY

Compare with Figure 30. Sample hot rolled at 1000 C and broken in impact at -75 C with an absorption of 14 ft-lb of energy. Hardness 240 DPH

500X Etchant: 3 Parts Hydrochloric Acid, 1 Part Nitric Acid, 4 Parts Water RM8456

FIGURE 40. IRON-30 w/o CHROMIUM-7 w/o ALUMINUM ALLOY CONTAINING 80 PPM CARBON AND 30 PPM OXYGEN

Annealed 1 hr at 1000 C. Hardness: 222 DPH.

Melting, Casting, and Impact Transition Studies

Not all of the tests reported in the preceding sections were performed at the outset of this program of research; many of the results were obtained or suggested by the behavior of materials during melting, casting, and fabrication. However, it became clear early in the program that precise control of raw materials and melting and casting techniques would be important to the recovery, quality, and ductility of the product. The notch sensitivity of the alloys and the existence of a brittle-ductile transition temperature with respect to cold rolling and with respect to notch-impact strength (see Figure 20) suggested that the low-temperature ductility of these alloys could best be evaluated quantitatively by means of standard V-notch Charpy impact tests.

With three exceptions, all of the ingots prepared during this research were made of commercial electrolytic iron flakes and commercial electrolytic chromium flakes. The aluminum used was commercially pure (2S) or high-purity (99.99 w/o) aluminum. The three exceptions involved the use of hydrogen-treated and vacuum-melted electrolytic iron or the use of iodide-refined chromium or both. Typical analyses of these materials are listed in Table 9.

All ingots prepared were melted in a vacuum of less than 10 μ absolute pressure to remove hydrogen, nitrogen, carbon dioxide, carbon monoxide, and any other volatiles which might be detrimental to the ductility of the alloys. Generally, only the iron and chromium were held in the molten state in a vacuum. It was believed that when the metal was deoxidized with aluminum-alloy additions there was small chance of removing any additional volatiles, except aluminum and chromium. Therefore, in all cases, helium was added to the system to about atmospheric pressure prior to adding aluminum to the melts just before pouring the ingots.

Effect of Raw Materials

The three exceptions mentioned above involved four ingots which were intended to test the effect of varying the purity of the raw materials. Each ingot contained a different combination of the materials, electrolytic iron, vacuum-melted iron, electrolytic chromium, or iodide chromium. The results in Figure 41 show that there is no correlation between carbon and oxygen contents of the raw materials and the products. Ingots 1 and 3 contained vacuum-melted iron, and Ingots 2 and 3 contained iodide chromium. There is, however, an apparent correlation between the analyses of the alloys and their transition temperatures. The high-oxygen alloy has the lowest transition temperature, and the high-carbon high-aluminum low-oxygen alloy has the highest transition temperature. A multitude of experiments described later have confirmed this correlation, but no basic understanding of the role of oxygen has been achieved. It has been suggested that carbon tends to associate with oxygen to some extent rather than precipitate as carbide. Perhaps oxygen tends to prevent the pickup of some unknown impurity or aids in the removal of impurities as gases or complex ions.

TABLE 9. MATERIALS USED IN MELTING OF IRON-CHROMIUM-ALUMINUM ALLOYS

Raw Material	Impurity Analysis, ppm			
	Carbon	Oxygen	Nitrogen	Hydrogen
Electrolytic iron	20	46	<10	1
Vacuum-melted iron	60	47	<10	<1
Electrolytic chromium	20	2990	<10	390
Iodide chromium	40	86	<10	3
99.99 w/o aluminum	20	23	<10	1.5

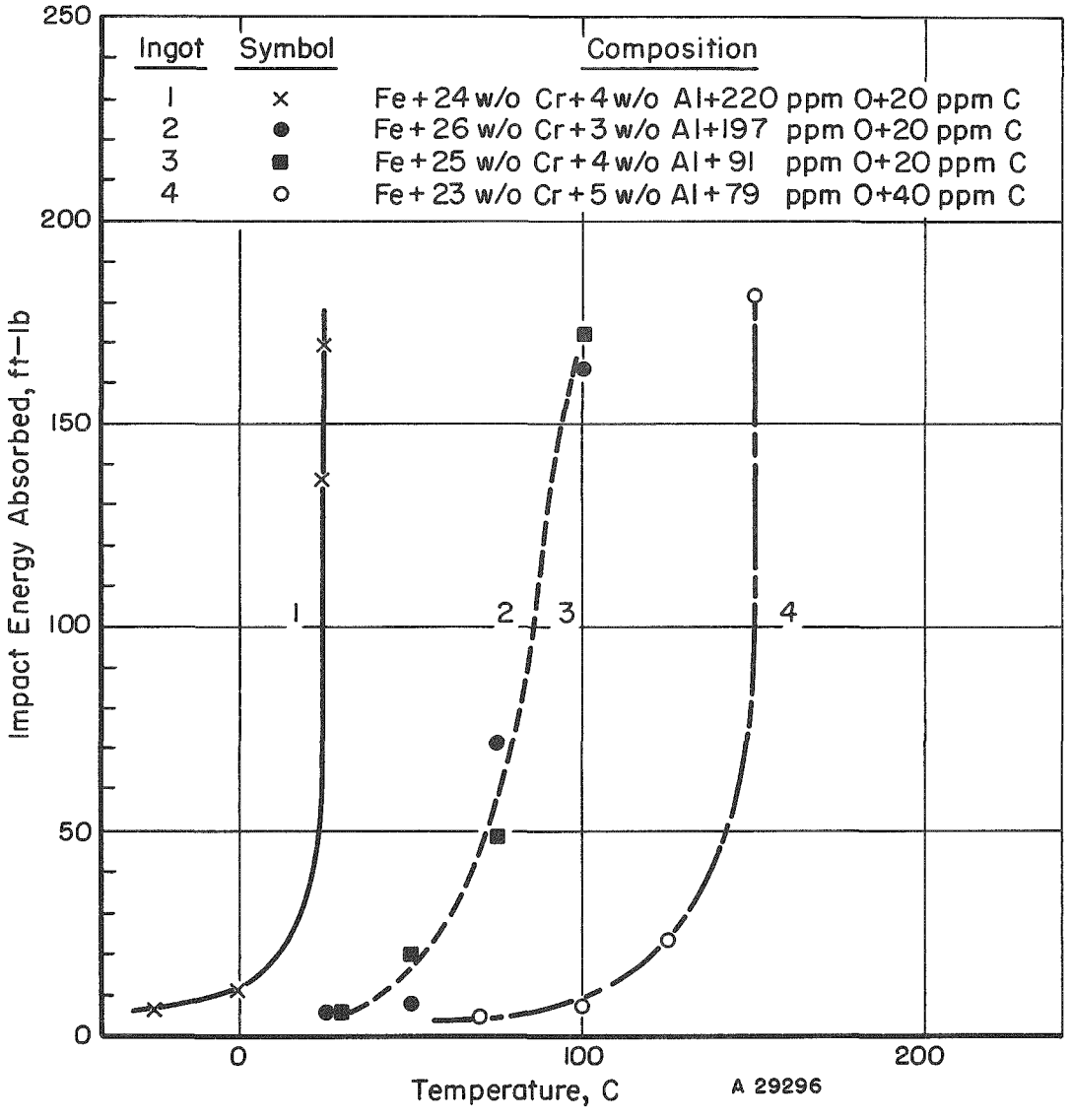

FIGURE 41. CHARPY IMPACT TESTS ON REPRESENTATIVE IRON-25 w/o CHROMIUM-5 w/o ALUMINUM ALLOYS HOT ROLLED AT 800 C

Effect of Crucible Materials

Because zirconia was known to be an extremely refractory material and has been used in melting of iron and iron-chromium alloys without difficulty, it was used as the crucible material for melting about 20 of the first experimental iron-chromium-aluminum alloys. This has been shown to be an unfortunate choice. It appears that at temperatures only slightly above the required pouring temperature for iron-chromium-aluminum alloys (about 1600 C) zirconia is dissolved by the reaction: $4Al + 3\ ZrO_2 \rightarrow 3\ Zr + 2Al_2O_3$. Zirconium is apparently very insoluble in solid iron; it appears as shown in Figure 42 in an iron-24 w/o chromium-5 w/o aluminum alloy containing 10 ppm carbon, 39 ppm oxygen, and 0.54 w/o zirconium. No zirconium was added to this alloy; however, it was melted in a zirconia crucible and was heated to 1650 C or higher just before pouring. The insoluble constituent observed in this sample must be the intermetallic compound $ZrFe_2$. The presence of this compound was indicated by X-ray diffraction measurements. This alloy showed rather poor fabrication characteristics in hot rolling at 800 C, failed in cold rolling at less than 10 per cent reduction in thickness, showed an impact transition temperature about 100 C above that of similar alloys containing no zirconium, and showed less than one-fourth the impact strength of similar alloys above the transition temperature. Figure 43 shows an impact specimen of this alloy which absorbed only 38 ft-lb of energy in breaking in half at 200 C. Next to it is the specimen of Alloy 1 (see Figure 41) which absorbed 170 ft-lb of energy at 25 C without breaking.

This result emphasized the importance of the role of crucible reactions in regard to ingot cleanliness and hot and cold fabricability. To avoid the problem of crucible reactions, alumina crucibles have been used for all heats melted subsequent to the above-mentioned discovery. Porous and low-fired alumina crucibles are not satisfactory because of impurities present in the alumina. Only high-density high-fired high-purity alumina crucibles (or similarly high-purity magnesia crucibles) are believed to be suitable for melting iron-chromium-aluminum alloys.

Effect of Casting and Fabrication Procedures

Kornilov[1,15] and Justusson, Zackay, and Morgan[34] have demonstrated the extreme dependence of the cast grain size of alloys of this type upon casting temperature. The lower the pouring temperature, the smaller the cast grain size will be. In practice this means that the pouring temperature must be closely controlled and held at or just below 1600 C if a fine-grained ingot is to be obtained. This is not an easy thing to do for vacuum-melted alloys containing chromium or aluminum because thermocouples tend to dissolve in the melt and metal vapors tend to obstruct optical measurements. Observation of the behavior of slags of known composition has been an aid to temperature control in this research and is described in detail later. In the absence of large quantities of embrittling impurities, the hot-fabrication characteristics of iron-chromium-aluminum alloys are dependent upon ingot quality, alloy composition, and ingot grain size. A fine-grained iron-chromium-aluminum alloy ingot containing ingot defects and small quantities of embrittling materials such as carbon, sulfur, or zirco-

500X 10 Per Cent Oxalic Acid, Electrolytic Etch N38270

FIGURE 42. IRON-24 w/o CHROMIUM-5 w/o ALUMINUM ALLOY CONTAINING 10 PPM CARBON, 39 PPM OXYGEN, AND 0.54 w/o ZIRCONIUM

The insoluble phase is probably $ZrFe_2$. Sample as hot rolled. Hardness, 207 DPH

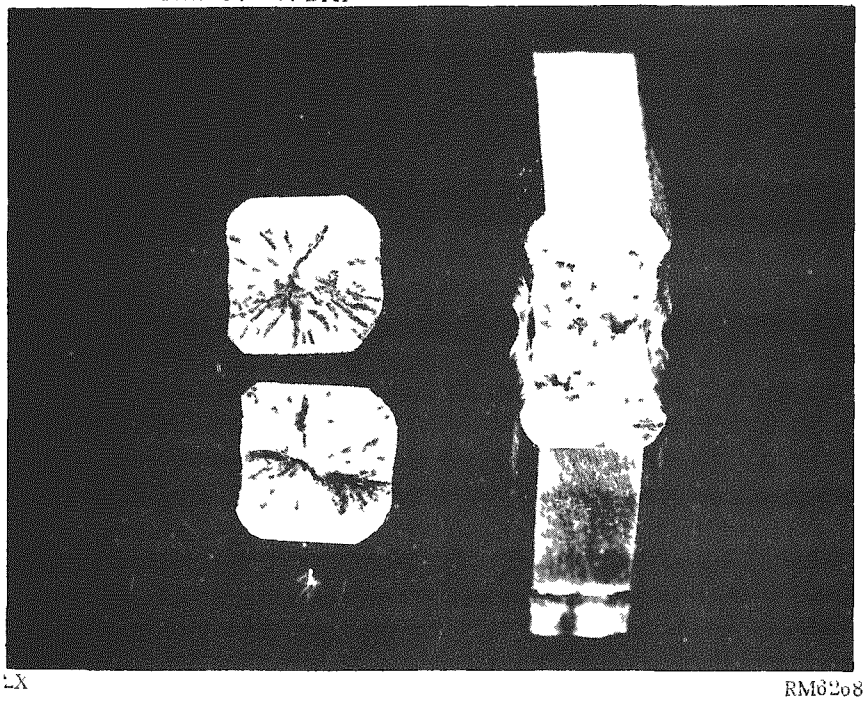

2X RM62o8

FIGURE 43. EXTREMES OF BEHAVIOR OF IMPACT BARS OF IRON-25 w/o CHROMIUM-5 w/o ALUMINUM ALLOY

Left Iron-24 w/o chromium-5 w/o aluminum alloy containing about 0.54 w/o zirconium. Broken at 200 C with 38 ft-lb of energy absorbed. Right Iron-24 w/o chromium-4 w/o aluminum alloy containing 220 ppm oxygen, 20 ppm carbon, and less than 100 ppm zirconium. Broken at 25 C with 170 ft-lb of energy absorbed.

nium will usually fabricate to sound wrought material; whereas a perfect ingot of purer metal of the same nominal composition but large grained will often crack into fragments in the initial breakdown. Figure 38 suggests that the iron-35 w/o chromium-7 w/o aluminum alloy can be forged at 1100 to 1200 C and hot rolled at 850 to 1000 C. The materials prepared in this research were usually forged from a furnace at 1260 C and rolled from a furnace at 1000 C. Once the initial breakdown was achieved, it was often found best to continue fabrication as rapidly as possible down to finished size without reheating to take advantage of the smaller grain size produced by working. Temperatures above 1260 C and lengthy reheating schedules were found undesirable because of rapid grain growth and resultant aggravation of any tendency for hot shortness from trace impurities. Some of the first ingots prepared of iron-25 w/o chromium-5 w/o aluminum alloy were hot rolled from a furnace at 800 C with excellent results except that the hot-rolled structures were excessively elongated in the rolling direction.

Figure 44 suggests that fabrication procedures may have some effect on the grain size and impact transition temperature of iron-chromium-aluminum alloys; because of this rolling procedures were standardized as much as possible by specifying 1000 C as the hot-rolling temperature regardless of composition. With the exception of the samples reported in Figure 44, all impact specimens were machined directly from hot-rolled stock, and were tested without further treatment. Figure 44 is believed to show a correlation with the grain-size data of Table 6. That is, it is very likely that the increase in transition temperature shown in Figure 44 was caused by the same increase in grain size and agglomeration of impurities in the grain boundaries as described in Table 6. It is not possible to separate these two effects of annealing at this time. Conversely, it is believed that the change in bend ductility in increasing the annealing temperature from 800 to 1000 C is related to a change in what might be called a transition temperature for bending; i.e., the sample in Table 6 annealed at 1000 C which cracked in bending at room temperature probably would not have cracked in bending at 50 or 75 C. This line of reasoning suggests that the impact transition temperature can be used to predict bending or cold-rolling ductility transitions, provided that a small temperature correction for the difference in deformation rates is applied. This deduced relation was used to predict a temperature for successful warm rolling of iron-35 w/o chromium-7 w/o aluminum alloys which are brittle at room temperature.

Because of the high thermal-expansion coefficients of iron-chromium-aluminum alloys, particularly the higher aluminum alloys, and because of the possibility of hot shortness of ingots, it is not desirable to chill cast iron-chromium-aluminum alloys for any reason. Chill casting promotes columnar grain growth and internal cracking from differential contraction. Ingots cast in copper during this research often showed columnar grains to the center, and some broke in half on removal from the mold. Ingots cast in fairly thin-walled steel or cast iron or graphite or zirconite molds are usually sound and show only an outer layer of columnar grains. It is very desirable to provide the ingot with a hot top of suitable heat content and capacity since these alloys are fully "killed" and show considerable solidification shrinkage and a pronounced tendency to pipe. Severe piping has very little effect on the fabrication behavior of these alloys, and is important only to the extent that it affects the internal soundness of the product. Heating of the mold and hot top to a red heat may be useful in cases where chill cracking seems to occur.

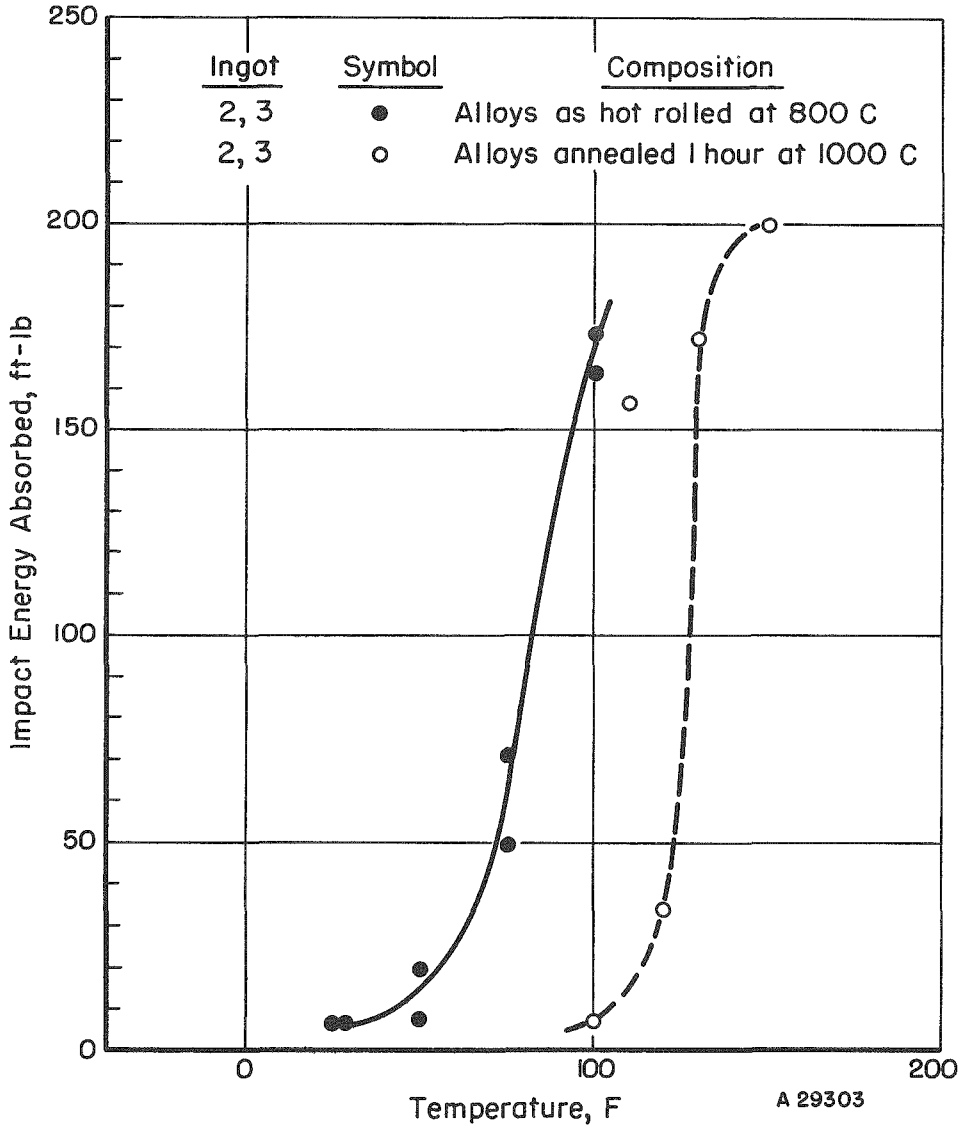

FIGURE 44. EFFECT OF AN ANNEALING TREATMENT ON THE IMPACT TRANSITION OF IRON-25 w/o CHROMIUM-4 w/o ALUMINUM

Effect of Basic Alloying Elements

Ham and Carr[28] have shown that vacuum-melted binary iron-chromium alloys containing 20 to 35 w/o chromium and 50 to 160 ppm carbon have impact transition temperatures in the range from -50 to +10 C. Figures 45 through 47 show the effect of increasing aluminum content upon these alloys. The data show that in the range of 25 to 35 w/o chromium and 3 to 8 w/o aluminum each per cent of aluminum added to the alloy raises the impact transition temperature by about 50 C. On the other hand, a comparison of these figures suggests that increasing the chromium content from 25 to 35 w/o has no appreciable effect on the impact transition temperature. This is in agreement with the work of Ham and Carr who showed no significant change in the impact transition of binary iron-chromium alloys from 20 to 35 w/o chromium.

The behavior of iron-35 w/o chromium-7 to 8 w/o aluminum alloys in impact tests at temperatures above the brittle-ductile transition temperature was interesting, and suggests a problem in handling of this alloy in manufacturing of parts. Figure 48 shows an impact specimen of iron-35 w/o chromium-8 w/o aluminum alloy containing 50 ppm carbon and which absorbed 100 ft-lb of energy in an impact test at 275 C. This alloy is definitely ductile at 275 C, yet the ground surfaces show signs of brittle cracking. It is believed that these cracks are grinding cracks produced by the high thermal-expansion coefficient of the metal combined with local heating by the grinding wheel while the mass of the material was at some temperature below 275 C. While this type of cracking is evidently not serious for a thick specimen such as an impact bar, cracks of this magnitude could have serious effects on thin sheet.

Effects of Special Alloying Additions

Carbon. Attempts to define the effect of carbon upon the impact strength of iron-chromium-aluminum alloys in the range from 20 to 100 ppm carbon have been futile. However, significant results have been achieved by adding carbon to these alloys. The results shown in Figure 49 seem to indicate a steady increase in transition temperature with increasing carbon content from 30 to 700 ppm. However, reference to Figure 45 shows that the iron-25 w/o chromium-5 w/o aluminum alloys containing 40 to 60 ppm carbon may have transition temperatures between 70 and 150 C. It is not clear, therefore, that carbon is responsible for the trend of increasing transition temperatures from 30 to 290 ppm carbon. It is clear, however, that 600 to 700 ppm carbon does significantly embrittle iron-25 w/o chromium-5 w/o aluminum alloys. The results suggest that for best results these alloys should contain a maximum of 100 ppm carbon if only because this represents a high level of alloy cleanliness.

Oxygen. The results shown in Figure 41 suggested that oxygen additions might aid in producing more ductile iron-chromium-aluminum alloys. Attempts to add oxygen in the form of Fe_3O_4 were unsuccessful, and it soon became clear that the raw electrolytic chromium contained more than enough oxygen to produce a voluminous dross which resulted in heavy skulls in the crucibles, and greatly reduced metal yields. Some of

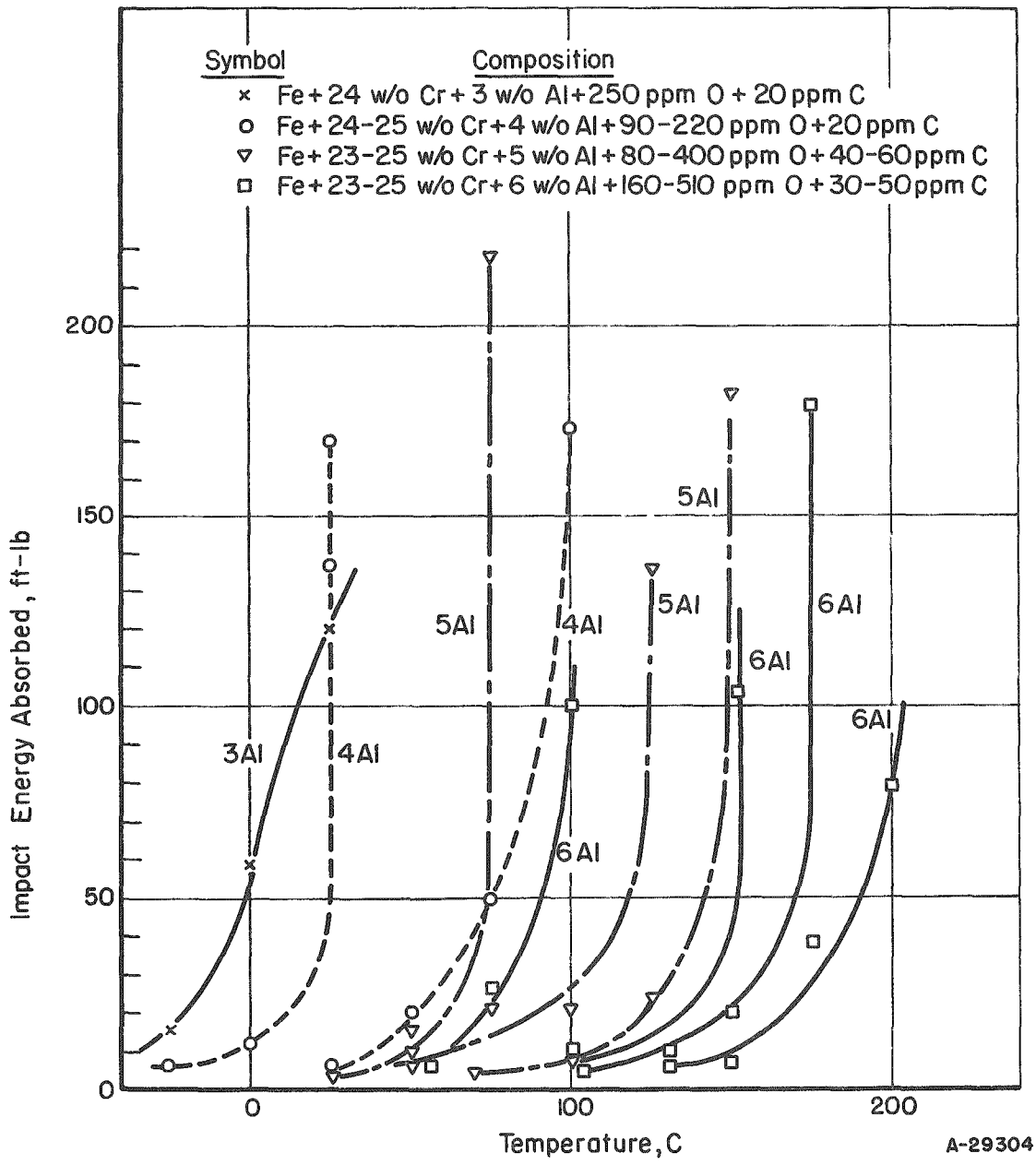

FIGURE 45. EFFECT OF ALUMINUM ON THE TRANSITION TEMPERATURE OF IRON-25 w/o CHROMIUM ALLOYS

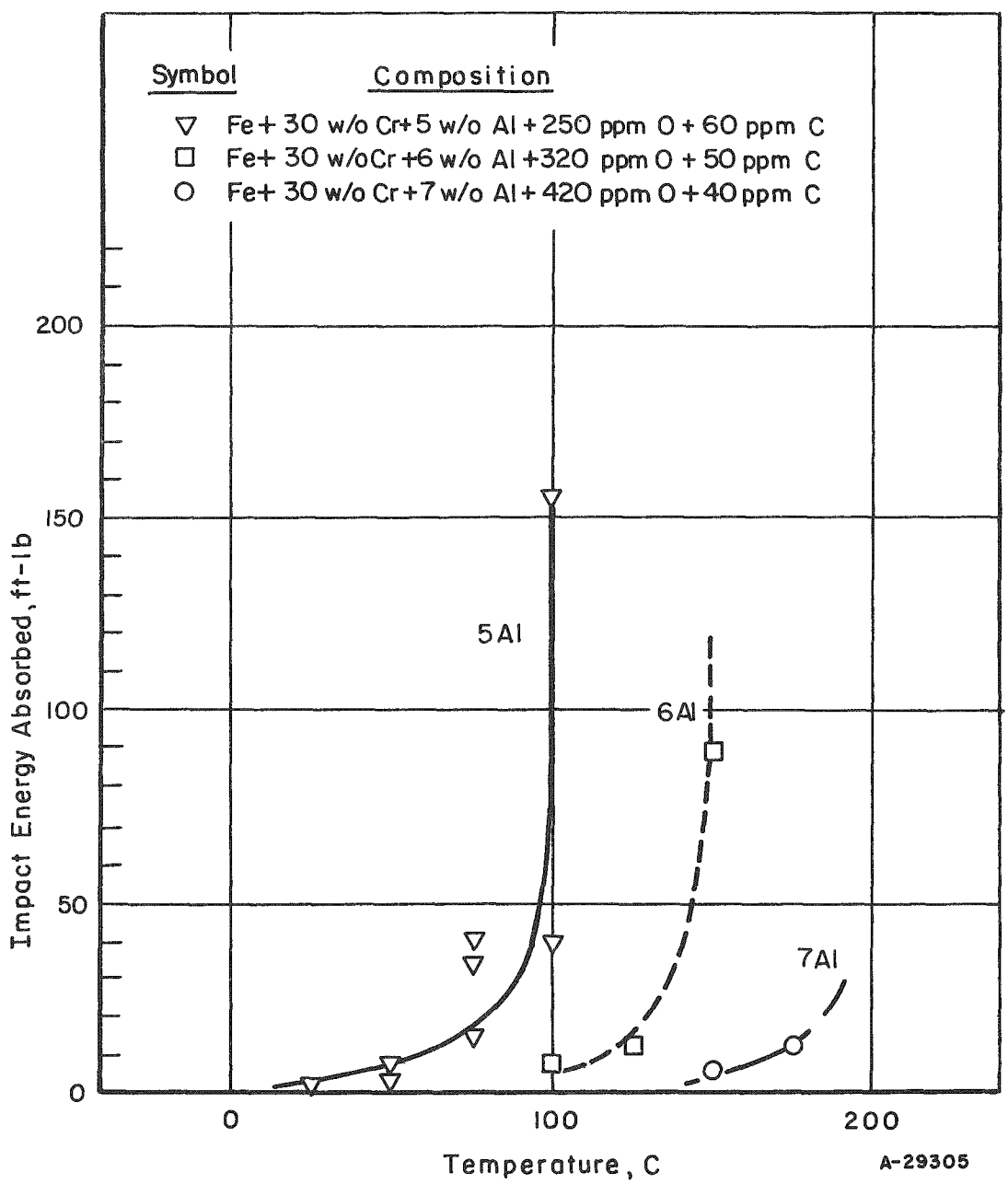

FIGURE 46. EFFECT OF ALUMINUM ON THE TRANSITION TEMPERATURE OF IRON-30 w/o CHROMIUM ALLOYS

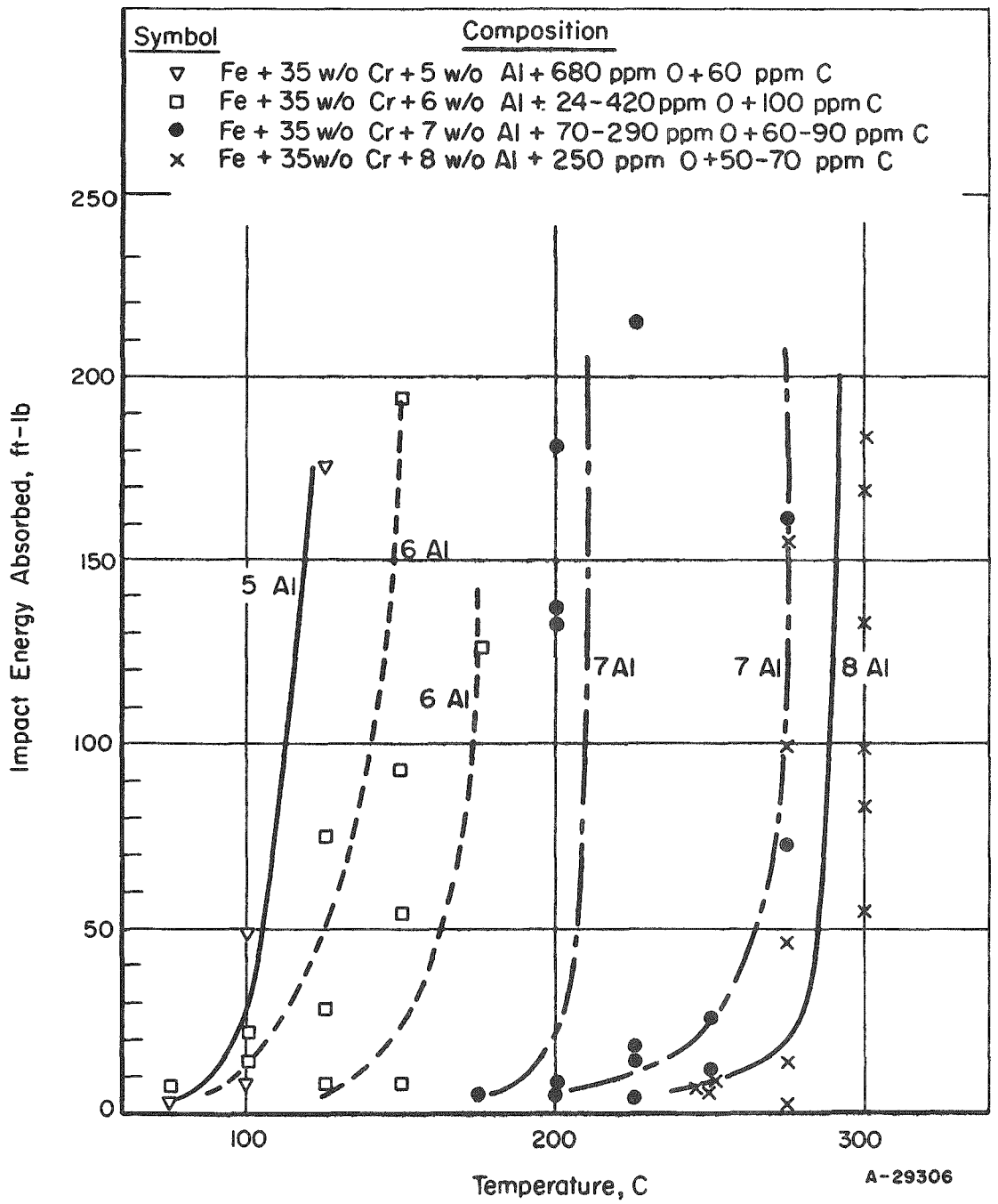

FIGURE 47. EFFECT OF ALUMINUM ON THE TRANSITION TEMPERATURE OF IRON-35 w/o CHROMIUM ALLOYS

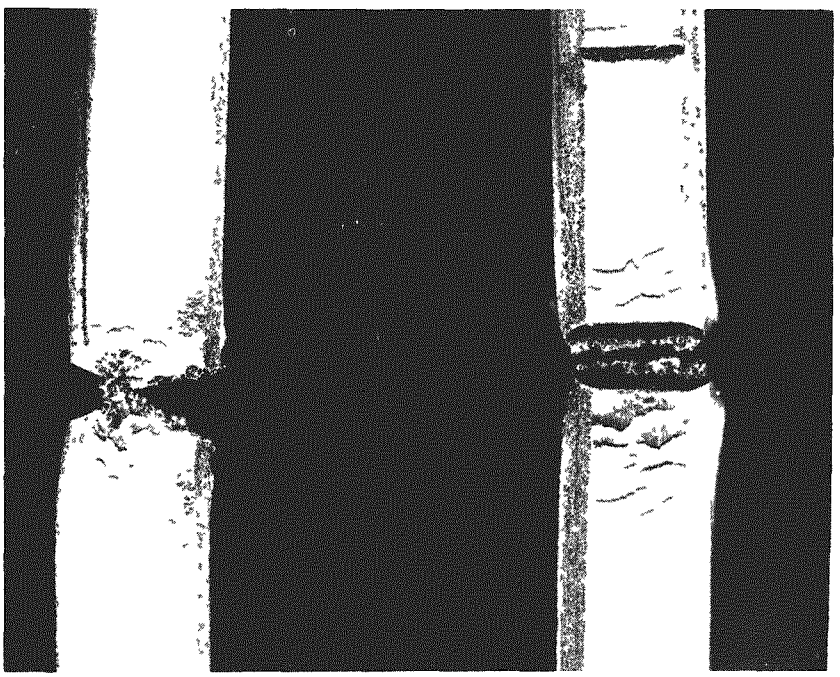

2X RM9342

FIGURE 48. GRINDING CRACKS OPENED DURING IMPACT TESTING OF AN IRON-35 w/o CHROMIUM-8 w/o ALUMINUM ALLOY

Sample absorbed 100 ft-lb at 275 C. Hardness 240 DPH

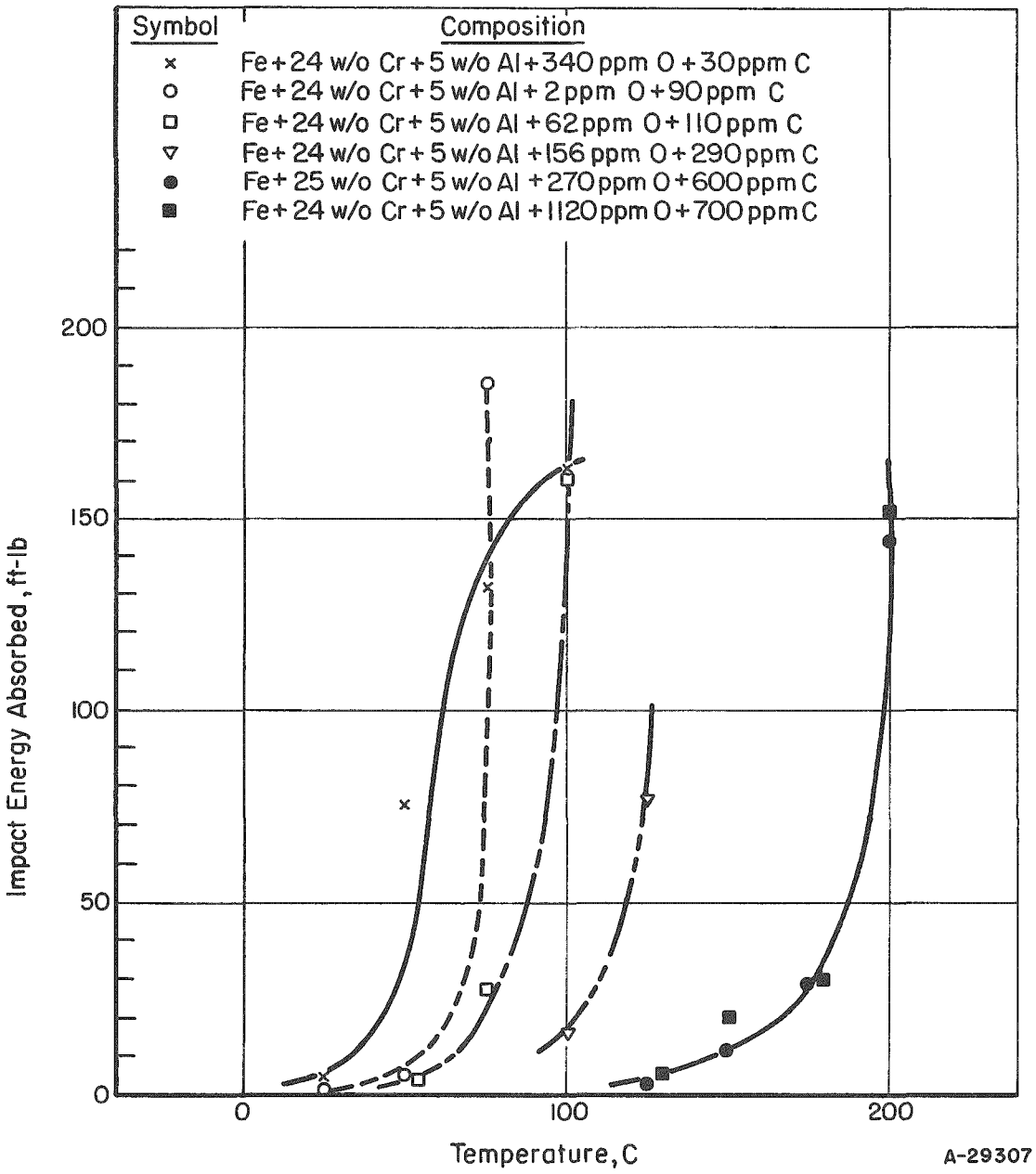

FIGURE 49. EFFECT OF CARBON ON THE TRANSITION TEMPERATURE OF IRON-25 w/o CHROMIUM-5 w/o ALUMINUM ALLOYS

these drosses were examined and were found to be mixtures of oxide (of unknown composition) and metal. A distinct sulfurous odor was given off when the dross was wet. To eliminate this dross and to increase metal fluidity and yields, a high calcium slag, corresponding to $3CaO \cdot Al_2O_3$ and melting at about 1500 C, was added to a number of melts just before pouring. The benefits of this procedure were manifold. Skulls and dross were almost completely eliminated and metal fluidity was noticeably improved. The cleanliness of the resultant metal with respect to oxide clusters and stringers was noticeably improved, and in some cases the oxygen content was reduced to less than 10 ppm. By observing the rate of melting of the artificial slag, the temperature of the molten bath could be judged and adjusted up, or more often down, just before pouring. No ill effects on ingot quality were observed from the use of this slag, but the amount of slag used had to be minimized to avoid crucible erosion. One-pound heats were observed to need about 1 w/o of slag to remove the dross without causing crucible erosion. It has been found desirable to use only about 1/2 w/o of slag on larger heats to avoid excessive crucible erosion.

It was shown earlier that when the aluminum alloy addition is made to the iron-chromium melt, all the oxygen present is removed as alumina, and most of this alumina can be removed as calcium aluminate slag. However, until the aluminum is added, the activity of oxygen in the iron-chromium melt may be very high, and it is possible to use this oxygen to form volatile gas molecules such as carbon monoxide and sulfur dioxide and phosphorus pentoxide. As a result of the reaction of carbon and oxygen to form volatile carbon monoxide, alloys containing as little as 20 ppm of carbon have been produced on occasion (see analyses, Figures 41 and 45). Attempts to use this refining process to produce alloys of superpurity have been unsuccessful. It was found that a 60-min vacuum-refining period readily reduced the carbon content of iron-chromium melts from about 100 ppm to about 10 ppm, but chromium losses were high, and after adding aluminum the carbon content was found to be at least 30 ppm. This result suggests that the aluminum, chromium, and iron should be melted and refined separately and combined in the molten state to avoid contamination by normal handling.

Nitrogen, Sulfur, Silicon, Boron, and Hydrogen. No nitrogen, sulfur, silicon, boron, or hydrogen has been intentionally added to any of the alloys investigated during this research. The raw materials each contained less than 10 ppm nitrogen, and six ingots analyzed for nitrogen all contained 10 ppm or less nitrogen. Electrolytic chromium contains variable amounts of sulfur, typically 100 to 300 ppm, and analyses of 14 ingots showed sulfur ranging from 50 to 90 ppm. No noticeable effect of this range of sulfur variation upon fabricability or impact behavior was observed. Analyses of 15 ingots for silicon showed amounts ranging from less than 100 ppm to 600 ppm, and no effect of this range of silicon was detected. A spot check for boron on two ingots of the same nominal alloy content but of vastly different properties disclosed that both contained less than 30 ppm boron, and it was assumed that boron could not be causing the difference between these alloys. Hydrogen analyses on over 50 ingots disclosed amounts ranging from 0.1 to 60 ppm, and no effect of this variation was observed. Most hydrogen analyses were less than 10 ppm, and it is suspected that the higher analyses represent water or hydrocarbons picked up in handling the specimens used for chemical analysis.

Manganese, Titanium, and Vanadium. It has been observed that the fabricability of many materials is very favorably affected by the addition of powerful deoxidants or carbide formers, generically falling in the category of "gettering agents". The possibility, however remote, that such agents might have utility in iron-chromium-aluminum alloys cannot be overlooked. Analyses for manganese on four ingots containing no added manganese disclosed less than 100 ppm. Typical results on a series of alloys to which 1 w/o manganese was added are shown in Figure 50. Analyses showed that each of the alloys intended to contain 1 w/o manganese actually contained between 0.9 and 1.0 w/o manganese. Figure 50 suggests that 1 w/o manganese has no effect on the ductility of iron-chromium-aluminum alloys. Actually, the fabrication behavior of some of these alloys suggests that manganese may have reduced hot shortness in forging at about 1100 C.

The addition of 0.1 w/o titanium and 1 w/o vanadium to a series of iron-35 w/o chromium-8 w/o aluminum alloys produced results similar to those shown for manganese in Figure 50. There was no significant effect of these additions upon transition temperature, hardness, or fabrication behavior. Neither manganese, titanium, nor vanadium produced any grain-refining effect in the castings.

Results of Arc-Melting Tests

Iron-chromium-aluminum alloys tend to be contaminated and embrittled by contact with most common refractory materials at temperatures above 1500 C. While pure alumina will not embrittle these alloys, the impurities present in all but the purest alumina refractories will cause some embrittlement. Since arc melting can be done in an inert atmosphere and involves almost no contact of molten metal with the crucible, it represents a method by which crucible contamination can be minimized. In an attempt to use this advantage of arc melting, six ingots were prepared by consumable-electrode arc melting. The first two ingots were prepared by cold pressing electrodes from electrolytic chromium, electrolytic iron, and high-purity aluminum shot. The metal appeared mushy and sluggish during melting, but produced satisfactory ingots, one of which is shown in Figure 31. Neither of these ingots could be forged at 1230 C, and both were sectioned and remelted. The remelted ingots appeared cleaner, but again both failed in forging at 1230 C. Figure 51 shows a vertical section of one of these ingots and the nature of the failure in forging. It is apparent that arc melting consolidates the few impurities in the metal into massive slag pockets in the ingot, and that the rapid cooling inherent in arc melting results in a pronounced columnar structure in the ingot. Both of these conditions are believed to contribute to the failure shown in Figure 51. These ingots which were nominally 35 w/o chromium-7 w/o aluminum contained 6.0 to 6.2 w/o aluminum and 200 to 300 ppm carbon.

Four additional ingots prepared from materials of different types, both with and without aluminum, produced essentially the same results. One ingot containing aluminum was badly cracked in the as-cast condition, probably from the rapid shrinkage produced by the chill-casting effect of the water-cooled copper mold. One ingot of iron-38 w/o chromium alloy was fabricated to bar stock for remelting, but the remelted ingot still contained slag pockets and showed a carbon content of 170 ppm. Two ingots of

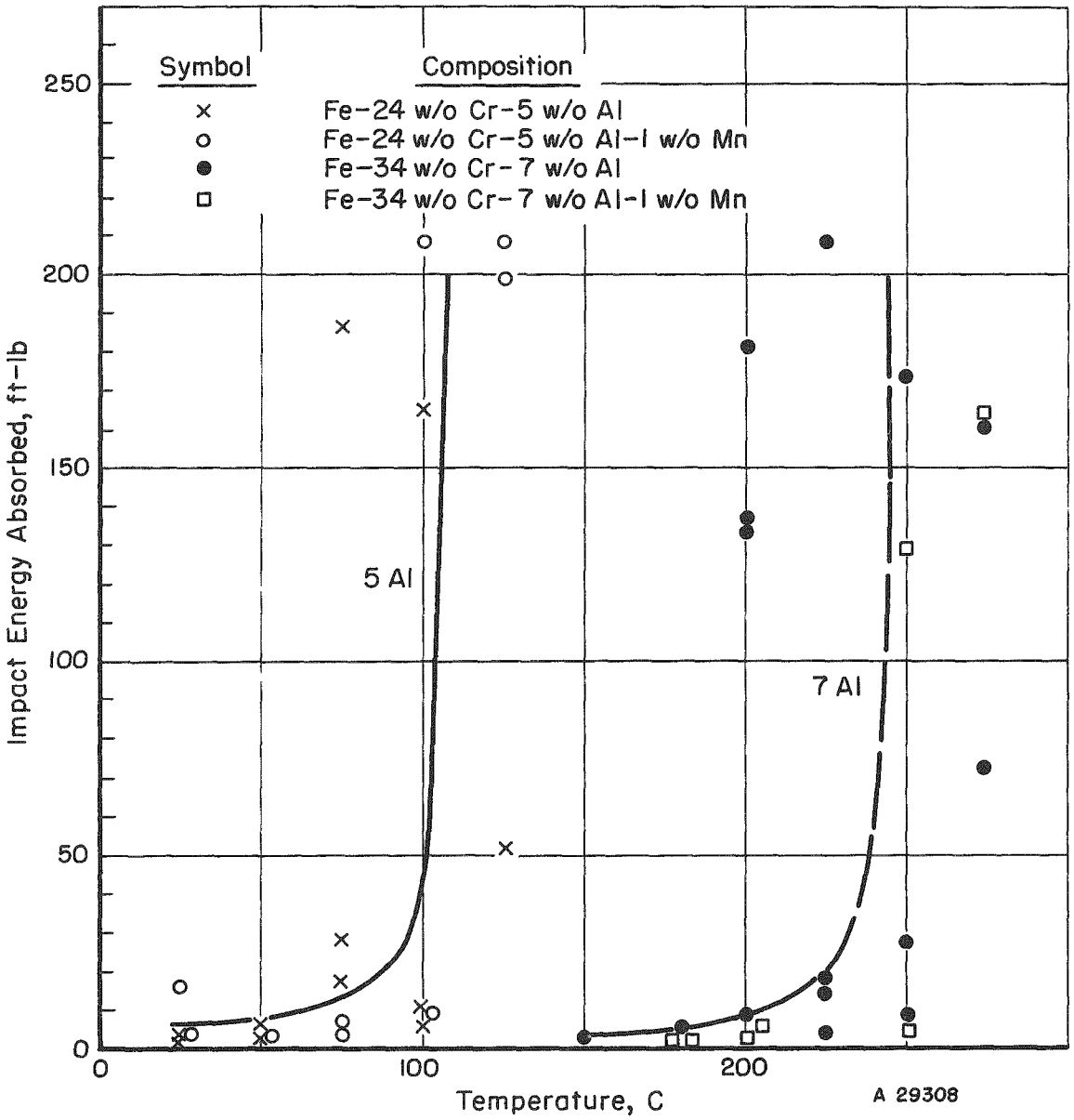

FIGURE 50. EFFECT OF MANGANESE ON THE TRANSITION TEMPERATURE OF IRON-CHROMIUM-ALUMINUM ALLOYS

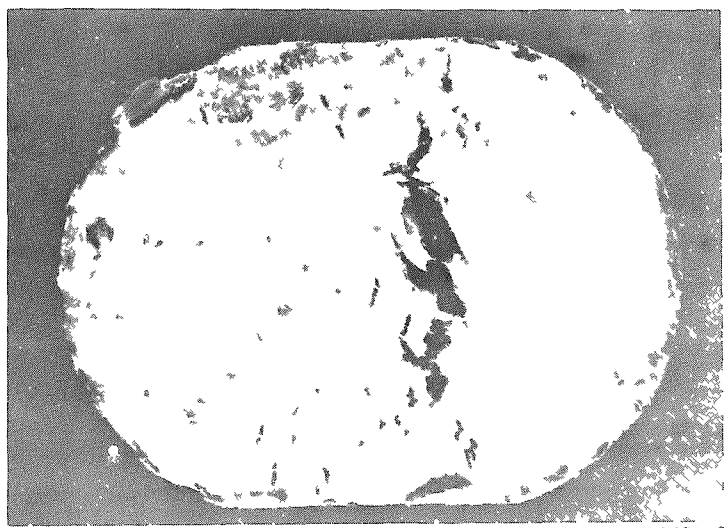

1X RM8668

a. Top of Ingot as Forged

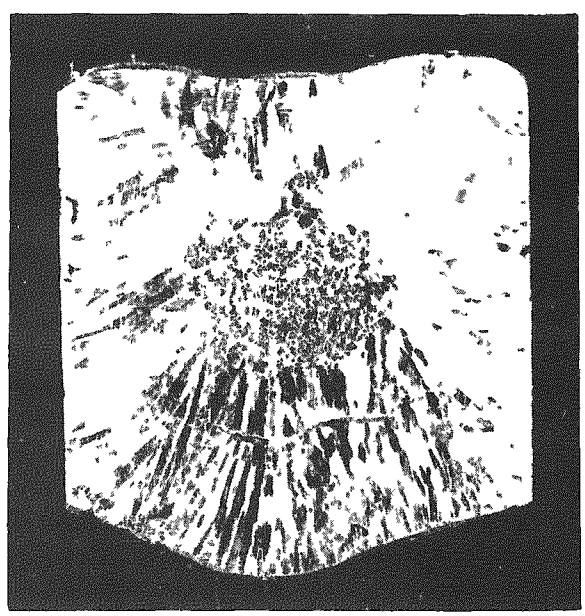

1X RM8794

b. Vertical Section of Same Ingot, Etched

FIGURE 51. IRON-35 w/o CHROMIUM-7 w/o ALUMINUM ALLOY PREPARED BY DOUBLE CONSUMABLE-ELECTRODE ARC MELTING IN A WATER-COOLED COPPER CRUCIBLE AND FORGED AT 1230 C

iron-38 w/o chromium alloy were prepared by vacuum arc melting rather than under a helium atmosphere. Both of these had extremely poor surfaces covered with pockets of dirt or slag, and one of them contained a deep center cavity from which it looked as if gases formed during solidification had been expelled explosively. These later two ingots showed carbon contents of 100 ppm.

These results show that while arc melting may eliminate crucible reactions, the process does not allow for liquation of slags and drosses normally formed during melting of iron-chromium-aluminum alloys, nor does it allow for removal of volatile impurities in a single melting operation; moreover, it results in a chill-cast structure which is difficult, if not impossible, to fabricate.

Conclusions and Recommendations

Iron-25 to 35 w/o chromium-3 to 8 w/o aluminum alloys are ferritic solid-solution type alloys which differ one from the other only in degree.

For alloys of the purity described in this report (alloys containing about 200 ppm oxygen and 50 ppm carbon), there appears to exist a ductility transition temperature which is a fundamental property of the solid solution and which is dependent primarily upon the aluminum content of the alloy. This ductility transition appears to be associated with the deformation mechanisms of the solid solution; plastic deformation occurs by twinning on definite crystallographic planes; brittle fracture occurs by cleavage on similar crystallographic planes. The ductility transition temperature for a particular mode of deformation, such as by the impact test, apparently may be defined as that temperature at which the critical stress for cleavage becomes equal to the critical stress for twinning.

Because of the tendency of the various alloying elements to combine with nearly all other elements, iron-chromium-aluminum alloys have very low solubilities for most impurity atoms. Those impurities, such as carbon, which are slightly soluble and which tend to concentrate at grain boundaries are particularly detrimental to the hot and cold ductility of iron-chromium-aluminum alloys. Because of the notch sensitivity of iron-chromium-aluminum alloys, grain-boundary impurities tend to promote brittleness and to raise the brittle-ductile transition temperature. It is not known whether or not a further increase in the purity of these alloys (to a level corresponding to perhaps 5 ppm carbon) would have an additional effect on the brittle-ductile transition temperature such as that described by Figures 20 and 49. Grain growth and the associated redistribution of impurities at the grain boundaries could not be separated as a cause of raised transition temperatures. Recrystallization, however, does not cause embrittlement.

Iron-chromium-aluminum alloys containing up to 35 w/o chromium and 8 w/o aluminum are fabricable both hot and cold. However, hot fabrication of these alloys is strongly dependent upon ingot cleanliness and grain structure. Dirt and columnar grain structures must be avoided. Fine-grained structures are desirable and are promoted by low casting temperatures. Recommended forging temperature is 1200 C for the iron-35 w/o chromium-7 w/o aluminum alloy; recommended rolling temperature is 1000 C. Slightly lower temperatures may be used for leaner alloys. Reheating for hot fabrication should be minimized.

The iron-25 w/o chromium-5 w/o aluminum alloy can be cold rolled more than 50 per cent at room temperature. The iron-35 w/o chromium-7 w/o aluminum alloy can be cold rolled in similar fashion at 350 C, but is brittle at room temperature.

Iron-chromium-aluminum alloys are highly reactive materials at temperatures above 1500 C. These alloys should be melted in a vacuum (approximately 10 μ absolute pressure or less). High-density high-purity alumina crucibles have proved to be most satisfactory for melting these alloys. Magnesia crucibles of similar purity, if available, are presumed to be equally satisfactory. The iron and chromium should be melted and thoroughly outgassed before any aluminum is added. It is not necessary to add the aluminum under vacuum; an inert atmosphere is equally satisfactory. After adding the aluminum to deoxidize the melt, it is desirable to remove the resultant dross by means of a high-calcium slag of the type $3CaO \cdot Al_2O_3$. The use of a slag of this type (melting at about 1500 C) increases melt fluidity and metal yields, reduces the oxide content of the metal, and allows the temperature of the melt to be reduced to the minimum desired for producing fine-grained ingots.

Arc melting is not a satisfactory method for obtaining high-purity iron-chromium-aluminum alloys. Arc melting provides no method for removal of oxide drosses, and the water-cooled copper hearth tends to produce columnar grain structures and internal cracking.

OXIDATION RESISTANCE OF IRON-23.7 w/o CHROMIUM-6.0 w/o ALUMINUM IN VARIOUS GAS ATMOSPHERES AT 1900 AND 2100 F

Background

The excellent oxidation resistance of iron-chromium-aluminum alloys makes them attractive for many applications requiring oxidation-corrosion resistance at very high temperatures. The behavior of these ferritic alloys from 1400 to 2300 F (760 to 1260 C) in air has been reported in previous investigations[2,3,4,44,67]; and it has been concluded that optimum oxidation resistance is obtained with iron-chromium-aluminum alloys containing about 6 w/o aluminum.

In commercial furnace atmospheres, small amounts of moisture, metal oxides, sulfur dioxide, carbon dioxide, and other gases are often encountered. To evaluate the usefulness of a high-temperature alloy in commercial air atmospheres, it is necessary to determine the effect of such trace gases present in the atmosphere. Data on the oxidation resistance of iron-30 w/o chromium-5 w/o aluminum and nickel-20 w/o chromium alloys at 1920 and 2190 F (1048 and 1199 C), respectively, in atmospheres of air, carbon dioxide, nitrogen, oxygen, and hydrogen, water gas, and city gas have been reported by Hessenbruch, et al.[45] They found that only a hydrogen atmosphere leaves the alloys entirely unchanged. With carbon-containing gases, e.g., water gas, a marked carburizing effect was observed. Nitrogen reacts with the alloys, forming nitrides of aluminum and/or chromium, and shortens the useful life of the alloy. Other data[46 through 66] serve to complement these results.

Data from oxidation tests of an iron-23.7 w/o chromium-6.0 w/o aluminum and a nickel-20.0 w/o chromium-1.1 w/o niobium alloy (tested for comparison purposes) at 1900 and 2100 F (1038 and 1150 C) in an air atmosphere containing various amounts of moisture and carbon dioxide were obtained. Alloy sheet specimens were exposed for 100 hr at temperature in the various gas atmospheres. Weight-gain and oxide-penetration measurements were chosen as a basis for evaluating the oxidation resistance of the alloys. Oxidation tests were made in the following atmospheres flowing at the rate of 1 liter per min:

(1) Dry air (0.005 volume per cent H_2O)

(2) Normal atmosphere (air plus 0.76 volume per cent H_2O)

(3) Air plus 2.5 volume per cent H_2O

(4) Air plus 2.5 volume per cent H_2O plus 2.5 volume per cent CO_2

(5) Air plus 5 volume per cent H_2O

(6) Dry air plus 5 volume per cent CO_2

(7) Air plus 5 volume per cent H_2O plus 5 volume per cent CO_2

(8) Nitrogen plus 9 volume per cent H_2O plus 6.3 volume per cent CO_2 plus 8.2 volume per cent oxygen.

Alloy Preparation and Testing

The iron-chromium-aluminum and nickel-chromium-niobium alloys used in this investigation were obtained in the form of 0.060-in. cold-rolled sheet. Chemical analyses of the sheet showed that the iron-chromium-aluminum alloy contained 23.7 w/o chromium, 6.0 w/o aluminum, 0.03 w/o carbon, 0.01 w/o silicon, and 0.01 w/o manganese and that the nickel-chromium-niobium alloy contained 78.9 w/o nickel, 20.0 w/o chromium, and 1.1 w/o niobium.

Both alloys were rolled to 0.030-in. sheet at 1500 F (815 C), water quenched, and cold rolled to 0.015-in. sheet. The iron-chromium-aluminum sheet was annealed at 1400 F (760 C) for 15 min, water quenched, and vapor blasted. The nickel-chromium-niobium sheet was annealed for 15 min at 1700 F (926 C) air cooled, and vapor blasted. Specimens about 1 by 0.5 by 0.015 in. were cut from the alloy sheets. The length, width, and thickness of each specimen were accurately measured with a micrometer and the dimensions subsequently used to calculate the surface area. The specimens were cleaned in acetone, dried, and weighed. They were placed in individual Alundum tubes and a combined weight was recorded.

Tests were conducted at 1900 and 2100 F (1038 and 1150 C) for 100 hr. Duplicate specimens were tested. At the conclusion of a 100-hr run each specimen was cooled and weighed with the accumulated oxide in the Alundum container, and weight-gain

values were determined. Each specimen was sheared in four parts and mounted in Bakelite such that the freshly cut edges were exposed for examination. The minimum and average thicknesses of the unaffected metal, measured with a micrometer eyepiece at suitable magnification, were subtracted from the original thickness of the specimen. The differences, divided by two, were taken as the maximum and average oxide penetrations into the specimen. These measurements were made with a filar micrometer eyepiece accurate to 0.0001 in.

Photomicrographs were taken of representative areas of the as-polished edges of each specimen.

The test apparatus used in this work is shown schematically in Figure 52. It consisted of a gas flowmeter, water bath with heater and thermostat, dew pointer, and horizontal Globar furnace. For tests in normal air, a small fan was used to obtain a flow rate of 1 liter of air per min.

Cylinders of dry air, dry air plus 5 volume per cent CO_2 mixture, and nitrogen plus 9 volume per cent H_2O plus 6.3 volume per cent CO_2 plus 8.2 volume per cent O_2 mixture, were purchased and supplied the various combinations of atmospheres used in the tests. A flow rate of 1 liter of gas per min at 70 F (21 C) and atmospheric pressure was obtained by manually operating the pressure regulators on the gas cylinders.

For atmospheres containing water vapor, the gas was passed through a frit bubbler into water. The amount of water vapor obtained was dependent on the temperature of the water, which was controlled by a water immersion thermostat and heater. Once it had passed through the water, the gas was maintained at a temperature above the dew point of the desired atmosphere. Four or five dew-point measurements were made each day to determine the amount of water vapor in the atmosphere prior to its passing through the Globar furnace. Accuracy of the dew-point determination was ± 0.5 volume per cent H_2O. The Alundum tubes containing the test specimen were fit snugly into a K-brick plug which was inserted in the Inconel sleeve.

Results and Discussion

Evaluation of the oxidation resistance of the iron-chromium-aluminum alloy (and the nickel-chromium-niobium alloy) has been made both on the basis of weight gain per unit area per 100 hr and on the basis of maximum and average oxide penetration following the 100-hr test. Since iron-chromium-aluminum alloys are being considered for engineering applications where the amount of sound, residual metal is of prime importance, discussion of the experimental data is based only on the maximum values of weight gain and oxide penetration.

The data of Table 10 indicate that the iron-chromium-aluminum alloy had much better oxidation resistance than the concurrently tested nickel-chromium-niobium alloy in all atmospheres at temperatures of 1900 and 2100 F (1037 and 1150 C). Weight-gain and oxide-penetration values for the nickel-chromium-niobium alloy were approximately 50 per cent greater in all atmospheres at both temperatures. One exception to this generalization was noted for certain tests in air containing 5 volume per cent water vapor at 1900 F. In these tests the iron-chromium-aluminum alloy exhibited a higher

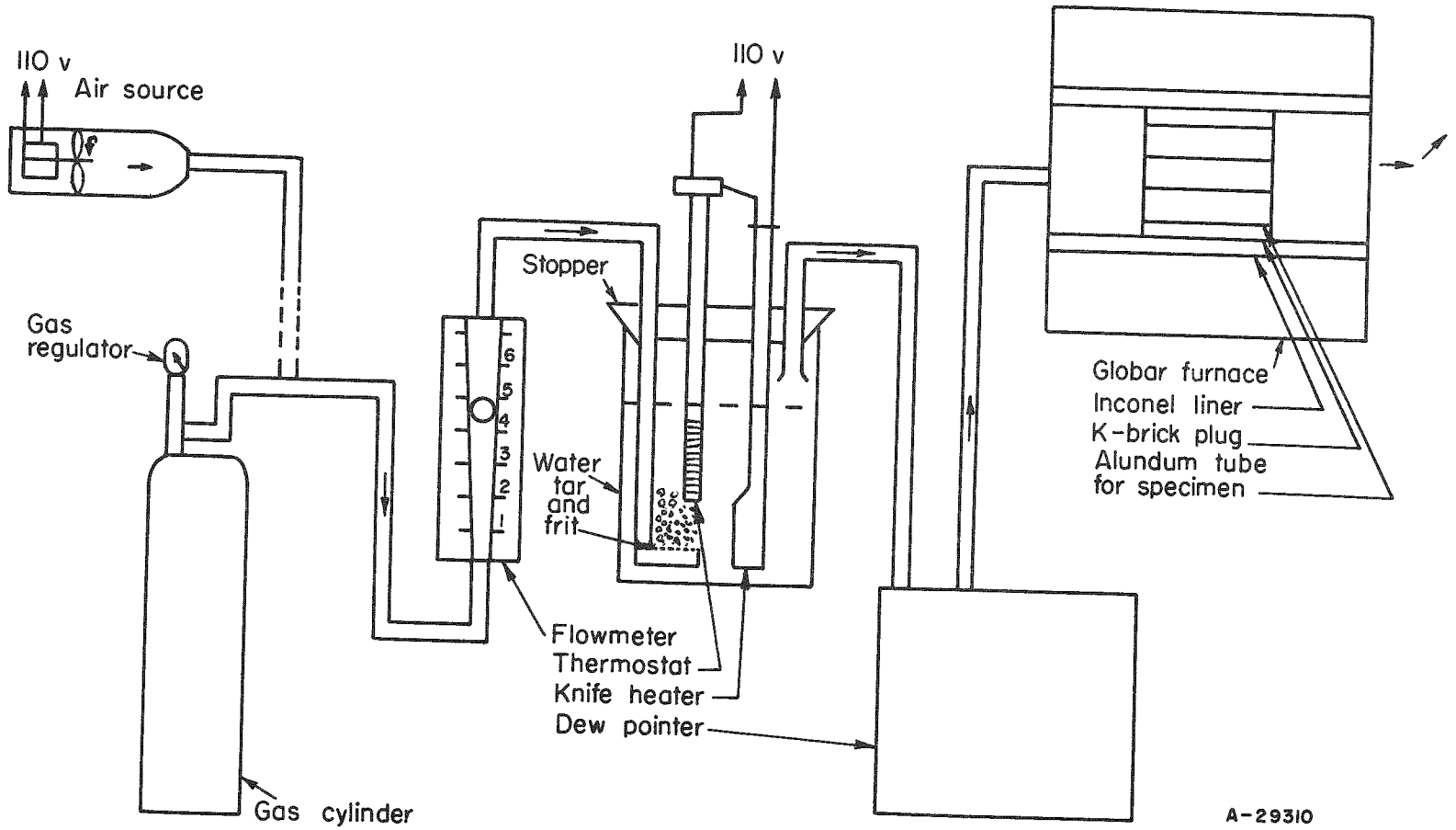

FIGURE 52. CIRCUIT OF FLOWING ATMOSPHERE

TABLE 10. OXIDATION TESTS OF IRON-23.7 w/o CHROMIUM-6.0 w/o ALUMINUM AND NICKEL-20.0 w/o CHROMIUM-1.1 w/o NIOBIUM ALLOYS IN VARIOUS GAS ATMOSPHERES AT 1900 AND 2100 F (1038 AND 1150 C)

Alloy	Temperature, F	Weight Gain, $g/(cm^2)(100\ hr)$	Penetration, 10^{-5} in. Maximum	Penetration, 10^{-5} in. Average
	Dry Air (0.005 Volume Per Cent H_2O)			
Fe-Cr-Al	1900	.0016	125	57
	1900	.0022	99	33
	2100	.0037	98	27
	2100	.0031	141	36
Ni-Cr-Nb	1900	.0041	240	195
	1900	.0024	102	74
	2100	.0051	166	128
	2100	.0037	273	204
	Normal Air (0.76 Volume Per Cent H_2O)			
Fe-Cr-Al	1900	.0014	175[a]	55
	1900	.0014	55	20
	2100	.0027	70	40
	2100	.0031	65	10
Ni-Cr-Nb	1900	.0030	160	70
	1900	.0025	165	60
	2100	.0066	190	85
	2100	.0050	215	75
	Air Plus 2.5 Volume Per Cent H_2O			
Fe-Cr-Al	1900	.0020	41	14
	1900	.0017	45	26
	2100	.0028	42	34
	2100	.0023	45	12
Ni-Cr-Nb	1900	.0024	102	26
	1900	.0020	87	29
	2100	.0047	130	98
	2100	.0050	149	113
	Air Plus 2.5 Volume Per Cent H_2O Plus 2.5 Volume Per Cent CO_2			
Fe-Cr-Al	1900	.0031	29	16
	1900	.0036	115	77
	2100	.0064	45	27
	2100	.0051	109	86
Ni-Cr-Nb	1900	.0051	151	103
	1900	.0027	77	42
	2100	.0081	269	215
	2100	.0099	269	218

TABLE 10. (Continued)

Alloy	Temperature, F	Weight Gain, $g/(cm^2)(100\ hr)$	Penetration, 10^{-5} in. Maximum	Penetration, 10^{-5} in. Average
		Air Plus 5 Volume Per Cent H_2O		
Fe-Cr-Al	1900	.0031	74	56
	1900	.0040	72	51
	2100	.0057	41	16
	2100	.0081	112	48
Ni-Cr-Nb	1900	.0028	96	51
	1900	.0026	131	66
	2100	.0190	250	220
	2100	.0207	269	238
		Dry Air Plus 5 Volume Per Cent CO_2		
Fe-Cr-Al	1900	.0022	133	51
	1900	.0022	48	9
	2100	.0021	149	32
	2100	.0022	114	25
Ni-Cr-Nb	1900	.0032	215	98
	1900	.0025	246	125
	2100	.0067	299	198
	2100	.0059	208	166
		Air Plus 5 Volume Per Cent H_2O Plus 5 Volume Per Cent CO_2		
Fe-Cr-Al	1900	.0038	125	112
	1900	.0027	123	41
	2100	.0039	143	86
	2100	.0029	29	22
Ni-Cr-Nb	1900	.0029	141	71
	1900	.0042	109	82
	2100	.0059	176	141
	2100	.0058	197	157
		Nitrogen Plus 9 Volume Per Cent H_2O Plus 6.3 Volume Per Cent CO_2 Plus 8.2 Volume Per Cent Oxygen		
Fe-Cr-Al	2100	.0086	113	45
	2100	.0061	97	45
	2100	.0073	58	40
	2100	.0062	51	33
Ni-Cr-Nb	1900	.0036	115	83
	1900	.0021	84	65
	1900	.0029	121	89
	1900	.0023	139	97

(a) The high value for oxide penetration probably resulted from a defect in the specimen prior to oxidation testing.

TABLE 11. PERFORMANCE RATINGS[a] OF IRON-23.7 w/o CHROMIUM-6/0 w/o ALUMINUM AND NICKEL-20.0 w/o CHROMIUM-1.1 w/o NIOBIUM ALLOYS IN VARIOUS GAS ATMOSPHERES AT 1900 AND 2100 F (1038 AND 1150 C)

Atmosphere	Fe-Cr-Al		Ni-Cr-Nb	
	1900 F	2100 F	1900 F	2100 F
Normal air	A	A	B	C
Dry air (0.005 volume per cent H_2O)	B	B	C	D
Air plus 2.5 volume per cent H_2O	A	A	A	B
Air plus 5 volume per cent H_2O	A	A	B	D
Air plus 2.5 volume per cent H_2O plus 2.5 volume per cent CO_2	B	B	B	D
Air plus 5 volume per cent H_2O plus 5 volume per cent CO_2	B	B	B	C
Dry air plus 5 volume per cent CO_2	B	B	D	D
Nitrogen plus 9 volume per cent H_2O plus 6 volume per cent CO_2 plus 8 volume per cent oxygen	(b)	A	B	(b)

(a) Based on maximum oxide penetration:

Rating	Maximum Oxide Penetration, 10^{-5} in.
A	45 to 110
B	111 to 176
C	177 to 242
D	243 to 299

(b) Not tested.

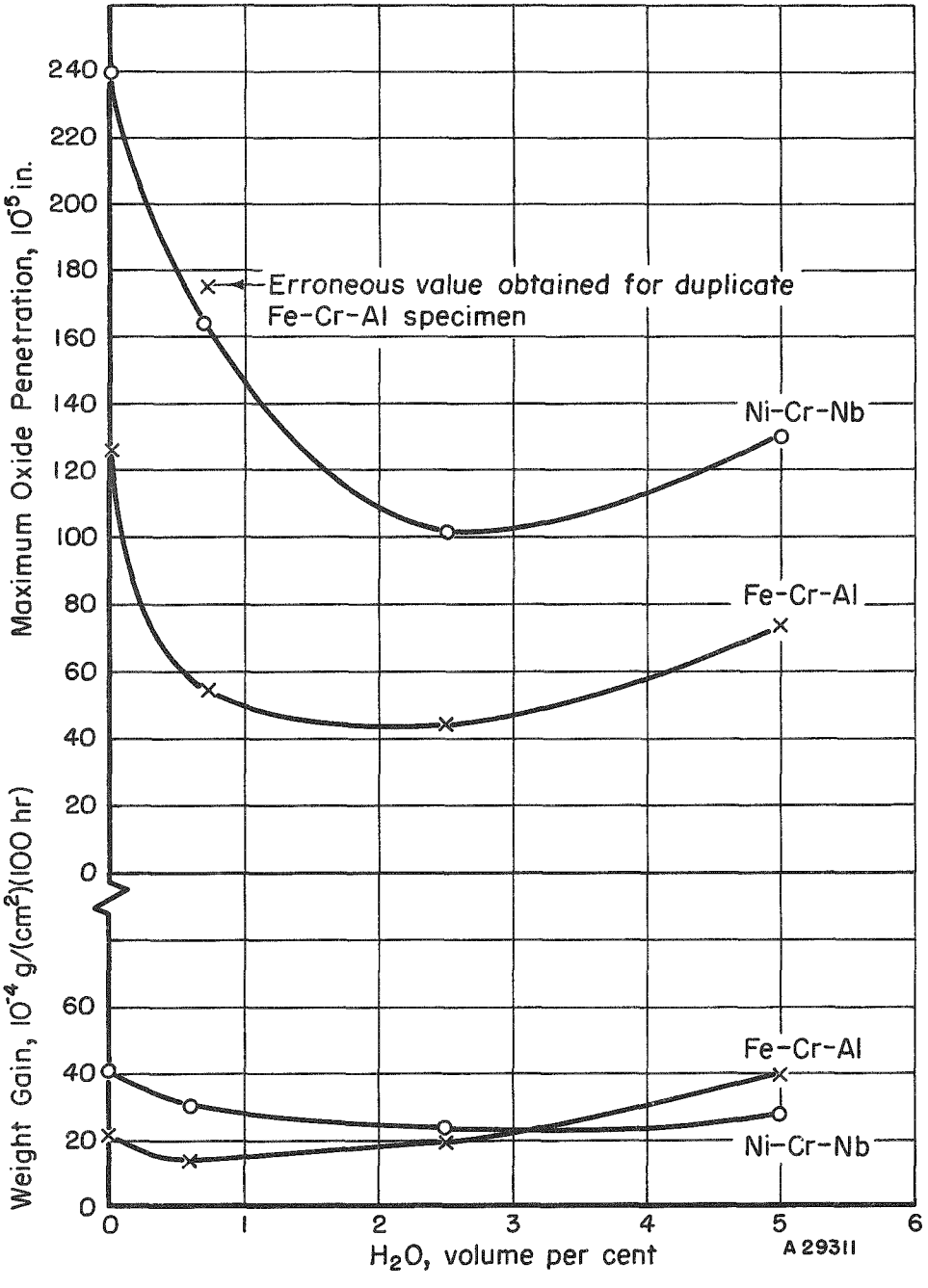

FIGURE 53. THE EFFECT OF WATER VAPOR ON THE OXIDATION BEHAVIOR OF IRON-23.8 w/o CHROMIUM-6.0 w/o ALUMINUM AND NICKEL-20.0 w/o CHROMIUM-1.1 w/o NIOBIUM ALLOYS AT 1900 F

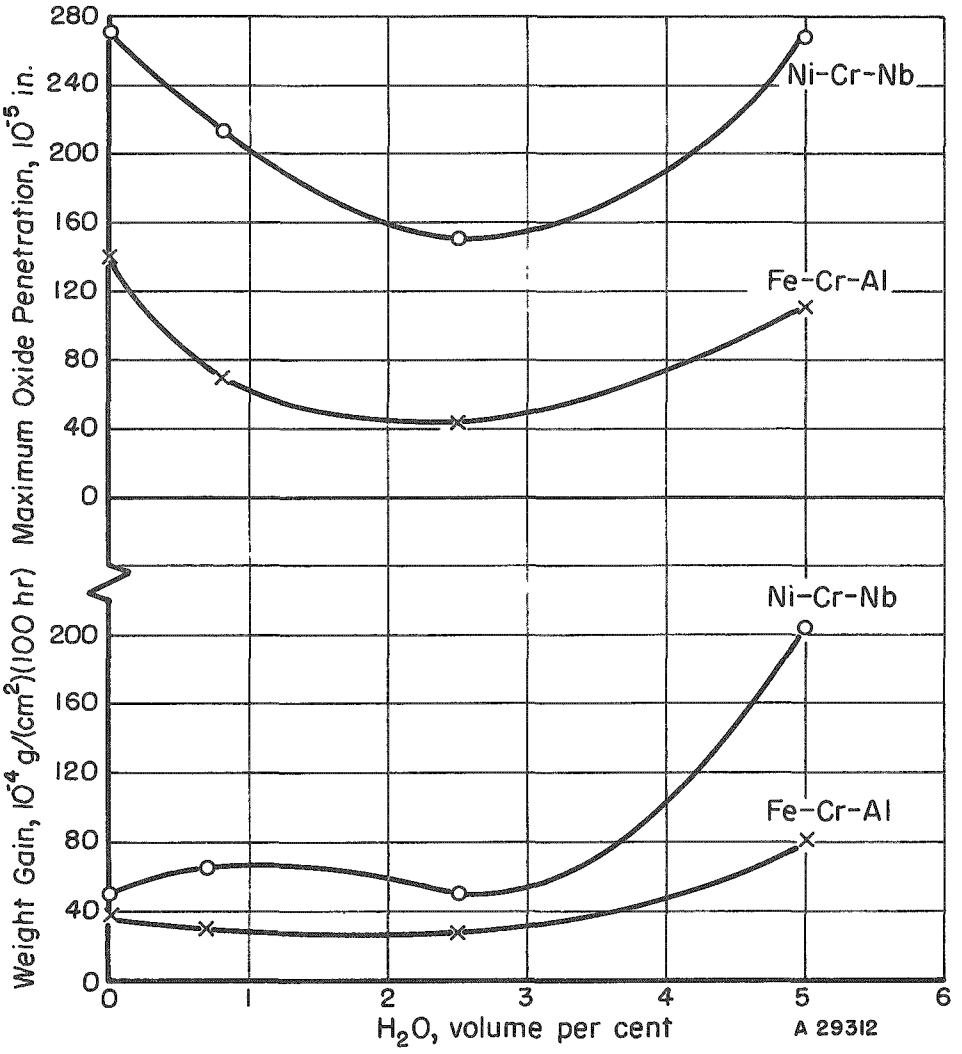

FIGURE 54. THE EFFECT OF WATER VAPOR ON THE OXIDATION BEHAVIOR OF IRON-23.8 w/o CHROMIUM-6.0 w/o ALUMINUM AND NICKEL-20.0 w/o CHROMIUM-1.1 w/o NIOBIUM ALLOYS AT 2100 F

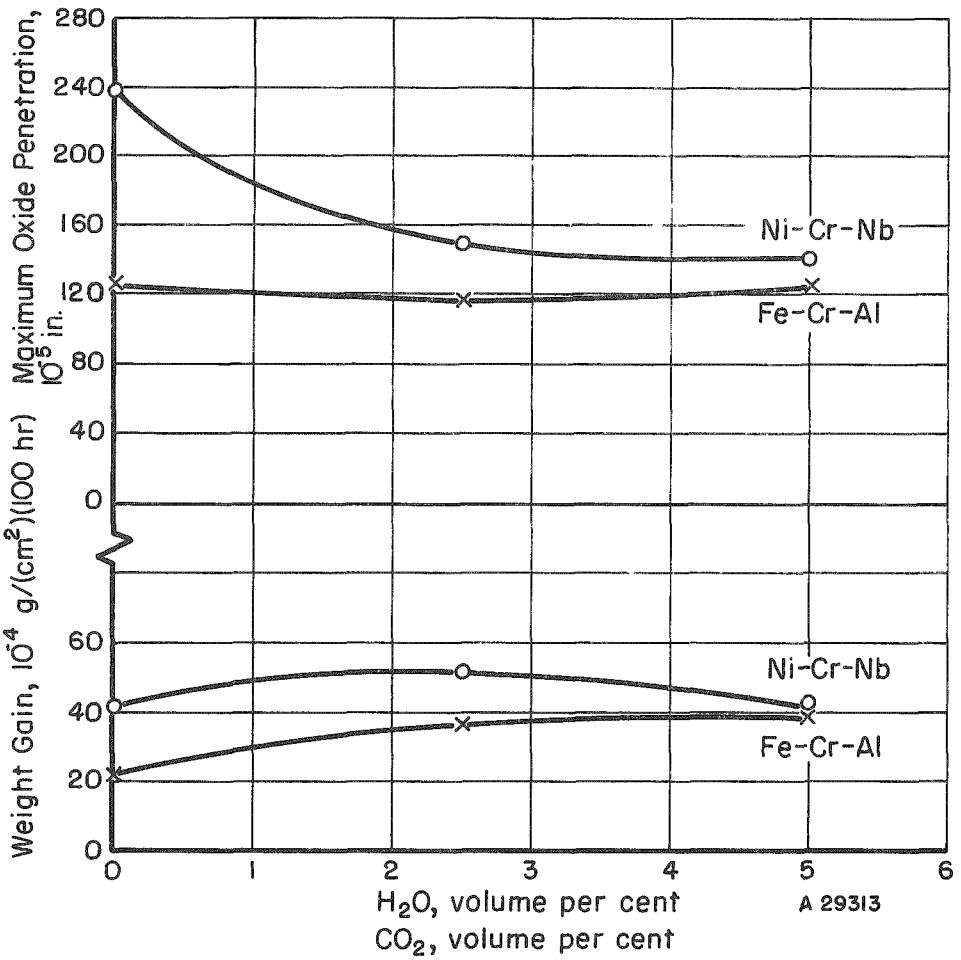

FIGURE 55. THE EFFECT OF H_2O AND CO_2 ON THE OXIDATION BEHAVIOR OF IRON-23.8 w/o CHROMIUM-6.0 w/o ALUMINUM AND NICKEL-20.0 w/o CHROMIUM-1.1 w/o NIOBIUM ALLOYS AT 1900 F

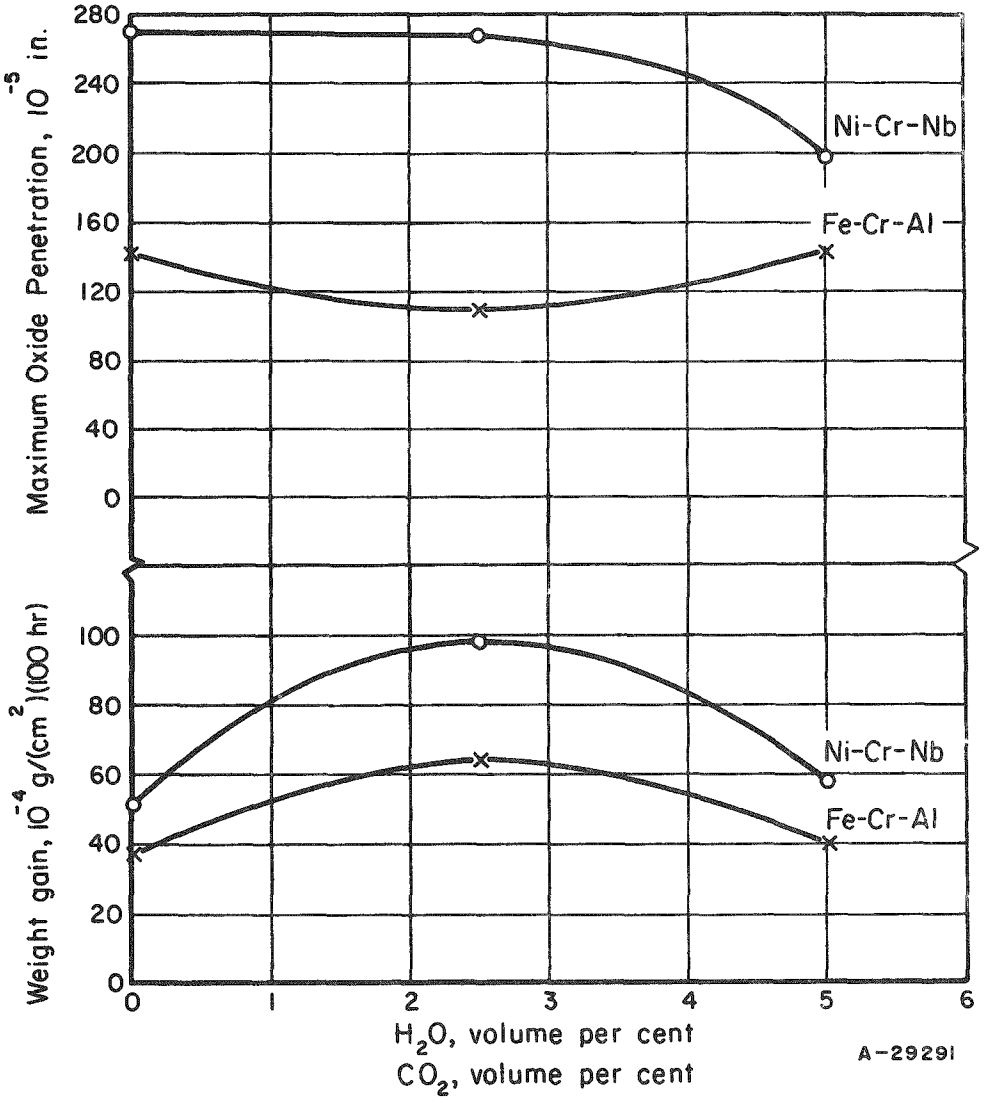

FIGURE 56. THE EFFECT OF H_2O AND CO_2 ON THE OXIDATION BEHAVIOR OF IRON-23.8 w/o CHROMIUM-6.0 w/o ALUMINUM AND NICKEL-20.0 w/o CHROMIUM-1.1 w/o NIOBIUM ALLOYS AT 2100 F

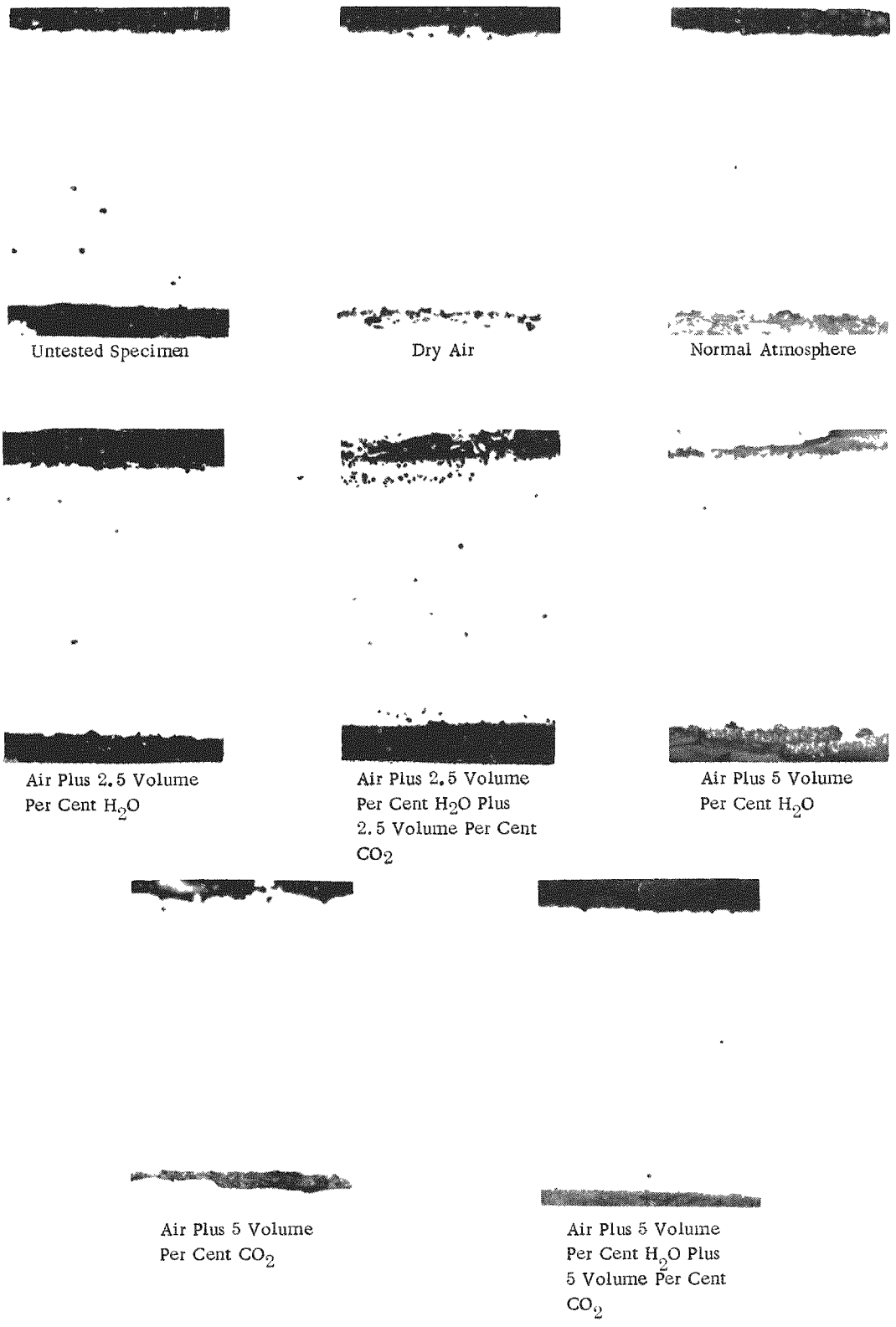

N43251

FIGURE 57. OXIDATION OF IRON-23.7 w/o CHROMIUM-6.0 w/o ALUMINUM ALLOY AT 1900 F IN VARIOUS GAS ATMOSPHERES

Duration of test, 100 hr. Original magnification 250X, reduced for presentation.

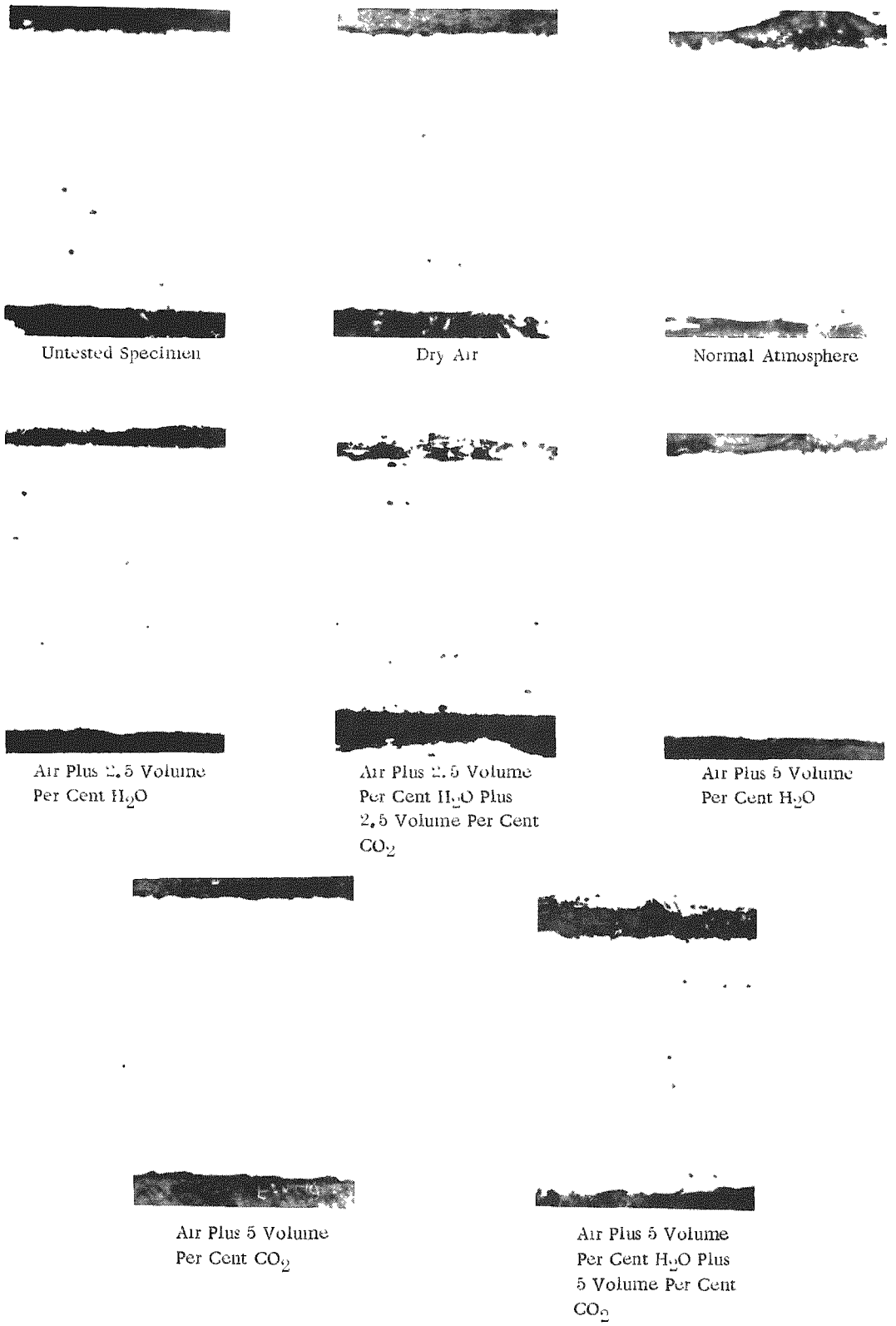

N43247

FIGURE 58. OXIDATION OF IRON-23.7 w/o CHROMIUM-6.0 w/o ALUMINUM ALLOY AT 2100 F IN VARIOUS GAS ATMOSPHERES

Duration of test, 100 hr. Original magnification 250X, reduced for presentation.

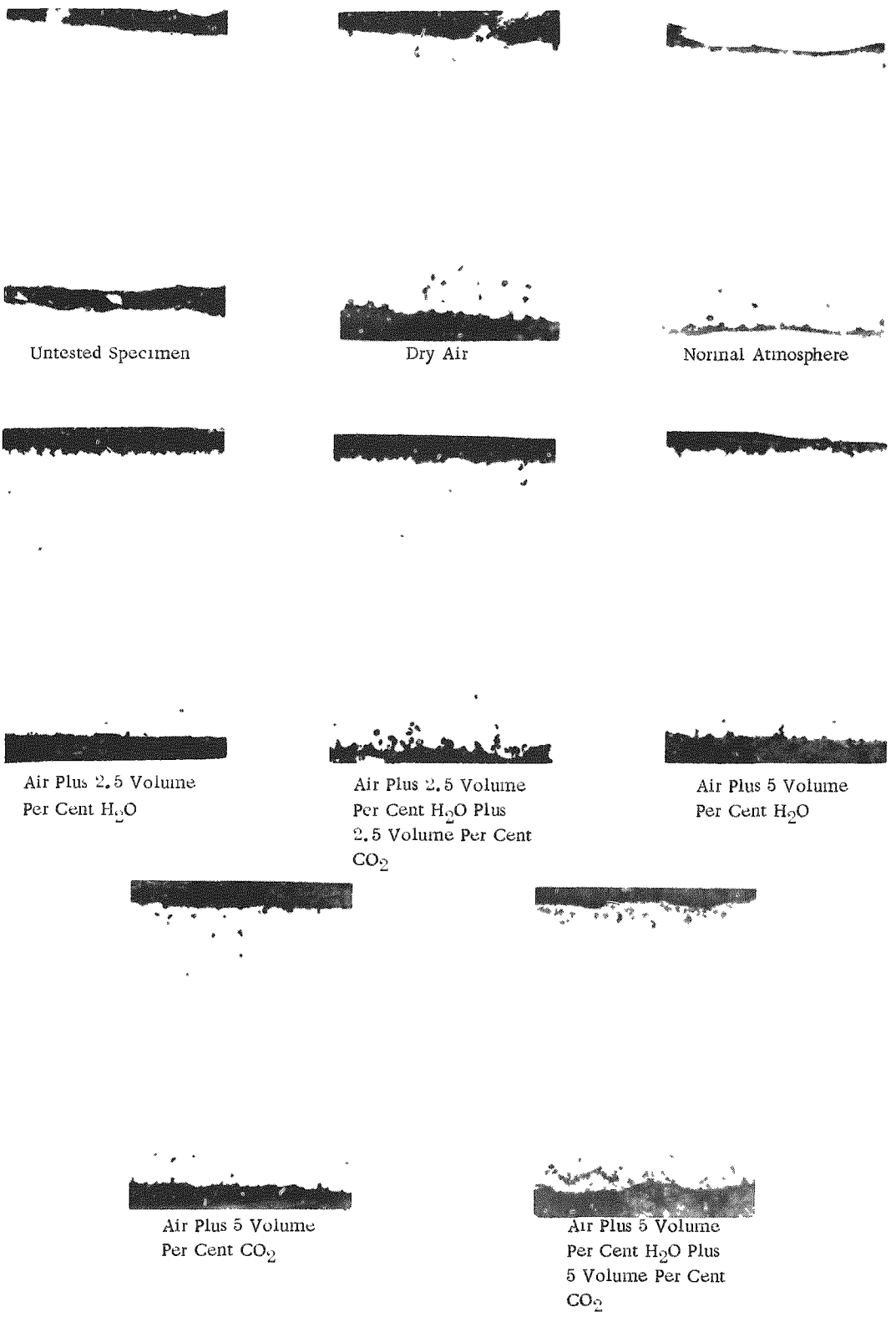

FIGURE 59. OXIDATION OF NICKEL-19.9 w/o CHROMIUM-1.1 w/o NIOBIUM ALLOY AT 1900 F IN VARIOUS GAS ATMOSPHERES

Duration of test, 100 hr. Original magnification 250X, reduced for presentation.

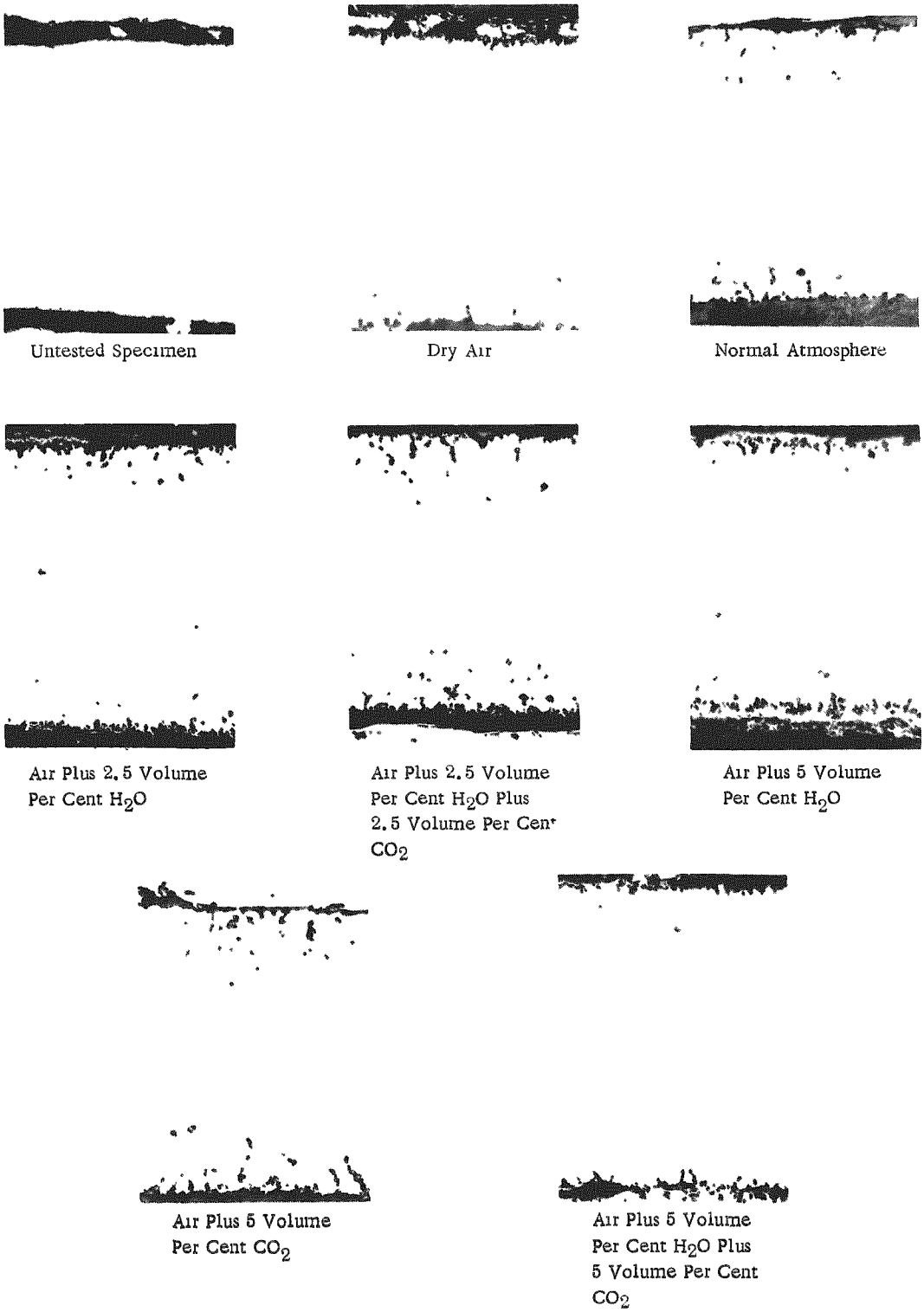

FIGURE 60. OXIDATION OF NICKEL-19.9 w/o CHROMIUM-1.1 w/o NIOBIUM ALLOY AT 2100 F IN VARIOUS GAS ATMOSPHERES

Duration of test, 100 hr. Original magnification 250X, reduced for presentation.

weight gain than the nickel-chromium-niobium alloy. No apparent reason was noted for this exceptional behavior. Weight gain and oxide penetration were slightly higher at 2100 F than at 1900 F for both alloys in all atmospheres. These data suggest increased diffusion rates at 2100 F for aluminum and chromium which provide the oxidation resistance of the alloys.[45] Table 11 shows performance ratings assigned to both alloys on the basis of maximum-oxide-penetration data obtained from the tests in all atmospheres at 1900 and 2100 F. These ratings form a basis for comparison of the oxidation resistance of the alloys as affected by test temperatures and test atmosphere. Maximum values of oxide penetration and weight gain have been plotted against volume per cent water vapor and volume per cent water vapor plus carbon dioxide in the test atmospheres at 1400 and 2100 F in Figures 53 through 56.

Figures 53 and 54 show that the minimum rate of oxidation occurs in atmospheres containing 2.5 volume per cent water vapor. More or less water vapor in the test atmosphere increases the oxidation rates of both alloys at each temperature. Addition of a like amount of CO_2 to atmospheres containing H_2O reverses the curves as shown in Figures 55 and 56; the maximum rates of oxidation were observed in an atmosphere of 2.5 volume per cent H_2O plus 2.5 volume per cent CO_2. The presence of CO_2 in the test atmosphere increased the rate of weight gain and the rate of oxide penetration into the alloys at both temperatures. The deleterious effects of CO_2 in the test atmospheres suggest a possible reaction of CO_2 and H_2O to form an acid environment which may tend to change the form or density of the oxidation products on the alloys. Deterioration of the protective aluminum oxide and chromium oxide films results in depletion of the aluminum and chromium content of the alloys near the surface with resultant accelerated corrosion.

The oxidation resistance of the alloy in dry air showed improvement with additions of water vapor. These results suggest a possible beneficial effect from free oxygen available from decomposed water vapor. The oxygen may serve to enhance the formation of a protective oxide coating on the alloys.

Photomicrographs were taken of the as-polished surface edge of each tested specimen with the exception of those tested in air plus 9 volume per cent H_2O plus 6 volume per cent CO_2. As seen in Figures 57 and 58, oxidation of the iron-chromium-aluminum alloys proceeded from the surface to the center of each specimen in a uniform manner. Ferritic alloys are not susceptible to intergranular attack by gases at high temperatures. However, Figures 59 and 60 show some evidence of an intergranular attack on the nickel-chromium-niobium alloy which may account for the higher rates of weight gain and oxide penetration noted for this material.

REFERENCES

(1) Case, S. L., and Van Horn, K. R., Aluminum in Iron and Steel, John Wiley and Sons, Inc., New York (1953), 478 pp.

(2) Jablonowski, E. J., Shober, F. R., and Dickerson, R. F., "High-Temperature Oxidation Resistance of Thin Iron-Chromium-Aluminum Alloy Sheet", BMI-1230 (October 22, 1957).

(3) Stacy, J. T., Peoples, R. S., Shober, F. R., and Boyd, W. K., "Effect of Aluminum on the Oxidation Resistance of Iron-Chromium-Aluminum Alloys at 2100 F", BMI-1131 (September 14, 1956). Secret.

(4) Saller, H. A., Stacy, J. T., and Eddy, N. S., "Investigation of Wrought Iron-Chromium-Aluminum Alloys for Service at 2200 F", BMI-922 (June 28, 1954).

(5) Saller, H. A., Stacy, J. T., and Porembka, S. W., "Investigation of Wrought Iron-Chromium-Aluminum Alloys Containing Platinum and Palladium", BMI-1017 (July 12, 1955).

(6) Saller, H. A., Stacy, J. T., and VanEcho, J. A., "Evaluation of Wrought Iron-Chromium-Aluminum Alloys for Service up to 2300 F in Air", BMI-1109 (July, 1956). Secret.

(7) Srawley, J. E., "Iron-Chromium-Aluminum Alloys", NRL-5124 (February 28, 1958).

(8) Chevenard, P., Recherches Experimentales sur les Alliages der Fer, de Nickel, et de Chrome, Dunod, Paris (1927), 144 pp.

(9) Bain, E. C., and Griffiths, W. E., "An Introduction to the Iron-Chromium-Nickel Alloys", Trans. AIME, 75, 166 (1927).

(10) Cook, A. J., and Jones, F. W., "The Brittle Constituent of the Iron-Chromium System (Sigma Phase)", J. Iron and Steel Inst., 148 (II), 217 (1943).

(11) Anderson, A. G. H., and Jette, E. R., "X-Ray Investigation of the Iron-Chromium-Silicon Phase Diagram", Trans. ASM, 24, 375 (1936).

(12) Vollers, C., "The Sigma Phase in Alloys Containing Iron and Chromium", Metalen, 5-6, 223 (1950-1951).

(13) Nicholson, M. E., Samans, C. H., and Shortsleeve, F. J., "Composition Limits of Sigma Formation in Nickel-Chromium Steels at 1200 F (650 C)", Trans. ASM, 44, 601 (1952).

(14) Tofaute, V. W., Küttner, C., and Büttinghaus, A., "Das System Eisen-Chrom-Chromkarbid Cr_7C_3-Zementit", Arch. Eisenhüttenw., 9, 606 (1936).

(15) Kornilov, I. I., Alloys of Iron-Chromium-Aluminum, Vol I, Academy of Sciences, U.S.S.R., Moscow (1945), 192 pp (Russian).

(16) Fisher, R. M., Dulis, E. J., and Carrol, K. G., "Identification of the Precipitate Accompanying 885°F Embrittlement in Chromium Steels", Trans. AIME, 197, 690 (1953).

(17) Williams, R. O., and Paxton, H. W., "The Nature of Aging of Binary Iron-Chromium Alloys Around 500 C", J. Iron and Steel Inst., 185, 358 (March, 1957).

(18) Williams, R. O., "Further Studies of the Iron-Chromium System", Trans. AIME, 212, 497 (1958).

(19) Tisinai, G. F., and Samans, C. H., "Some Observations on 885°F Embrittlement", Trans. AIME, 207, J. Metals, 9, 1221 (October, 1957).

(20) Wright, W. V., Jr., "Precipitation Embrittlement Studies in Vacuum Melted Iron-Chromium Alloys", Doctoral dissertation, California Institute of Technology (1955).

(21) Lorrel, J. M., "Some Aspects of 475°C Embrittlement", M. S. Thesis, Illinois Institute of Technology (1954).

(22) Metals Handbook, 1948 Edition, American Society for Metals, Cleveland (1948), pp 438-443.

(23) Olds, L. E., and Rengstorff, G., "Effects of Oxygen, Nitrogen, and Carbon on the Ductility of Cast Molybdenum", Trans. AIME, 206, 150-155 (February, 1956).

(24) Wain, H. L., Henderson, F., and Johnstone, S. T. M., "A Study of the Room Temperature Ductility of Chromium", Australia Commonwealth, Dept. Supply, Research, and Development Branch, ARL/MET 1, 33 pp (April, 1954).

(25) Abrahamson, E. P., and Grant, N. J., "Brittle to Ductile Transition Temperatures of Binary Chromium Base Alloys", Trans. ASM, 50, 705-721 (1958).

(26) Lorig, C. H., "Metallurgical Aspects", Symposium on the Effect of Temperature on the Brittle Behavior of Metals (1954), ASTM Special Publication No. 158, p 147.

(27) McLennan, J. E., Johnstone, S. T. M., and Wain, H. L., "Research Report on Brittleness of Metals", Australasian Engr., 67-75 (September, 1955).

(28) Ham, J. L., and Carr, F. L., "Impact Properties of Vacuum-Melted Iron-Chromium-Alloys", Vacuum Metallurgy, J. Electrochem. Soc., 102, 35-48 (1955).

(29) Nachman, J. F., and Buehler, W. J., "16% Al-Fe Alloy Cold-Rolled in the Order-Disorder Temperature Range", J. Appl. Phy., 25, 307-313 (1954).

(30) Morgan, E. R., and Zackay, V. F., "Ductile Iron-Aluminum Alloys", Metal Progr., 68, 126-128 (October, 1955).

(31) Morgan, E. R., "Method of Preparation of Iron-Aluminum Alloys", U. S. Patent 2,726,952 (December 13, 1955).

(32) Nachman, J. F., Buehler, W. J., Zackay, V. F., and Morgan, E. R., "Iron-Aluminum Alloys", Metal Progr., 69, 93-94 (February, 1956).

(33) Zackay, V. F., and Goering, W. A., "The Air-Melting of Iron-Aluminum Alloys", Trans. AIME, 212, 203-204 (April, 1958).

(34) Justusson, W., Zackay, V. F., and Morgan, E. R., "The Mechanical Properties of Iron-Aluminum Alloys", Trans. ASM, 49, 905-923 (1957).

(35) Rees, W. P., "The Mechanical Properties of Iron and Some Iron Alloys of High Purity", Proceedings of the First World Metallurgical Congress, American Society for Metals (1952), pp 506-534.

(36) Gokcen, N. A., and Chipman, J., "Aluminum-Oxygen Equilibrium in Liquid Iron", Trans. AIME, 197, 173-178 (February, 1953).

(37) Green, H. T., and Brick, R. M., "Effect of Aluminum on the Low Temperature Properties of Ferrite", Trans. AIME, 200, 906-913 (August, 1954).

(38) Wessel, E. T., "Abrupt Yielding and the Ductile-to Brittle Transition in Body-Centered-Cubic Metals", Trans. AIME, 209, 930-935 (July, 1957).

(39) Metal Interfaces, American Society for Metals, Cleveland (1952), "Mechanical Effects of Interfaces" (B. Chalmers), pp 299-311.

(40) Metals Handbook, 1948 Edition, American Society for Metals, Cleveland (1948), p 1249.

(41) Bastien, P., "Diffusion of Gases in Metals. Case of the Iron-Hydrogen System", Métaux & corrosion, 25, 248-262 (October, 1950).

(42) Cottrell, A. H., "Theory of Brittle Fracture in Steel and Similar Metals", Trans. AIME, 212, 192-203 (April, 1958).

(43) Smith, W. H., "Solid Solubility of Carbon in Chromium", Trans. AIME, 209, 47-49 (January, 1957).

(44) Saller, H. A., Stacy, J. T., and Eddy, N. S., "An Investigation of Wrought Iron-Chromium-Aluminum-Nitrogen Alloys for Service at 2200 F", BMI-1082 (April 10, 1956). Secret.

(45) Hessenbruch, W., Horst, E., and Schichtel, K., "The Behavior of Electrical Heating Wire Alloys in Different Gases at High Temperatures", Arch. Eisenhüttenw., 11, 225-229 (1937). Brutcher Translation No. 1640.

(46) Houdremont, E., and Bandel, G., "Heat Resisting Steels Under Attack by Hot Gases", Arch. Eisenhüttenw., 11, 131-138 (1937). Brutcher Translation No. 564.

(47) Bandel, G., "Changes in Structure and Properties of Heat Resisting Chromium-Aluminum and Chromium-Silicon Steels Due to Absorption of Nitrogen", Arch. Eisenhüttenw., 11, 139-144 (1937). Brutcher Translation No. 553.

(48) Scheil, E., and Schulz, E. H., "Heat-Resistant Chromium-Aluminum Steels", Arch. Eisenhüttenw., 6, 155-160 (1932). Brutcher Translation No. 98.

(49) Houdremont, E. , and Schrader, H. , "Effect of Alloying Elements Upon the Behavior of Steels in Case Hardening", Arch. Eisenhüttenw. , 8, 445-459 (1935).

(50) Hessenbruch. W. , "Choice of Material for Electric Production of Heat", Chem. Fabrik, 9, 525-529 (1936).

(51) Houdremont, E. , Introduction to Special Steels, Julius Springer Verlag, Berlin (1935), p 462.

(52) Ipavic, H. , Sulphur Resisting Alloys, 1923-1933, Hanau Albertis Verlagsbuchhandlung (1933), Heraus Vacuum-Schmelze 10th Anniversary Volume, p 290. Brutcher Translation No. 905.

(53) Clark, F. H. , Metals at High Temperature, Reinhold Publishing Co. , New York (1950).

(54) Kubaschewski, O. , and Hopkins, B. E. , Oxidation of Metals and Alloys, Academic Press, New York (1953).

(55) Evans, U. R. , Metallic Corrosion, Passivity, Protection, Longman's Green and Co. , New York (1946).

(56) Grunert, A. , Hessenbruch, W. , and Schichtel, K. , "Highly Heat-Resisting Chrome-Aluminum-Iron Alloys", Elektrowärme, 5, 2-11 (1935).

(57) Fry, A. , "Theory and Practice of Hardening by Nitriding", Tech. Mitt. Krupp, 1, 44-47 (1933).

(58) Gruber, H. , "Heat-Resistant and Sulfur-Resistant Alloys", Z. Metallk. , 23, 151-157 (1931).

(59) "Articles Resistant to Hydrogen Sulfide", German Patent 641,405 (January, 1937).

(60) "Chemical Treatment of Iron-Aluminum or Iron-Aluminum-Chromium Alloys", German Patent 645,306 (May, 1937).

(61) Kornilov, I. , "New Heat Resisting Chromium-Aluminum Steels With High Electrical Resistance", Doklady Akad. Nauk S. S. S. R. , 24, 904-914 (1939); Stal, 10, 59-60 (1940). Brutcher Translation No. 1250.

(62) Kornilov, I. , and Shpikelman, A. I. , "Rate of Oxidation of Iron-Chromium-Aluminum Alloys With High Chromium Content", Doklady Akad. Nauk S. S. S. R. , 53, 805-808 (1946). Brutcher Translation No. 1965.

(63) Mikheev, V. S. , "Tubes of Heat Resisting Alloys", Vestnik Akad. Nauk S. S. S. R. , 26, 40-42 (1956).

(64) Hatfield, W. H. , "Heating Resisting Steels", J. Iron and Steel Inst. , 115, 483 (1927).

(65) Lustman, B. , "Resistance of Metals to Scaling", Metal Progr. , 50, 850-856 (1946).

(66) Grum-Grzhimailo, N. V., "Heat Resistance of Some Alloy Steels", Metallurg, 15, 21-25 (1940). Brutcher Translation No. 1050.

WC/SA/AAB/EJJ/FRS/RFD:all